

REPORT DOCUMENTATION PAGE

Public reporting burden for this collection of information is estimated to average 1 hour per response, including the time for reviewing instructions, the collection of information. Send comments regarding this burden estimate or any other aspect of this collection of information, including its operations and reports, 1215 Jefferson Davis Highway, Suite 1204, Arlington, VA 22202-4302, and to the Office of Management and Budget, P.

AFRL-SR-BL-TR-00-

nd reviewing
Information

1. AGENCY USE ONLY (Leave blank)		2. REPORT DATE December, 1997		3. REP 0972	
4. TITLE AND SUBTITLE 1997 Summer Research Program (SRP), High School Apprenticeship Program (HSAP), Final Reports, Volume 15A, Wright Laboratory				5. FUNDING NUMBERS F49620-93-C-0063	
6. AUTHOR(S) Gary Moore					
7. PERFORMING ORGANIZATION NAME(S) AND ADDRESS(ES) Research & Development Laboratories (RDL) 5800 Uplander Way Culver City, CA 90230-6608				8. PERFORMING ORGANIZATION REPORT NUMBER	
9. SPONSORING/MONITORING AGENCY NAME(S) AND ADDRESS(ES) Air Force Office of Scientific Research (AFOSR) 801 N. Randolph St. Arlington, VA 22203-1977				10. SPONSORING/MONITORING AGENCY REPORT NUMBER	
11. SUPPLEMENTARY NOTES					
12a. DISTRIBUTION AVAILABILITY STATEMENT Approved for Public Release				12b. DISTRIBUTION CODE	
13. ABSTRACT (Maximum 200 words) The United States Air Force Summer Research Program (USAF-SRP) is designed to introduce university, college, and technical institute faculty members, graduate students, and high school students to Air Force research. This is accomplished by the faculty members (Summer Faculty Research Program, (SFRP)), graduate students (Graduate Student Research Program (GSRP)), and high school students (High School Apprenticeship Program (HSAP)) being selected on a nationally advertised competitive basis during the summer intersession period to perform research at Air Force Research Laboratory (AFRL) Technical Directorates, Air Force Air Logistics Centers (ALC), and other AF Laboratories. This volume consists of a program overview, program management statistics, and the final technical reports from the HSAP participants at the Wright Laboratory.					
14. SUBJECT TERMS Air Force Research, Air Force, Engineering, Laboratories, Reports, Summer, Universities, Faculty, Graduate Student, High School Student				15. NUMBER OF PAGES	
				16. PRICE CODE	
17. SECURITY CLASSIFICATION OF REPORT Unclassified	18. SECURITY CLASSIFICATION OF THIS PAGE Unclassified	19. SECURITY CLASSIFICATION OF ABSTRACT Unclassified	20. LIMITATION OF ABSTRACT UL		

UNITED STATES AIR FORCE
SUMMER RESEARCH PROGRAM -- 1997
HIGH SCHOOL APPRENTICESHIP PROGRAM FINAL REPORTS

VOLUME 15A

WRIGHT LABORATORY

RESEARCH & DEVELOPMENT LABORATORIES

5800 Uplander Way

Culver City, CA 90230-6608

Program Director, RDL
Gary Moore

Program Manager, AFOSR
Major Linda Steel-Goodwin

Program Manager, RDL
Scott Licoscas

Program Administrator, RDL
Johnetta Thompson

Program Administrator, RDL
Rebecca Kelly

Submitted to:

AIR FORCE OFFICE OF SCIENTIFIC RESEARCH
Bolling Air Force Base
Washington, D.C.
December 1997

20010321 044

NA M61-06-1271

PREFACE

Reports in this volume are numbered consecutively beginning with number 1. Each report is paginated with the report number followed by consecutive page numbers, e.g., 1-1, 1-2, 1-3; 2-1, 2-2, 2-3.

Due to its length, Volume 15 is bound in three parts, 15A, 15B and 15C. Volume 15A contains #1-20. Volume 15B contains reports #21-40 and Volume 15C contains reports 41-56. The Table of Contents for Volume 15 is included in all parts.

This document is one of a set of 16 volumes describing the 1997 AFOSR Summer Research Program. The following volumes comprise the set:

<u>VOLUME</u>	<u>TITLE</u>
1	Program Management Report
	<i>Summer Faculty Research Program (SFRP) Reports</i>
2A & 2B	Armstrong Laboratory
3A & 3B	Phillips Laboratory
4A & 4B	Rome Laboratory
5A , 5B & 5C	Wright Laboratory
6	Arnold Engineering Development Center, United States Air Force Academy and Air Logistics Centers
	<i>Graduate Student Research Program (GSRP) Reports</i>
7A & 7B	Armstrong Laboratory
8	Phillips Laboratory
9	Rome Laboratory
10A & 10B	Wright Laboratory
11	Arnold Engineering Development Center, Wilford Hall Medical Center and Air Logistics Centers
	<i>High School Apprenticeship Program (HSAP) Reports</i>
12A & 12B	Armstrong Laboratory
13	Phillips Laboratory
14	Rome Laboratory
15A, 15B & 15C	Wright Laboratory
16	Arnold Engineering Development Center

HSAP FINAL REPORT TABLE OF CONTENTS

i-xv

1. INTRODUCTION	1
2. PARTICIPATION IN THE SUMMER RESEARCH PROGRAM	2
3. RECRUITING AND SELECTION	3
4. SITE VISITS	4
5. HBCU/MI PARTICIPATION	4
6. SRP FUNDING SOURCES	5
7. COMPENSATION FOR PARTICIPATIONS	5
8. CONTENTS OF THE 1995 REPORT	6

APPENDICIES:

A. PROGRAM STATISTICAL SUMMARY	A-1
B. SRP EVALUATION RESPONSES	B-1

HSAP FINAL REPORTS

SRP Final Report Table of Contents

author	University/Institution Report Title	Armstrong Laboratory Directorate	Vol-Page
Brandi L Black	Red Mountain High School , Mesa , AZ	AL/HRA	12- 1
Kimberly K Blazer	Oakwood High School , Dayton , OH Repeatability Evaluation of Night Vision Goggles for Geometric Measurements	AL/CFHV	12- 2
Kristen R Bonnema	Wayne High School , Huber Heights , OH The Effects of Individual Differences and team processes on Team Member schema similarity and task P	AL/CFHI	12- 3
David M Brogan	Robert E. Lee High School , San Antonio , TX The use of 3-Dimensional modeling in the widespread Dissemination of complex scientific data	AL/OERS	12- 4
Matthew S Caspers	MacArthur High School , San Antonio , TX A Study of the 39-40 Hz Signal to determine an index of Gravitational induced loss of Consciousness	AL/CFTF	12- 5
Elizabeth M Cobb	Belmont High School , Dayton , OH A Study fo Pitch and Contact Associated with the Opening and Closing of Vocal Cords	AL/CFBA	12- 6
Linda E Cortina	Theodore Roosevelt High School , San Antonio , TX The Effect of Hyperbaric Oxygenation on the Mitotic Div of Prostate Cancer Cells	AL/AOH	12- 7
Maria A Evans	John Jay High School , San Antonio , TX Mercury Analysis By Cold Vapor By Atomic Absorption	AL/OEAO	12- 8
Daniel L Hardmeyer	James Madison High School , San Antonio , TX Neuropsychological Examinations For Pilots	AL/AOC	12- 9
Nafisa Islam	Centerville High School , Centerville , OH Effects of timed exposure to Dibromobenzene on /arachidonic acid levels in skin using a methyl Ester	AL/OET	12- 10
Kathleen S Kao	Keystone School , San Antonio , TX Effects of Brain Temperature ofn Fatigue in Rats Due to Maziarl Exercise and Radio Frequency Radiati	ALOERB	12- 11

SRP Final Report Table of Contents

Author	University/Institution Report Title	Armstrong Laboratory Directorate	Vol-Page
Lauren M Lamm	Keystone School , San Antonio , TX Analyses of Metal Concentrations By Flame Atomic Absorption Spectroscopy	AL/OEAO	12- 12
Evan D Large	Northwestern High School , Springfield , OH ABDAR Remote Enginecrigng	AL/HRGO	12- 13
Jason L Law	Oliver Wendell Holmes High , San Antonio , TX	AL/CFT	12- 14
Shaun M Little	Floresville High School , Floresville , TX The role of Microsoft's directx 3 software development Kit in the rapid development of high fidelity	AL/HRCC	12- 15
Katie E Lorenz	Chaminade-Julienne High School , Dayton , OH Visual Acuity between 6 and 60 Meters	AL/CFHP	12- 16
Darby M Mahan	Tippecanoe High School , Tipp City , OH	AL/CF	12- 17
Priscilla M Medina	PSJ High School , Port Saint Joe , FL A Look into the Air Force's Computer Department	AL/EQP	12- 18
Mark T Meiners	Dobson High , Mesa , AZ A Study of Accuracy and Response Time in Tests of Spatial Ability	AL/HRA	12- 19
David J Miller	Texas Academy of Mathematics , Denton , TX An Analysis of Radiofrequency Radiation Induced Temperature gradients in the Rat Brain	AL/OERS	12- 20
Joseph R Moate	Rutherford High School , PANAMA CITY , FL	AL/EQM	12- 21
Shannon J Murphy	Keystone School , San Antonio , TX An Investigation of The Precision of the El-Mar Fixation Analysis Software Technology	AL/CFTF	12- 22

SRP Final Report Table of Contents

author	University/Institution Report Title	Armstrong Laboratory Directorate	Vol-Page
Catrina A Navalta	Health Careers High School , San Antonio , TX Metals Analysis by Atomic Absorption Using A Graphite Furnace	AL/OEAO	12 - 23
Christine P Pan	Health Careers High School , San Antonio , TX Spinning a Web	AL/HRCC	12 - 24
Kavitha K Reddy	Miami Valley School , Dayton , OH Study of factors Influencing Injury Potential Associated with Emergency Egress	AL/CFBE	12 - 25
Anitha K Reddy	Miami Valley School , Dayton , OH A Study of the Methodology Used In An Experiment Testing The Effect of Localizing Auditory Signals O	AL/CFBA	12 - 26
Ester I Resendiz	William Howard Taft High School , San Antonio , TX A study of the shifts in scene perception memory	AL/CFTF	12 - 27
Amanda M Scheidt	Wayne High School , Huber Heights , OH	AL/OET	12 - 28
Rachel A Sharp	William Howard Taft High School , San Antonio , TX A study of the Analysis of Urinary Benzodiazepines Using Enzyme Hydrolysis	AL/AOEL	12 - 29
James E Sovel	Rutherford High School , PANAMA CITY , FL	AL/EQA	12 - 30
Curtis J Sparks	Xenia High School , Xenia , OH ABDR:Remote Engineering Requests	AL/HRGO	12 - 31
Lauren M Spencer	Rutherford High School , PANAMA CITY , FL Alternative Training Agents Laboratory-Scale Work	AL/EQL	12 - 32
Tyler W Standage	Gilbert High School , Gilbert , AZ A Study of Accuracy and Response time in tests of Spatial Ability	AL/HRA	12 - 33

SRP Final Report Table of Contents

Author	University/Institution Report Title	Armstrong Laboratory Directorate	Vol-Page
Rachel J Strickland	A. Crawford Mosely High School , Lynn Haven , FL the Process of Technical Publication/Documentation Via Electronic Media For the Armstrong Laboratory	AL/EQP	12- 34
Lydia R Strickland	A. Crawford Mosely High School , Lynn Haven , FL Anaerobic Degradation Products of Toluene and Laboratory MSDS Management	AL/EQL	12- 35
Kelly C Todd	Theodore Roosevelt High School , San Antonio , TX The Effect of Hyperbaric Oxygenation on the Mitotic Div of Prostate Cancer Cells	AL/AOH	12- 36
Tammy L Venema	Stebbins High School , Dayton , OH Cerebral hemodynamic Response to a Squat-Stand at IG	AL/CFBS	12- 37
Max P Vilimpoc	Beavercreek High School , Dayton , OH A Study of Psycho-Physiological Effects on Brainwave Activity During Varying levels of Activity	AL/CFHP	12- 38
Elizabeth A Walker	Theodore Roosevelt High School , San Antonio , TX The Effect of Hyperbaric Oxygenation on the Mitotic Div of Prostate Cancer Cells	AL/AOH	12- 39
Nathan L Wright	Dayton Christian High School , Dayton , OH CG and MOI Study of Human and Manikin Segments	AL/CFBV	12- 40
Muchieh A Yu	Theodore Roosevelt High School , San Antonio , TX Detection of Clostridium Difficile Toxins by Polymerase Chain Reaction	AL/AOE	12- 41

SRP Final Report Table of Contents

author	University/Institution Report Title	Phillips Laboratory Directorate	Vol-Page
Emily R Blundell	Rosamond High School , Rosamond , CA Engineering Assistant	PL/RKO	13- 1
Lauren A Ferguson	Moriarity High School , Moriarity , NM Experimental Validation of Three-Dimensional Reconstruction of Inhomogeneity Images in turbid Media	PL/LIMI	13- 2
Erica S Gerken	Manzano High School , Albuquerque , NM Chaotic Dynamics in a Nd:YAG laser	PL/LIDD	13- 3
Ngan B Kha	Chelmsford High School , North Chelmsford , MA	PL/GPOS	13- 4
Paul G Loftsgard	Quartz Hill High School , Quartz Hill , CA A Study on Optical Paternation	PL/RKS	13- 5
Fawn R Miller	Manzano High School , Albuquerque , NM A Study of Space Structure's Isolation	PL/VTV	13- 6
Amy W Mok	Newton North High School , Newtonville , MA A study of the Effect of fuel Sulfur Content on the Production of Aerosols in Aircraft Exhaust Plum	PL/GPID	13- 7
Martin P Morales	Palmdale High School , Palmdale , CA the Separations and Reacrions of Cyclohexyl Poss Compounds	PL/RKS	13- 8
David D Parker	Boron High School , Boron , CA Intranet Web Page, Design and Development	PL/RKD	13- 9
Kimberly A Robinson	Sandia High School , All-uquerque , NM Scientific Visualization methods at the Center for Plasma Theory and Computation	PL/WSQA	13- 10
Michael P Schoenfeld	NewMexico Military Ins. , Roswell , NM Study of the Effect of Heat Flow on the Performance of an Alkali Metal Thermal-to-Electric Converter	PL/VTV	13- 11

SRP Final Report Table of Contents

Author	University/Institution Report Title	Phillips Laboratory Directorate	Vol-Page
Thomas J Shea	Tehachapi High School , Tehachapi , CA A study of the Characterization of reduced Toxicity Monoporopellants	PL/RKS	13- 12
Carl W Steinbach	Lincoln-Sudbury Regional High , Sudbury , MA A Study of the Interrelation of Cloud Thickness and Cloud Liquid Water Content in Maritime Stratocum	PL/GPAB	13- 13
Nhi T Tran	Manzano High School , Albuquerque , NM Optically Addressed Spatial Light Modulators as real-time Holographic Media	PL/LMS	13- 14
Jeremy L White	Sandia High School , Albuquerque . NM Constructing a Computer Model of the Space Shuttle and The Effects of Lassers on Materials in Space	PL/WSAT	13- 15
Joanne Wu	Newton North High School , Newtonville , MA Development of Algorithms to Objectively Forecast Present Weather and Surface VisibilityBy Means fo	PL/GPAB	13- 16
Aaron Zimmerman	Sandia High School , All uquerque . NM IDASS ADDITIONS	PL/WSAT	13- 17

SRP Final Report Table of Contents

Author	University/Institution Report Title	Rome Laboratory Directorate	Vol-Page
Christine A Angell	Camden High School , Camden , NY HTML Computer Language	RL/C3CA	14 - 1
Stephen M Enjem	Whitesboro Senior High School , Marcy , NY Writing World-Wide Web (WWW) Pages	RL/IRAE	14 - 2
David S Feldman	Rome Free Academy , Rome , NY AFOSR SUMMER 1997 INTERNSHIP	RL/ERDR	14 - 3
Douglas M Feldmann	Oneida Senior High School , Oneida , NY Examination of the nearest-neighbor rule in voice pattern Classification	RL/OCSS	14 - 4
Patrick X Fitzgerald	Holland Patent High School , Holland Patent , NY The Multi-Temporal Trainable Delay(MTTD) neural Network Architecture	RL/IRDS	14 - 5
Daniel E Grabski	Holland Patent High School , Holland Patent , NY RF Module Life Test System Design	RL/ERDA	14 - 6
Sandra L Jablonka	Oneida Senior High School , Oneida , NY Antenna Pattern Measurements Using Infrared Imaging Techniques	RL/ERST	14 - 7
Colin M Kinsella	Oneida Senior High School , Oneida , NY A Study of Genetic Algorithms	RL/C3CA	14 - 8
Matthew A Miling	VVS Senior High School , Verona , NY A Study of Hostile Electromagnetic Environments within Multichip Modules	RL/ERST	14 - 9
Francis P Ruiz	Rome Free Academy , Rome , NY	RL/ERDD	14 - 10
Roshan P Shah	Camden High School , Camden , NY Multi-Paradigmatic Programming: Integrating Prolog and Visual Basic	RL/C3CA	14 - 11

SRP Final Report Table of Contents

Author	University/Institution Report Title	Rome Laboratory Directorate	Vol-Page
Brian B Tuch	New Hartford Senior High School , New Hartford , NY A Study of the Application, Uses, and Performance of Spread Spectrum Technology in Digital Signal Pr	RL/IRAA	14- 12
Brian S Walsh	Whitesboro High School , Whitesboro , NY Web based Computer Programming	RL/IRDS	14- 13
David A Young	Rome Free Academy , Rome , NY Reproducing the Copper/Gold Eutectic Curve Using Computer Simulations	RLERDR	14- 14

SRP Final Report Table of Contents

Author	University/Institution Report Title	Wright Laboratory Directorate	Vol-Page
Michael C Austin	Fairborn High School , Fairborn , OH System Administration	WL/AASE	15- 1
Gaurav K Bedi	Wayne High School , Huber Heights , OH Synthesis & Characterization of Melt Intercalated Nanocomposites	WL/MLBP	15- 2
Crystal W Bhagat	Dayton Christian High School , Dayton , OH A Study of the Effects of Varying Pulse Width and Duty Cycle On Polymer Dispersed	WL/MLPJ	15- 3
Margaret A Brun	Dixie High School , New Lebanon , OH Surface Structure and Optical Properties of a Sensitive Snake Infared Detector	WL/DOR	15- 4
Shannon M Campbell	Carroll High School , Dayton , OH Window Design for Laser Velocimetre Data Aquisition	WL/POTF	15- 5
Percio B Castro	Belmont High School , Dayton , OH	WL/AACF	15- 6
Jason R Caudill	Fairborn High School , Fairborn , OH 2 Photon Ionization and Disassociative Attachment of Eletrons To Excited Molcules	WL/POOX	15- 7
Bernardo V Cavour	Fairmont High School , Kettering , OH High School Appentice Program Accomplishments	WL/FIBT	15- 8
Christopher R Clark	Niceville Senior High School , Niceville , FL Neural Networks & Digital Image Processing	WL/MNGA	15- 9
Aaron Davis	Niceville Senior High School , Niceville , FL Electronic Studies of Polypyrrole Films Grown on Semiconductor Wafers	WL/MNMF	15- 10
Debbie L Dressler	Centerville High School , Centerville , OH Traction Models	WL/POSL	15- 11

SRP Final Report Table of Contents

Author	University/Institution Report Title	Wright Laboratory Directorate	Vol-Page
Molly M Flanagan	Chaminade-Julienne High School , Dayton , OH	WL/POTF	15 - 12
Landon W Frymire	Laurel Hill High School , Laurel Hill , FL Technical Report Library User's Manual	WL/MNAV	15 - 13
Allison D Gadd	Carroll High School , Dayton , OH	WL/FIVS	15 - 14
Matthew A Gerding	Fairborn High School , Fairborn , OH The Study of the Electro-Optic Coefficients of DR-1 and Dans	WL/MLPO	15 - 15
Jon M Graham	Carroll High School , Riverside , OH The Flight Dynaics Lab	WL/DOR	15 - 16
Trenton Hamilton	Rocky Bayou Christian School , Niceville , FL Cast Ductile Iron (CDI) (A Controlled Fragmentation Study)	WL/MNM	15 - 17
Neil Harrison	Ft Walton Beach High SC , Ft Walton BEACH , FL Comparison of Experimental Penetration Data with Various Penetration Prediction Methodologies	WL/MNM	15 - 18
Angela C Helm	Carroll High School , Dayton , OH	WL/AACT	15 - 19
Anna S Hill	Carroll High School , Dayton , OH Window design for Laser velocimeter Data Aquisition	WL/POTF	15 - 20
Erek A Kasse	Bellbrook High School , Bellbrook . OH Friction and Solid Lubricants	WL/MLBT	15 - 21
Maria Lee	Wayne High School , Huber Heights , OH the Database Design for a Configuration Mnagement Library	WL/AAST	15 - 22

SRP Final Report Table of Contents

Author	University/Institution Report Title	Wright Laboratory Directorate	Vol-Page
Colleen A Lefevre	Lehman High School , Sidney , OH the Effect of Chain Lengths on Bond Orders and Geometry in Simple Cyanines0	WL/DOR	15 - 23
John P Lightle	Tippecanoe High School , Tipp City , OH A Study of two methods for Predicting fin Center of Pressure position	WL/FIGC	15 - 24
Alexander R Lippert	Choctawhatchee High School , Ft Walton BEACH , FL Nanoparticle Doped Organic Electronic Junction Devices	WL/MNMF	15 - 25
Marcus W Mac Nealy	Chaminade-Julienne High School , Dayton , OH Web Page Design to Display Infrared Imagery	WL/AACA	15 - 26
Jonathan S Mah	Centerville High School , Centerville , OH The Integration of Circuit synthesis and Schematic Programs Using Prolog, ad Evaluatation of a Graph	WL/AASH	15 - 27
David Mandel	Niceville Senior High School , Niceville , FL Terminal Ballistics Data Acquisition & Analysis	WL/MNM	15 - 28
Michele V Manuel	Crestview High School , Crestview , FL The Mechanical & Metallurgical Characterization of Liquid Phase Sintered Tungsten Alloyw	WL/MNM	15 - 29
Lori M Marshall	Carroll High School , Dayton , OH A Study of Chemical Vapor Deposition and Pulse Laser Deposition	WL/DOR	15 - 30
Terrence J McGregor	Fairborn High School , Fairborn , OH Chain Armor Ballistic Testing : Establishing the Ballistic Limit	WL/FIVS	15 - 31
Deborah S Mills	West Liberty-Dalem Jr./Sr. High School , West Liberty , OH A Summer at Wright Patterson Air Force Base	WL/DOR	15 - 32
Ryan M Moore	Centerville High School . Centerville , OH Studies in Computational Chemistry and Biomimetics	WL/MLPJ	15 - 33

SRP Final Report Table of Contents

Author	University/Institution Report Title	Wright Laboratory Directorate	Vol-Page
Jeremy M Mount	Bellbrook High School , Bellbrook , OH	WL/FIIB	15- 34
John D Murchison	Ft Walton Beach High SC , Ft Walton BEACH , FL Methodology for the Creation of a Randomized Shot-Line Generator	WL/MNSA	15- 35
Disha J Patel	Fairmont High School , Kettering , OH	WL/AACT	15- 36
Neill W Perry	Crestview High School , Crestview , FL Empirical Characterization of Mid-Infrared Photodetectors for a Dual-Wavelength Ladar System	WL/MNGS	15- 37
Kathleen A Pirog	Niceville Senior High School , Niceville , FL The Implications of Photomodeler on the Generation of 3D Models	WL/MNGA	15- 38
Nathan A Power	Heritage Christian School , Xenia , OH The World Wide Web and Hyper Text Markup Language	WL/AAOP	15- 39
Shaun G Power	Heritage Christian School , Xenia , OH	WL/AACI	15- 40
Josh J Pressnell	Fairmont High School , Kettering , OH A Study n Internet Programming and World Wide Web Publishing	WL/AACN	15- 41
Stephanie M Puterbaugh	Beavercreek High School , Dayton , OH Initial Experimental evaluation of an Axial Groove Heat Pipe for Aircraft Applications	WL/POOS	15- 42
Matthew R Rabe	Carroll High School , Dayton , OH	WL/POSC	15- 43
Kristan M Raymond	Ft Walton Beach High SC , Ft Walton BEACH , FL Immersion Corrosion Testing of Tungsten Heavy-Metal Alloys	WL/MNSE	15- 44

SRP Final Report Table of Contents

Author	University/Institution Report Title	Wright Laboratory Directorate	Vol-Page
David S Revill	Choctawhatchee High School . Ft Walton BEACH , FL Verification of State of Chemical Equations & Generation of Textures for Phenomenology Modeling	WL/MNGA _____	15 - 45
Harris T Schneiderman	Miami Valley School , Dayton . OH A Study of the capabilities of computational fluid dynamics technology to simulate the flight perfor	WL/FIMC _____	15 - 46
Nicole L Speelman	Stebbins High School , Dayton , OH Development and Application of Materials Characterization web Site	WL/MLIM _____	15 - 47
Kari D Sutherland	Dayton Christian High School . Dayton , OH A Study of the Effects of the Performance of Polymer Dispersed Liquid Crystal Holographic Gratings w	WL/MLPJ _____	15 - 48
Christine M Task	Stebbins High School , Dayton , OH	WL/MLIM _____	15 - 49
Rebecca M Thien	Chaminade-Julienne High School , Dayton , OH A Study of the Corrosion Resistance of Sol-Gels	WL/DOR _____	15 - 50
Jonathan D Tidwell	Rocky Bayou Christian School , Niceville . FL Data Reduction for Blast Arena Lethality Enhancement	WL/MNM _____	15 - 51
Robert L Todd	Carroll High School , Dayton . OH The Characterization of A Scud Fragment	WL/MLLI _____	15 - 52
Elizabeth A Walker	Niceville Senior High School . Niceville , FL Concept vs Reality:Developing a Theoretical Sequencing Program for Shock Induced Combustion	WL/MNA _____	15 - 53
Darren C Wells	Bellbrook High School , Bellbrook , OH A Study of the Tension and Shear Strength of Bidirectional Epoxy-Resin Composites	WL/DOR _____	15 - 54
Tuan P Yang	Choctawhatchee High School , Ft Walton BEACH , FL Thermal Characterization of the 1,3,3-Trinitroazetidine (ADNAZ) Binary Mixture	WL/MNM _____	15 - 56

SRP Final Report Table of Contents

Author	University/Institution Report Title	Arnold Engineering Development Center Directorate	Vol-Page
Karllee R Barton	Coffee County Central High , Manchester , TN A Math Model of the Flow Characteristics of The J4 gaseous Nitrogen Reprass Systems	AEDC	16 - 1
Jason G Bradford	Franklin County Senior High School , Winchester , TN Design of A Serchable Data Retreving Web Based Page	AEDC	16 - 2
James R Brandon	Coffee County Central High , Manchester , TN	AEDC	16 - 3
Barbara E King	Franklin County Senior High School , Winchester , TN Assessment of Microwave Horn Antenna Radiation Pattern	AEDC	16 - 4
Kaitrin T Mahar	Coffee County Central High , Manchester , TN Analysis of DWSG Characterizations	AEDC	16 - 5
Steven W Marlowe	Franklin County Senior High School , Winchester , TN Writing a Cost Estimate Program Using The Java Programming Language	AEDC	16 - 6
Michael R Munn	Coffee County Central High , Manchester , TN Construction of a Graphical User Interface for the Thermally Perfect Gas Code	AEDC	16 - 7
Jason A Myers	Coffee County Central High , Manchester , TN Intranet Development Problem with Powerpoint	AEDC	16 - 8
James P Nichols	Tullahoma High School , Tullahoma , TN Assessment of Reflecting Microwave Horn Data Within A Plasma	AEDC	16 - 9
James M Perryman	Shelbyville Central High School , Shelbyville , TN Computer Manipulation of Raman Spectroscopy Test	AEDC	16 - 10
Kristin A Pierce	Coffee County Central High , Manchester , TN Evaluation of Arc Heater Performance and Operational Stability	AEDC	16 - 11

SRP Final Report Table of Contents

author	University/Institution Report Title	Arnold Engineering Development Center Directorate	Vol-Page
Daniel M Thompson	Shelbyville Central High School , Shelbyville , TN Maintenance of Facilities	AEDC	16 - 12
James R Williamson	Franklin County Senior High School , Winchester , TN Access Conversions	AEDC	16 - 13

1. INTRODUCTION

The Summer Research Program (SRP), sponsored by the Air Force Office of Scientific Research (AFOSR), offers paid opportunities for university faculty, graduate students, and high school students to conduct research in U.S. Air Force research laboratories nationwide during the summer.

Introduced by AFOSR in 1978, this innovative program is based on the concept of teaming academic researchers with Air Force scientists in the same disciplines using laboratory facilities and equipment not often available at associates' institutions.

The Summer Faculty Research Program (SFRP) is open annually to approximately 150 faculty members with at least two years of teaching and/or research experience in accredited U.S. colleges, universities, or technical institutions. SFRP associates must be either U.S. citizens or permanent residents.

The Graduate Student Research Program (GSRP) is open annually to approximately 100 graduate students holding a bachelor's or a master's degree; GSRP associates must be U.S. citizens enrolled full time at an accredited institution.

The High School Apprentice Program (HSAP) annually selects about 125 high school students located within a twenty mile commuting distance of participating Air Force laboratories.

AFOSR also offers its research associates an opportunity, under the Summer Research Extension Program (SREP), to continue their AFOSR-sponsored research at their home institutions through the award of research grants. In 1994 the maximum amount of each grant was increased from \$20,000 to \$25,000, and the number of AFOSR-sponsored grants decreased from 75 to 60. A separate annual report is compiled on the SREP.

The numbers of projected summer research participants in each of the three categories and SREP "grants" are usually increased through direct sponsorship by participating laboratories.

AFOSR's SRP has well served its objectives of building critical links between Air Force research laboratories and the academic community, opening avenues of communications and forging new research relationships between Air Force and academic technical experts in areas of national interest, and strengthening the nation's efforts to sustain careers in science and engineering. The success of the SRP can be gauged from its growth from inception (see Table 1) and from the favorable responses the 1997 participants expressed in end-of-tour SRP evaluations (Appendix B).

AFOSR contracts for administration of the SRP by civilian contractors. The contract was first awarded to Research & Development Laboratories (RDL) in September 1990. After completion of the

1990 contract, RDL (in 1993) won the recompetition for the basic year and four 1-year options.

2. PARTICIPATION IN THE SUMMER RESEARCH PROGRAM

The SRP began with faculty associates in 1979; graduate students were added in 1982 and high school students in 1986. The following table shows the number of associates in the program each year.

YEAR	SRP Participation, by Year			TOTAL
	SFRP	GSRP	HSAP	
1979	70			70
1980	87			87
1981	87			87
1982	91	17		108
1983	101	53		154
1984	152	84		236
1985	154	92		246
1986	158	100	42	300
1987	159	101	73	333
1988	153	107	101	361
1989	168	102	103	373
1990	165	121	132	418
1991	170	142	132	444
1992	185	121	159	464
1993	187	117	136	440
1994	192	117	133	442
1995	190	115	137	442
1996	188	109	138	435
1997	148	98	140	427

Beginning in 1993, due to budget cuts, some of the laboratories weren't able to afford to fund as many associates as in previous years. Since then, the number of funded positions has remained fairly constant at a slightly lower level.

3. RECRUITING AND SELECTION

The SRP is conducted on a nationally advertised and competitive-selection basis. The advertising for faculty and graduate students consisted primarily of the mailing of 8,000 52-page SRP brochures to chairpersons of departments relevant to AFOSR research and to administrators of grants in accredited universities, colleges, and technical institutions. Historically Black Colleges and Universities (HBCUs) and Minority Institutions (MIs) were included. Brochures also went to all participating USAF laboratories, the previous year's participants, and numerous individual requesters (over 1000 annually).

RDL placed advertisements in the following publications: *Black Issues in Higher Education*, *Winds of Change*, and *IEEE Spectrum*. Because no participants list either *Physics Today* or *Chemical & Engineering News* as being their source of learning about the program for the past several years, advertisements in these magazines were dropped, and the funds were used to cover increases in brochure printing costs.

High school applicants can participate only in laboratories located no more than 20 miles from their residence. Tailored brochures on the HSAP were sent to the head counselors of 180 high schools in the vicinity of participating laboratories, with instructions for publicizing the program in their schools. High school students selected to serve at Wright Laboratory's Armament Directorate (Eglin Air Force Base, Florida) serve eleven weeks as opposed to the eight weeks normally worked by high school students at all other participating laboratories.

Each SFRP or GSRP applicant is given a first, second, and third choice of laboratory. High school students who have more than one laboratory or directorate near their homes are also given first, second, and third choices.

Laboratories make their selections and prioritize their nominees. AFOSR then determines the number to be funded at each laboratory and approves laboratories' selections.

Subsequently, laboratories use their own funds to sponsor additional candidates. Some selectees do not accept the appointment, so alternate candidates are chosen. This multi-step selection procedure results in some candidates being notified of their acceptance after scheduled deadlines. The total applicants and participants for 1997 are shown in this table.

1997 Applicants and Participants			
PARTICIPANT CATEGORY	TOTAL APPLICANTS	SELECTEES	DECLINING SELECTEES
SFRP	490	188	32
(HBCU/MI)	(0)	(0)	(0)
GSRP	202	98	9
(HBCU/MI)	(0)	(0)	(0)
HSAP	433	140	14
TOTAL	1125	426	55

4. SITE VISITS

During June and July of 1997, representatives of both AFOSR/NI and RDL visited each participating laboratory to provide briefings, answer questions, and resolve problems for both laboratory personnel and participants. The objective was to ensure that the SRP would be as constructive as possible for all participants. Both SRP participants and RDL representatives found these visits beneficial. At many of the laboratories, this was the only opportunity for all participants to meet at one time to share their experiences and exchange ideas.

5. HISTORICALLY BLACK COLLEGES AND UNIVERSITIES AND MINORITY INSTITUTIONS (HBCU/MIs)

Before 1993, an RDL program representative visited from seven to ten different HBCU/MIs annually to promote interest in the SRP among the faculty and graduate students. These efforts were marginally effective, yielding a doubling of HBCU/MI applicants. In an effort to achieve AFOSR's goal of 10% of all applicants and selectees being HBCU/MI qualified, the RDL team decided to try other avenues of approach to increase the number of qualified applicants. Through the combined efforts of the AFOSR Program Office at Bolling AFB and RDL, two very active minority groups were found, HACU (Hispanic American Colleges and Universities) and AISES (American Indian Science and Engineering Society). RDL is in communication with representatives of each of these organizations on a monthly basis to keep up with their activities and special events. Both organizations have widely-distributed magazines/quarterlies in which RDL placed ads.

Since 1994 the number of both SFRP and GSRP HBCU/MI applicants and participants has increased ten-fold, from about two dozen SFRP applicants and a half dozen selectees to over 100 applicants and two dozen selectees, and a half-dozen GSRP applicants and two or three selectees to 18 applicants and 7 or 8 selectees. Since 1993, the SFRP had a two-fold applicant increase and a two-fold selectee increase. Since 1993, the GSRP had a three-fold applicant increase and a three to four-fold increase in selectees.

In addition to RDL's special recruiting efforts, AFOSR attempts each year to obtain additional funding or use leftover funding from cancellations the past year to fund HBCU/MI associates. This year, 5 HBCU/MI SFRPs declined after they were selected (and there was no one qualified to replace them with). The following table records HBCU/MI participation in this program.

SRP HBCU/MI Participation, By Year				
YEAR	SFRP		GSRP	
	Applicants	Participants	Applicants	Participants
1985	76	23	15	11
1986	70	18	20	10
1987	82	32	32	10
1988	53	17	23	14
1989	39	15	13	4
1990	43	14	17	3
1991	42	13	8	5
1992	70	13	9	5
1993	60	13	6	2
1994	90	16	11	6
1995	90	21	20	8
1996	119	27	18	7

6. SRP FUNDING SOURCES

Funding sources for the 1997 SRP were the AFOSR-provided slots for the basic contract and laboratory funds. Funding sources by category for the 1997 SRP selected participants are shown here.

1997 SRP FUNDING CATEGORY	SFRP	GSRP	HSAP
AFOSR Basic Allocation Funds	141	89	123
USAF Laboratory Funds	48	9	17
HBCU/MI By AFOSR (Using Procured Addn'l Funds)	0	0	N/A
TOTAL	9	98	140

SFRP - 188 were selected, but thirty two canceled too late to be replaced.
GSRP - 98 were selected, but nine canceled too late to be replaced.
HSAP - 140 were selected, but fourteen canceled too late to be replaced.

7. COMPENSATION FOR PARTICIPANTS

Compensation for SRP participants, per five-day work week, is shown in this table.

1997 SRP Associate Compensation

PARTICIPANT CATEGORY	1991	1992	1993	1994	1995	1996	1997
Faculty Members	\$690	\$718	\$740	\$740	\$740	\$770	\$770
Graduate Student (Master's Degree)	\$425	\$442	\$455	\$455	\$455	\$470	\$470
Graduate Student (Bachelor's Degree)	\$365	\$380	\$391	\$391	\$391	\$400	\$400
High School Student (First Year)	\$200	\$200	\$200	\$200	\$200	\$200	\$200
High School Student (Subsequent Years)	\$240	\$240	\$240	\$240	\$240	\$240	\$240

The program also offered associates whose homes were more than 50 miles from the laboratory an expense allowance (seven days per week) of \$50/day for faculty and \$40/day for graduate students. Transportation to the laboratory at the beginning of their tour and back to their home destinations at the end was also reimbursed for these participants. Of the combined SFRP and GSRP associates, 65 % (194 out of 286) claimed travel reimbursements at an average round-trip cost of \$776.

Faculty members were encouraged to visit their laboratories before their summer tour began. All costs of these orientation visits were reimbursed. Forty-three percent (85 out of 188) of faculty associates took orientation trips at an average cost of \$388. By contrast, in 1993, 58 % of SFRP associates took

orientation visits at an average cost of \$685; that was the highest percentage of associates opting to take an orientation trip since RDL has administered the SRP, and the highest average cost of an orientation trip. These 1993 numbers are included to show the fluctuation which can occur in these numbers for planning purposes.

Program participants submitted biweekly vouchers countersigned by their laboratory research focal point, and RDL issued paychecks so as to arrive in associates' hands two weeks later.

This is the second year of using direct deposit for the SFRP and GSRP associates. The process went much more smoothly with respect to obtaining required information from the associates, only 7% of the associates' information needed clarification in order for direct deposit to properly function as opposed to 10% from last year. The remaining associates received their stipend and expense payments via checks sent in the US mail.

HSAP program participants were considered actual RDL employees, and their respective state and federal income tax and Social Security were withheld from their paychecks. By the nature of their independent research, SFRP and GSRP program participants were considered to be consultants or independent contractors. As such, SFRP and GSRP associates were responsible for their own income taxes, Social Security, and insurance.

8. CONTENTS OF THE 1997 REPORT

The complete set of reports for the 1997 SRP includes this program management report (Volume 1) augmented by fifteen volumes of final research reports by the 1997 associates, as indicated below:

1997 SRP Final Report Volume Assignments

LABORATORY	SFRP	GSRP	HSAP
Armstrong	2	7	12
Phillips	3	8	13
Rome	4	9	14
Wright	5A, 5B	10	15
AEDC, ALCs, WHMC	6	11	16

APPENDIX A – PROGRAM STATISTICAL SUMMARY

A. Colleges/Universities Represented

Selected SFRP associates represented 169 different colleges, universities, and institutions,
GSRP associates represented 95 different colleges, universities, and institutions.

B. States Represented

SFRP - Applicants came from 47 states plus Washington D.C. Selectees represent 44 states.

GSRP - Applicants came from 44 states. Selectees represent 32 states.

HSAP - Applicants came from thirteen states. Selectees represent nine states.

Total Number of Participants	
SFRP	189
GSRP	97
HSAP	140
TOTAL	426

Degrees Represented			
	SFRP	GSRP	TOTAL
Doctoral	184	0	184
Master's	2	41	43
Bachelor's	0	56	56
TOTAL	186	97	298

SFRP Academic Titles	
Assistant Professor	64
Associate Professor	70
Professor	40
Instructor	0
Chairman	1
Visiting Professor	1
Visiting Assoc. Prof.	1
Research Associate	9
TOTAL	186

Source of Learning About the SRP		
Category	Applicants	Selectees
Applied/participated in prior years	28%	34%
Colleague familiar with SRP	19%	16%
Brochure mailed to institution	23%	17%
Contact with Air Force laboratory	17%	23%
<i>IEEE Spectrum</i>	2%	1%
<i>BIIHE</i>	1%	1%
Other source	10%	8%
TOTAL	100%	100%

APPENDIX B -- SRP EVALUATION RESPONSES

1. OVERVIEW

Evaluations were completed and returned to RDL by four groups at the completion of the SRP. The number of respondents in each group is shown below.

Table B-1. Total SRP Evaluations Received

Evaluation Group	Responses
SFRP & GSRPs	275
HSAPs	113
USAF Laboratory Focal Points	84
USAF Laboratory HSAP Mentors	6

All groups indicate unanimous enthusiasm for the SRP experience.

The summarized recommendations for program improvement from both associates and laboratory personnel are listed below:

- A. Better preparation on the labs' part prior to associates' arrival (i.e., office space, computer assets, clearly defined scope of work).
- B. Faculty Associates suggest higher stipends for SFRP associates.
- C. Both HSAP Air Force laboratory mentors and associates would like the summer tour extended from the current 8 weeks to either 10 or 11 weeks; the groups state it takes 4-6 weeks just to get high school students up-to-speed on what's going on at laboratory. (Note: this same argument was used to raise the faculty and graduate student participation time a few years ago.)

2. 1997 USAF LABORATORY FOCAL POINT (LFP) EVALUATION RESPONSES

The summarized results listed below are from the 84 LFP evaluations received.

1. LFP evaluations received and associate preferences:

Table B-2. Air Force LFP Evaluation Responses (By Type)

Lab	Evals Recv'd	How Many Associates Would You Prefer To Get ?								(% Response)			
		SFRP				GSRP (w/Univ Professor)				GSRP (w/o Univ Professor)			
		0	1	2	3+	0	1	2	3+	0	1	2	3+
AEDC	0	-	-	-	-	-	-	-	-	-	-	-	-
WHMC	0	-	-	-	-	-	-	-	-	-	-	-	-
AL	7	28	28	28	14	54	14	28	0	86	0	14	0
USAF A	1	0	100	0	0	100	0	0	0	0	100	0	0
PL	25	40	40	16	4	88	12	0	0	84	12	4	0
RL	5	60	40	0	0	80	10	0	0	100	0	0	0
WL	46	30	43	20	6	78	17	4	0	93	4	2	0
Total	84	32%	50%	13%	5%	80%	11%	6%	0%	73%	23%	4%	0%

LFP Evaluation Summary. The summarized responses, by laboratory, are listed on the following page. LFPs were asked to rate the following questions on a scale from 1 (below average) to 5 (above average).

2. LFPs involved in SRP associate application evaluation process:
 - a. Time available for evaluation of applications:
 - b. Adequacy of applications for selection process:
3. Value of orientation trips:
4. Length of research tour:
5.
 - a. Benefits of associate's work to laboratory:
 - b. Benefits of associate's work to Air Force:
6.
 - a. Enhancement of research qualifications for LFP and staff:
 - b. Enhancement of research qualifications for SFRP associate:
 - c. Enhancement of research qualifications for GSRP associate:
7.
 - a. Enhancement of knowledge for LFP and staff:
 - b. Enhancement of knowledge for SFRP associate:
 - c. Enhancement of knowledge for GSRP associate:
8. Value of Air Force and university links:
9. Potential for future collaboration:
10.
 - a. Your working relationship with SFRP:
 - b. Your working relationship with GSRP:
11. Expenditure of your time worthwhile:

(Continued on next page)

12. Quality of program literature for associate:
13. a. Quality of RDL's communications with you:
 b. Quality of RDL's communications with associates:
14. Overall assessment of SRP:

Table B-3. Laboratory Focal Point Responses to above questions

	<i>AEDC</i>	<i>AL</i>	<i>USAFA</i>	<i>PL</i>	<i>RL</i>	<i>WHMC</i>	<i>WL</i>
<i># Evals Recv'd</i>	0	7	1	14	5	0	46
<i>Question #</i>							
2	-	86 %	0 %	88 %	80 %	-	85 %
2a	-	4.3	n/a	3.8	4.0	-	3.6
2b	-	4.0	n/a	3.9	4.5	-	4.1
3	-	4.5	n/a	4.3	4.3	-	3.7
4	-	4.1	4.0	4.1	4.2	-	3.9
5a	-	4.3	5.0	4.3	4.6	-	4.4
5b	-	4.5	n/a	4.2	4.6	-	4.3
6a	-	4.5	5.0	4.0	4.4	-	4.3
6b	-	4.3	n/a	4.1	5.0	-	4.4
6c	-	3.7	5.0	3.5	5.0	-	4.3
7a	-	4.7	5.0	4.0	4.4	-	4.3
7b	-	4.3	n/a	4.2	5.0	-	4.4
7c	-	4.0	5.0	3.9	5.0	-	4.3
8	-	4.6	4.0	4.5	4.6	-	4.3
9	-	4.9	5.0	4.4	4.8	-	4.2
10a	-	5.0	n/a	4.6	4.6	-	4.6
10b	-	4.7	5.0	3.9	5.0	-	4.4
11	-	4.6	5.0	4.4	4.8	-	4.4
12	-	4.0	4.0	4.0	4.2	-	3.8
13a	-	3.2	4.0	3.5	3.8	-	3.4
13b	-	3.4	4.0	3.6	4.5	-	3.6
14	-	4.4	5.0	4.4	4.8	-	4.4

3. 1997 SFRP & GSRP EVALUATION RESPONSES

The summarized results listed below are from the 257 SFRP/GSRP evaluations received.

Associates were asked to rate the following questions on a scale from 1 (below average) to 5 (above average) - by Air Force base results and over-all results of the 1997 evaluations are listed after the questions.

1. The match between the laboratories research and your field:
2. Your working relationship with your LFP:
3. Enhancement of your academic qualifications:
4. Enhancement of your research qualifications:
5. Lab readiness for you: LFP, task, plan:
6. Lab readiness for you: equipment, supplies, facilities:
7. Lab resources:
8. Lab research and administrative support:
9. Adequacy of brochure and associate handbook:
10. RDL communications with you:
11. Overall payment procedures:
12. Overall assessment of the SRP:
13.
 - a. Would you apply again?
 - b. Will you continue this or related research?
14. Was length of your tour satisfactory?
15. Percentage of associates who experienced difficulties in finding housing:
16. Where did you stay during your SRP tour?
 - a. At Home:
 - b. With Friend:
 - c. On Local Economy:
 - d. Base Quarters:
17. Value of orientation visit:
 - a. Essential:
 - b. Convenient:
 - c. Not Worth Cost:
 - d. Not Used:

SFRP and GSRP associate's responses are listed in tabular format on the following page.

Table B-4. 1997 SFRP & GSRP Associate Responses to SRP Evaluation

	Arnold	Brooks	Edwards	Eglin	Griffis	Hanseum	Kelly	Kirtland	Lackland	Robins	Tyndall	WPAFB	average
# res	6	48	6	14	31	19	3	32	1	2	10	85	257
1	4.8	4.4	4.6	4.7	4.4	4.9	4.6	4.6	5.0	5.0	4.0	4.7	4.6
2	5.0	4.6	4.1	4.9	4.7	4.7	5.0	4.7	5.0	5.0	4.6	4.8	4.7
3	4.5	4.4	4.0	4.6	4.3	4.2	4.3	4.4	5.0	5.0	4.5	4.3	4.4
4	4.3	4.5	3.8	4.6	4.4	4.4	4.3	4.6	5.0	4.0	4.4	4.5	4.5
5	4.5	4.3	3.3	4.8	4.4	4.5	4.3	4.2	5.0	5.0	3.9	4.4	4.4
6	4.3	4.3	3.7	4.7	4.4	4.5	4.0	3.8	5.0	5.0	3.8	4.2	4.2
7	4.5	4.4	4.2	4.8	4.5	4.3	4.3	4.1	5.0	5.0	4.3	4.3	4.4
8	4.5	4.6	3.0	4.9	4.4	4.3	4.3	4.5	5.0	5.0	4.7	4.5	4.5
9	4.7	4.5	4.7	4.5	4.3	4.5	4.7	4.3	5.0	5.0	4.1	4.5	4.5
10	4.2	4.4	4.7	4.4	4.1	4.1	4.0	4.2	5.0	4.5	3.6	4.4	4.3
11	3.8	4.1	4.5	4.0	3.9	4.1	4.0	4.0	3.0	4.0	3.7	4.0	4.0
12	5.7	4.7	4.3	4.9	4.5	4.9	4.7	4.6	5.0	4.5	4.6	4.5	4.6
Numbers below are percentages													
13a	83	90	83	93	87	75	100	81	100	100	100	86	87
13b	100	89	83	100	94	98	100	94	100	100	100	94	93
14	83	96	100	90	87	80	100	92	100	100	70	84	88
15	17	6	0	33	20	76	33	25	0	100	20	8	39
16a	-	26	17	9	38	23	33	4	-	-	-	30	
16b	100	33	-	40	-	8	-	-	-	-	36	2	
16c	-	41	83	40	62	69	67	96	100	100	64	68	
16d	-	-	-	-	-	-	-	-	-	-	-	0	
17a	-	33	100	17	50	14	67	39	-	50	40	31	35
17b	-	21	-	17	10	14	-	24	-	50	20	16	16
17c	-	-	-	-	10	7	-	-	-	-	-	2	3
17d	100	46	-	66	30	69	33	37	100	-	40	51	46

4. 1997 USAF LABORATORY HSAP MENTOR EVALUATION RESPONSES

Not enough evaluations received (5 total) from Mentors to do useful summary.

5. 1997 HSAP EVALUATION RESPONSES

The summarized results listed below are from the 113 HSAP evaluations received.

HSAP apprentices were asked to rate the following questions on a scale from
1 (below average) to 5 (above average)

1. Your influence on selection of topic/type of work.
2. Working relationship with mentor, other lab scientists.
3. Enhancement of your academic qualifications.
4. Technically challenging work.
5. Lab readiness for you: mentor, task, work plan, equipment.
6. Influence on your career.
7. Increased interest in math/science.
8. Lab research & administrative support.
9. Adequacy of RDL's Apprentice Handbook and administrative materials.
10. Responsiveness of RDL communications.
11. Overall payment procedures.
12. Overall assessment of SRP value to you.
13. Would you apply again next year? Yes (92 %)
14. Will you pursue future studies related to this research? Yes (68 %)
15. Was Tour length satisfactory? Yes (82 %)

	Arnold	Brooks	Edwards	Eglin	Griffiss	Hanscom	Kirtland	Tyndall	WPAFB	Totals
# resp	5	19	7	15	13	2	7	5	40	113
1	2.8	3.3	3.4	3.5	3.4	4.0	3.2	3.6	3.6	3.4
2	4.4	4.6	4.5	4.8	4.6	4.0	4.4	4.0	4.6	4.6
3	4.0	4.2	4.1	4.3	4.5	5.0	4.3	4.6	4.4	4.4
4	3.6	3.9	4.0	4.5	4.2	5.0	4.6	3.8	4.3	4.2
5	4.4	4.1	3.7	4.5	4.1	3.0	3.9	3.6	3.9	4.0
6	3.2	3.6	3.6	4.1	3.8	5.0	3.3	3.8	3.6	3.7
7	2.8	4.1	4.0	3.9	3.9	5.0	3.6	4.0	4.0	3.9
8	3.8	4.1	4.0	4.3	4.0	4.0	4.3	3.8	4.3	4.2
9	4.4	3.6	4.1	4.1	3.5	4.0	3.9	4.0	3.7	3.8
10	4.0	3.8	4.1	3.7	4.1	4.0	3.9	2.4	3.8	3.8
11	4.2	4.2	3.7	3.9	3.8	3.0	3.7	2.6	3.7	3.8
12	4.0	4.5	4.9	4.6	4.6	5.0	4.6	4.2	4.3	4.5
Numbers below are percentages										
13	60%	95%	100%	100%	85%	100%	100%	100%	90%	92%
14	20%	80%	71%	80%	54%	100%	71%	80%	65%	68%
15	100%	70%	71%	100%	100%	50%	86%	60%	80%	82%

System Administration

Michael Austin
AASW

WL/AASW
2241 Avionic Circle Suite 32
WPAFB OH 45433-7334

Final Report for;
High School Apprenticeship Program

Sponsored by:
Wright Laboratories
and
Air Force Office of Scientific Research
Bolling Air Force Base, Washington DC

August 1, 1997

System Administration

Michael Austin
WL/AASW

Abstract

A system administrator is the person who maintains the integrity of a computer system. He must watch over the system and make sure that the system is running smoothly. The administrator chooses what programs will be at the highest of importance. If the system grows too large, he must know how to allow it to enlarge. A system administrator is the one that fixes any problems that the system may receive from improper or unauthorized use.

In a working environment where several people are using the same system from different terminals, it is necessary for that system to be controlled. The job of the system administrator is to insure that the system runs without errors and that the people using the system get their fair share of time. This is accomplished by correcting errors in the system, keeping the system up to date, backing up the system, and placing different levels of importance on different jobs. The job of the system administrator is to do these things and to protect it from unauthorized use.

A system administrator must first know where to find the documentation that describes the commands that are needed. The first and most important of these sources are the man and xman pages. They contain reference material, but they do not teach how to use the page. These pages are the main source for information dealing with individual daemons, commands, and files. They locate and print titled entries from the on-line reference sources that contain the information. The pages are not always user friendly, but are important for remembering how to use the system.

The man pages are found by typing `# man` and then the name of the program the administrator wants to find. Man pages will give information about the program in this order: user commands, application programs, and programming commands, then system calls, file formats, miscellaneous information, and the device file information. It will also give the system administration commands, network communication commands, graphical applications, functions, games, and special files about hardware peripherals. The xman program is a manual page that is designed for the xwindows system. It displays a list of

programs that the administrator can search through for man pages. It can be used by typing `# xman`. Another database to use which finds information is the `whatis` database. It gives a short description of every man page. The administrator can access this database by typing `# man -k` at the prompt. Release notes are also excellent sources to learn about a specific release. These can be accessed by typing `# relnotes` to find which programs have release notes with them. If the administrator uses `# grelnotes`, he can use the graphical interface to the release notes. The `insight` tool could also be used to find information. It provides an easy-to-use interface that lets you search through online information. The command that accesses it is `# insight`. Every command can be found in one of these pages.

Another job of the administrator is to keep track of new and old users. The administrator can add new user accounts, delete old user's account, control the user's environment, and communicate information to the user. The administrator also needs to keep each user's work private from the other users, thus protecting the system from inexperienced or unauthorized users is also important. They must track who is doing what on the system, and optimize the resources shared by the network. This job is one of the most important of the system administrators.

There are seven steps an administrator should follow to manage user accounts. First the administrator must identify user account characteristics. Then he must add the account to `/etc/passwd` and establish group memberships in `/etc/group`. He must then create the user's configuration files, and the file must be verified and given directory

permissions. The administrator will then assign a temporary password to the account, and have the user verify setup and change his password. If these steps are not followed, the system may have problems.

When the user account is made, certain information must be put in the database. The unique user login password guarantees the safety of the users account. The user identification number is used to keep track of users on the system. A group identification number will tell the administrator what group the user is working within and the login shell will tell the computer what shell to put the user in at login. Specialized group memberships must also be put in the account to designate privileges. This information will help the computer and the administrator identify who a particular user is when they are on the system.

The password entries have specific requirements for the information in them. The username must be unique to the system. The password that appears in the next field is empty unless the user puts a password there. The user ID must also be unique, because it identifies the default group membership. The comment field defines the user's name and phone number, but is optional. The login dir is the home directory of the user. In the group account password entry, a unique familiar group name is needed. An encoded password and group ID number is necessary for the entry. It will include a list of additional users and groups who have access to group-owned files. The administrator could use a system manager to handle accounts. This would ensure accuracy and consistency, but it is more time consuming, especially when many users are being added.

The administrator may need to delete a user from the system. The recommended way to delete a user starts by locking the account by placing an asterisk before its password field. The administrator should then back up the user's data files and directories for future reference. He will then remove the user's data files, directories, and mailbox. The user's name will finally be deleted from the group lists. This process, if followed, will ensure that the user is completely deleted from the systems with no ill affects to the system.

It is often necessary for the administrator to communicate to his users. He can use the message of the day command to send a message on a particular day or he could also use a crontab file to send a message at regular intervals. The process scheduler can be used to send cron jobs at a specific time of a particular day. These programs are very useful for system communication.

Another important job of the administrator is to monitor the system. By monitoring the system, the administrator will know who was on the system, when they were on the system, and what files were used. The administrator would use the `# du -s` command to find the amount of the disk space was used. The `# df [-k]` command tells him the amount of disk space that is free. The `find` command, followed by further information, can be used to find specific types of files. Examples of specific types are large files or inactive files. The log files and accounting files must also be monitored, because they grow constantly. It is important for the administrator to keep the disk space clean for important jobs.

The administrator must also keep track of the people that are on the system, and who has been on the system. It is important this be taken care of so that any unauthorized entries on the system can be found. The `who` command can be used to show who is on the system, and when they came on. It displays it with name first, then `tty` with a number following it, and finally the date and time. The command `w` shows who is on the system, and what they are doing. The `last [name]` command will show the last log-ins of users.

An administrator must also understand processes and how to manipulate them. A process is an instance of a running program. There are three processes. They are: the interactive process that is associated with a login, terminal, or window session, batch processes which are not associated with a specific login and are submitted from a queue, and daemons, which are initiated at boot time and wait in the background until an active process requests their service. The process table can be used to keep track of all processes maintained by the kernel. The table stores the process identification number, scheduling, and resource utilization. The `ps` command allows the administrator to see a portion of the process table. If the administrator needs to stop a process, the `kill` command can be used. It allows the program to clean-up after itself before ending. If the program does not respond and the need is urgent, The `kill -9` command can be used. It ends the program instantly without allowing any preparation that the program may need to safely shut down. A process is given a priority value that ranges from zero to 254. The higher the value of the priority value, the lower its priority is. A process that has a

high number takes longer to complete because it gets less system time. The nice command raises its priority number 10 points. The process number can be changed by the administrator by using the npri command. This is used to make the time share more even, especially if a process is a time consumer. The management of processes is important because of the need for system efficiency.

It is very important to have file systems that are well organized in a system, and it is the job of the administrator to keep it organized. File systems organize data on disks by mapping names to data on disks. They provide a uniform interface to accessing disk files, and are created on a partition or a logical volume. One type of file system is EFS, or an Extent File system. It has free blocks that are indicated with a bitmap. The inodes contain single, double, and triple indirects. Inodes point to extents in the file system and are of variable size of 1-248 blocks. The more modern file system is the XFS file system. It has a 64-bit file capability, journalled file system, and it is a high-performance file system. It has no performance penalty as file system size grows, and inodes are dynamically allocated. These file systems must be mounted to be used. When mounted they are part of the IRIX hierarchical directory tree. They are automatically mounted when the system is started, if it is specified in the /etc/fstab directory.

It is important to keep file systems free from corruption, because the system cannot work without them. Corruption can occur when the memory and disk versions of the system become inconsistent. It is often caused by software or hardware failures. Fsck can clean up the corruption. It is only available on the EFS file systems, though.

File systems must be kept up to date so that the system runs efficiently.

Within an IRIX system, there may not be enough physical memory to hold all of believe the program that is running. In this case, it may be necessary to make swap space available. Swap space is memory in the hard drive that the hard memory writes part or all of a program to if it runs out of memory. It can be designated in files, partitions, or separate disks. It is recommended that the system have twice the swap space of its hard memory.

Swap space is needed for some programs that take up large amounts of memory. Sometime a program needs to know that there is a certain amount of swap space available. If it is impossible to put real swap space in, virtual swap can be used. It makes the computer think that there is swap space that there is not. Swap management helps the computer run at optimum levels.

A system needs a way to transfer data to other systems. It can use network file systems to achieve this. One host can both be a client and a server. The client is the system that mounts a remote file system, while the server exports the file system. This transfer can be done by different brands of computers to each other, such as SGI with Sun. The configuration of this system is done by the system administrator. NFS, network file system, is an optional product that needs to be loaded on the system. Once it is loaded the administrator must enable the server. The Export status of the sever can be determined by typing `# showmount` and `# exportfs`. All the specified file systems are

mounted automatically when the system goes to multi-user run level.

There are two types of mounts. Soft mounts will try to get information from the server, and if no message is received it returns an error message. A hard mount keeps trying for the file system until it receives an answer. It is uninteruptible unless the `intr` option is used. There are two setups for mounts at boot. One is the foreground boot. It tries to mount until it mounts, and does not continue booting until it mounts. A background mount will continue booting while trying to mount.

A system administrator may find that certain file systems need more memory. A logical volume spreads a file system over two or more partitions. A grown logical volume is used to expand a file system without repartitioning. Striped logical volumes alternate information between partitions to increase speed. The fastest method is to have two disks for best performance with striped logical volumes. When growing a file system, the administrator must unmount the file system. The logical volume he creates contains that file system and an empty partition. He then grows the file system and mounts it. XLVs allow file systems to grow bigger than single disks, and it supports `efs` and `xfs` file systems. It also uses XFS journaling, without performance penalty. XLVs have many daemons that assist in handling the I/O operations. These are run by the system automatically. The administrator has many duties in a XLV. He must first create it. He must also get information about objects in it, grow it, delete objects in it, and delete an entire XLV. When an `efs` file system is converted to XLV, the limit on

memory is only 8 gigabytes. Xlvm is a graphical tool that can be used to show information about XLVs. The administrator can use it to add a new volume, plex, or volume element. He can also attach, detach, or remove XLV components. This tool is the easiest way to manipulate XLVs.

IRIX has run levels that have different purposes. There is a Multi-user run level used for networking, a single-user level for system maintenance, software installation, and troubleshooting. There is also a run level for system shutdown and a reboot level to reboot. There are also less significant run levels. The system is always in one of the run levels. Each run level has a designated number. Zero is the shutdown level, and 1,S, and s are the single user levels. Two allows multi-user mode, and 6 is the mode that reboots the system. By typing `# who -r`, the administrator can find the current run level. Init is the program that looks to see what run level the system needs to be in. It starts or stops the programs that are necessary for creating a run level. The `inittab` directory holds the default run level for the system. The administrator can change it by typing in number in the entry. Each run level has scripts, such as `rc2` for run level 2. These scripts mount and unmount file systems, start and stop processes, and run programs for the directories of the run levels. If anything goes wrong with the programs that control run levels, the system will not work well or possibly not at all.

System backup is one of the most important jobs of the system administrator. If the system is not backed up, and something happens to the system, all information in the system is lost. One of the places that system backups are placed are tape drives. A tape

device needs a file to access the drive. They are located in the /dev/rmt directory. The status of the tape drive can be seen by typing # mt stat. # mt erase will erase the tape. There are three types of backups. A full backup saves all files on a system, and an incremental backup saves only the files that have changed since the last backup. User backups save only a particular users directory. There are five tools that are used for backup. They are: tar, bru, backup, dump, and xfsdump. The backup command calls the bru command. The information after putting the command in is used to tell the system where to start the backup. Restore restores the programs that were saved with the backup command. The dump command only works on efs systems. It only backs up file systems by starting at the top directory of the file system. The files are restored by the restore command. Xfsdump works only for mounted XFS file systems and requires root privileges. It is similar to dump, but only works on XFS systems. Xfsrestore restores the data saved by xfsdump. If the system is saved or restored incorrectly, or not often enough, the system will not work properly.

There are many things that a system needs to have done that it can not do for itself. The system administrator is the person that takes care of the systems needs for both the system and the users. Without his help, the system would not be able to correct its mistakes or protect itself from outside influence. The system administrator is an essential part of a group when a system is used.

References

Hudson, Chuck. IRIX System Administration. California: Silicon Graphics, 1996.

**SYNTHESIS AND CHARACTERIZATION OF
MELT INTERCALATED NANOCOMPOSITES**

Gaurav K Bedi

**Wayne High School
5400 Chambersburg Road
Huber Heights, OH 45424**

**Final Report for:
High School Apprentice Program
Wright Laboratory**

**Sponsored by:
Air Force Office of Scientific Research
Bolling Air Force Base, DC**

and

**Wright Laboratory
Wright Patterson Air Force Base, Dayton, OH**

August 1997

SYNTHESIS AND CHARACTERIZATION OF MELT INTERCALATED NANOCOMPOSITES

**Gaurav K. Bedi
Wayne High School**

Abstract

The objective of my summer's research was to synthesize a polymer/clay nanocomposite via melt intercalation, under the direction of Captain Derrick Dean, Ph.D. and Captain Richard Vaia, Ph.D.. In order to successfully disperse the clay within the monomer, a method of sonication was utilized. This melt was then polymerized as shown by results. The interpretation of the results was accomplished using Infrared Spectroscopy, X-Ray Diffraction, and Differential Scanning Calorimetry. Two types of clays were utilized in this study. Suprisingly, experiments indicate intercalation of the polymer into the SCPx-781 Clay. However, our original hypothesis was that the polymer would not react with the SCPx-781 Clay, rather; we believed the polymer would intercalate into the Montmorillonite Clay.

SYNTHESIS AND CHARACTERIZATION OF MELT INTERCALATED NANOCOMPOSITES

Gaurav K. Bedi

Introduction

Nanocomposites, comprised of organic polymers and inorganic clay components, are emerging as new and useful materials that have multiple potential applications. Recent research has uncovered new and improved properties [1] . Some of these possible applications include use as barrier materials and space applications for rocket motors [2] . In solid rocket motors, nanocomposites can be used as cases, nozzles, and even insulation. Such composites could also be used in liquid rocket motors as tanks, turbines, injectors, propellant feed lines, hot gas ducting, valve bodies, and pump housings (Figure 1). Since the inorganic clay will be dispersed at the nanoscopic level, the thermal and mechanical properties are expected to be even better than micro- or macro- composites [3] .

My work this summer has primarily focused on the synthesis and characterization of an organic/inorganic composite comprised of the polymer poly(oxybenzoate) (pABA) and organically modified mica-type silicates (OMTS). Such a composite would be beneficial in many of the above space applications. Two different OMTS's were tested for possibly interacting with the ABA. The significant difference between these two OMTS's exists in the functional groups on the surface. One clay has a carboxylic organic group while the other has an alcohol organic group. Both were chosen because of their potential reactivity with the polymer's acetoxy group.

Methodology

The synthesis of both composites was done in a melt intercalated system composed of different ratios of clay to monomer components. The SCPx-781 clay contains an alcohol group, while the Montmorillonite clay contains a carboxylic group. As a control, pABA was synthesized from the ABA

monomer by a similar method shown below, and then characterized by Infrared Spectroscopy (IR) and Differential Scanning Calorimetry (DSC). To synthesize both composites, an oil bath was placed on a stirring hot plate and the oil was heated to 190°C and continually stirred. The monomer, which lay in a regular glass test tube, was then immersed approximately halfway into the hot oil bath and clamped in place onto a ring stand. When the monomer melted, the clay was dumped into the melt and a stirring bar was added to maintain a homogenous mixture. Then the system was sonicated for 1 minute using a Fisher Model 300 Sonic Dismembrator in order to disperse the clay on the nanoscopic level. Sonication was repeated several times to achieve complete dispersion and uniformity in the mixture. The length of polymerization varied from 1 hour to 48 hours. It was observed in every synthesis that some of the monomer would incessantly sublime up the test tube to right above the oil level. This sublimate was repeatedly pushed back into the melt only to sublime again.

Results and Discussion

For the SCPx-781 Clay/ABA nanocomposite, trials 1, 2, and 3 with clay compositions of 1.5%, 15%, and 75%, respectively, were attempted. Trial 1's composite, polymerized for 24 hours, was tested on IR and showed peaks at 1739 cm^{-1} and 1690 cm^{-1} (Figure 2). The formation of an ester group is prevalent at peak 1739 cm^{-1} while peak 1690 cm^{-1} represents the carboxylic group from the ABA. A portion of trial 1 composite was then heat treated at 400°C via Differential Scanning Calorimetry (DSC) in order to post-polymerize the composite, converting the lower molecular weight (MW) polymer/clay composite to higher molecular weight polymer [5]. IR on this higher MW polymer/clay composite showed a significant decrease in the 1690 cm^{-1} peak and the formation of a new 1640 cm^{-1} peak (Figure 3). The loss of the ABA carboxylic acid peak at 1690 cm^{-1} indicates that the ABA is reacting, while the carboxylic group from the clay gives a peak at 1640 cm^{-1} , indicative of intercalation. During the melt polymerization of trial 2, samples were removed at 1, 2, 3, and 4 hours. Characterization of trial 2 was d

done via X-Ray Diffraction (XRD) performed by a fellow co-worker. Results of XRD of trial 2's → composite indicate the possibility of intercalation because the longer the composite was polymerized the flatter the clay peak appeared (Figure 4). This means that the clay is probably layered in-between the polymer ABA. However this data is still inconclusive because the clay peak is not completely gone. Trial 3's initial composition of 75% clay is inaccurate because when the 75% component clay was added to the ABA melt, much of the clay did not react with the ABA. After polymerization, this unreacted clay was stored in a separate vial. Thermal Gravimetric Analysis (TGA) done by Marlene Houtz showed the trial 3 composite to actually have approximately 25% clay (Figure 5). XRD was performed by a fellow co-worker on a trial 3 sample annealed for 20 hours, verifying intercalation (Figure 6). Because the SCPx-781 clay peak has disappeared in this XRD data, clay intercalation has probably occurred. Thus, XRD and IR data indicate that the SCPx-781 clay/ABA composite, formed from an OMTS with an alcohol group, appears to be intercalated.

The Montmorillonite Clay, which has a carboxylic functional group, used in this experiment was synthesized by a fellow co-worker. Due to the shortage of time, only one trial, a 3 hour melt polymerization, was performed on the Montmorillonite Clay/ABA composite. However, the procedure was identical to the SCPx-781 clay/ABA composite. IR and XRD were performed to characterize this composite. IR data indicates that the clay does not appear to intercalate because no 1644 cm^{-1} peak exists in the spectrum (Figure 7) after polymerization. Even if the sample is annealed at 200°C for 18 hours, no 1644 cm^{-1} peak appears in the IR data (Figure 7). XRD data reveals that the Montmorillonite clay peak is still visible when the composite is annealed at 200°C for 18 hours (Figure 9) or at 400°C (Figure 10). Intercalation does not seem to be occurring as indicated from this IR and XRD data.

Conclusion

Polymer ABA/OMTS was synthesized with the goal of producing a new material which could be

used in barrier and space applications. Although future work is needed to confirm intercalation of the clay in the polymer matrix, my experiment proved useful in showing the intercalation of the SCPx-781 Clay/ABA composite. In this nanocomposite, intercalation does, in fact, appear to be occurring. Future research to be done the SCPx-781 Clay/ABA Nanocomposite includes a model reaction to verify reactivity of functional groups on the surface of clay with ABA and further mechanical and thermal testing of the Nanocomposite. For reasons unknown at this time, the ABA/Montmorillonite Clay does not seem to intercalate. However, with future research this nanocomposite may also become intercalated like the SCPx-781 Clay/ABA composite.

References

- [1] P.B. Messersmith and E.P. Giannelis, *Chemical Materials.*, 6, 1719 (1994) .
- [2] D. Dean, private conversation. (1997)
- [3] A. Okada and A. Usuki, *Materials Science and Engineering.*, C3. 109 (1995) .
- [4] P.B. Messersmith and E.P. Giannelis, *Journal of Polymer Science, Part A: Polymer Chemistry.*, 33, 1047 (1995) .
- [5] P. Geil, presented at 28th ACS Central Regional Meeting, Dayton, OH, June 1996

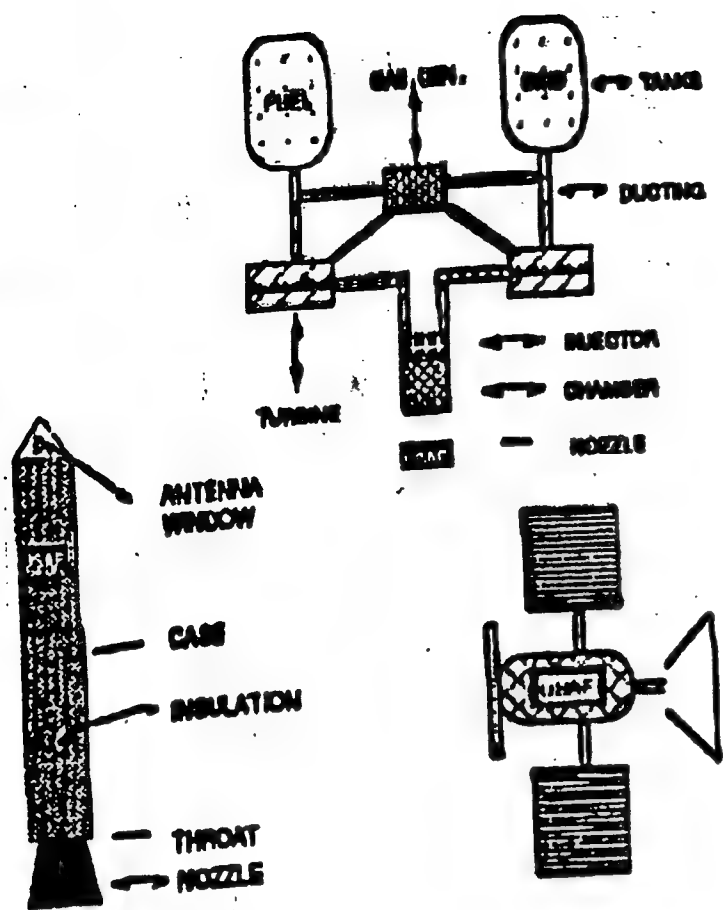


FIGURE 1
Potential applications for Nanocomposites.

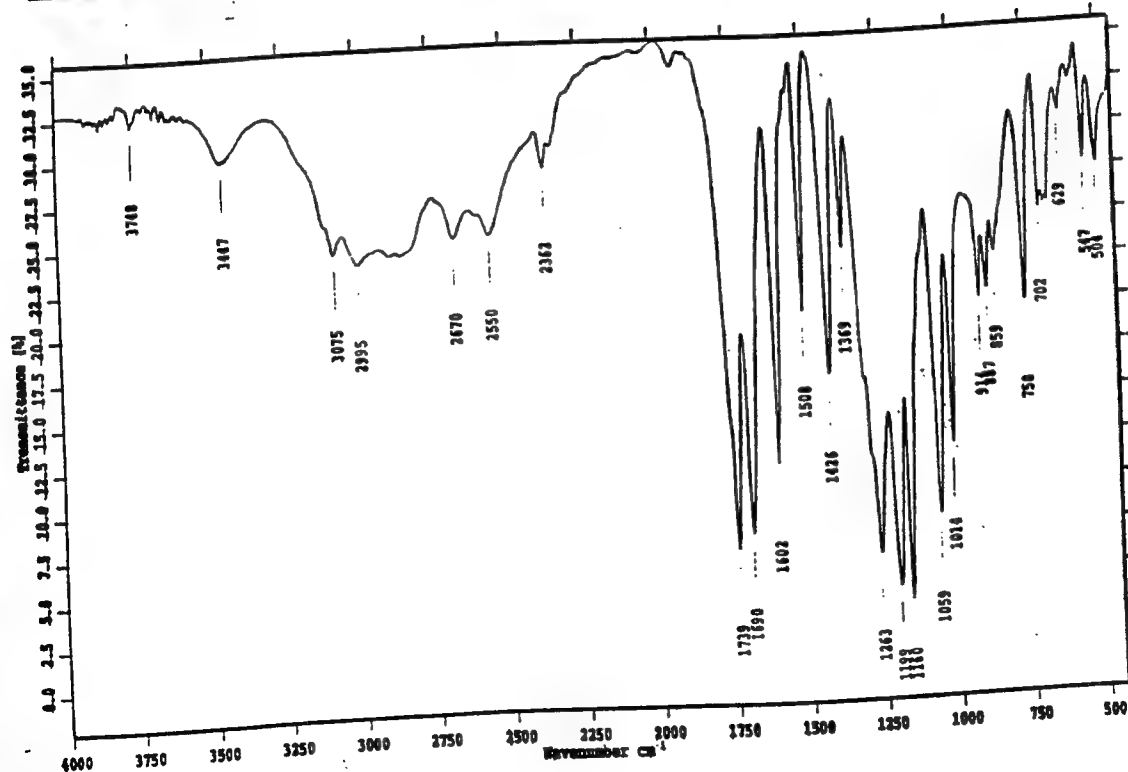


FIGURE 2
IR scan of SCPx-781 Clay/ABA Nanocomposite.

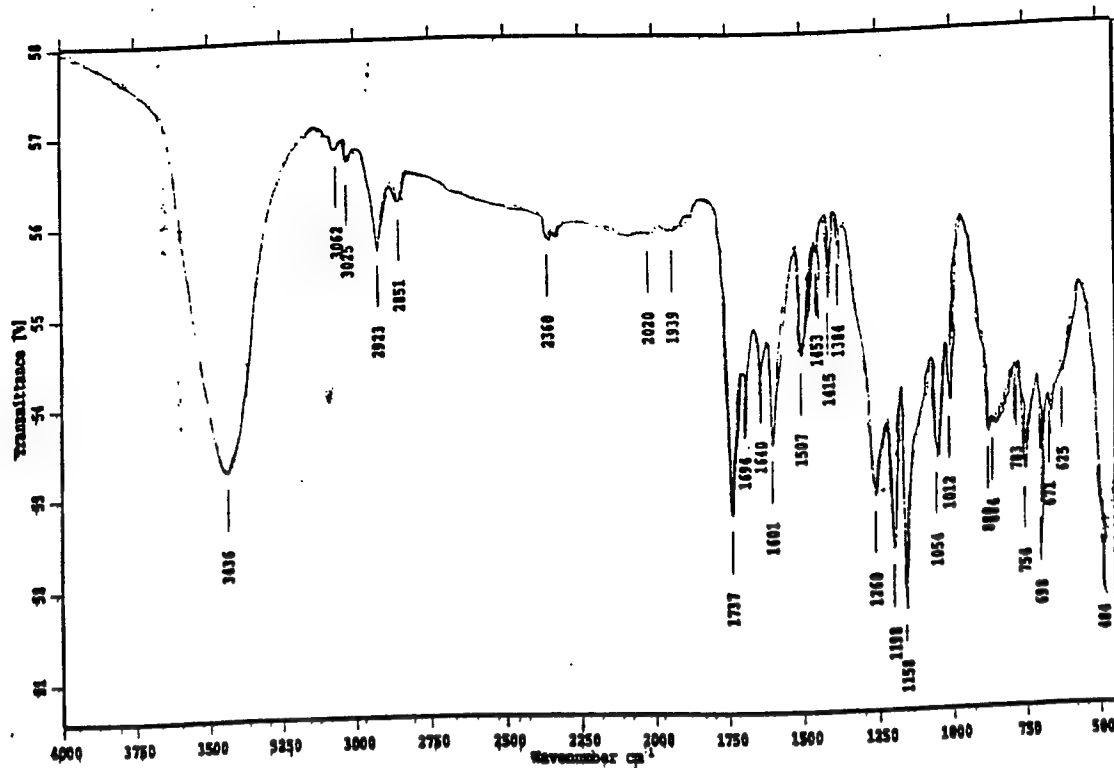


FIGURE 3

IR scan of SCPx-781 Clay/ABA Nanocomposite annealed at 400°C.

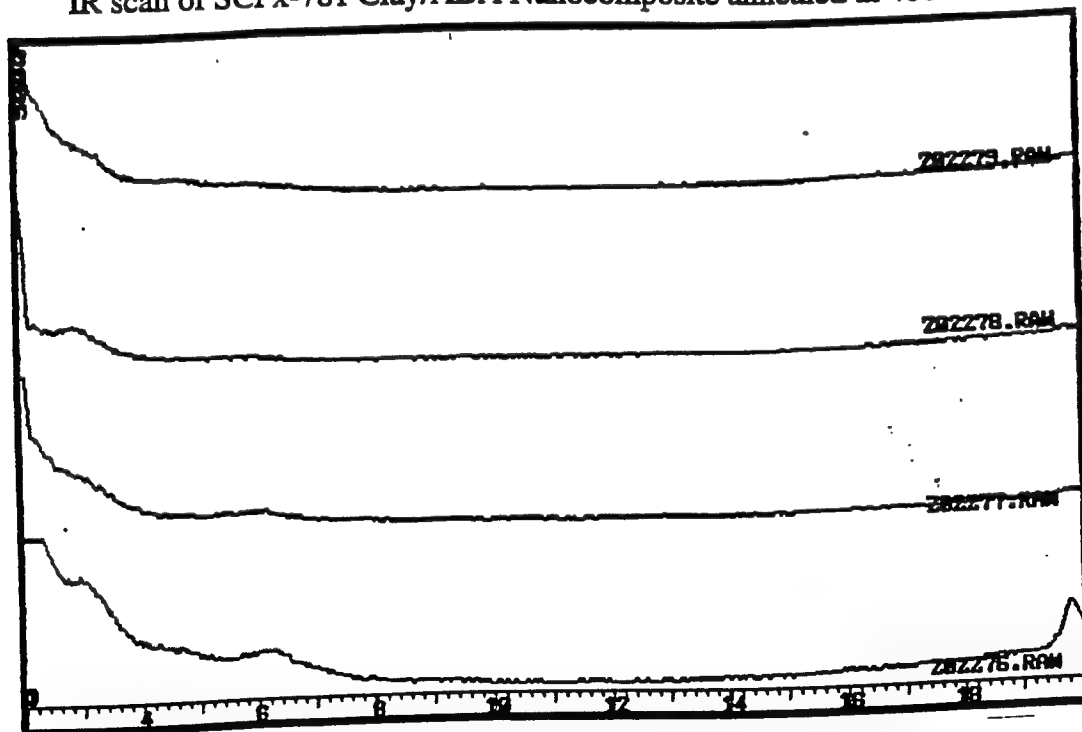


FIGURE 4

XRD scan of SCPx-781 Clay/ABA Nanocomposite reacting as a function of reaction time from bottom to top, 1 hour, 2 hours, 3 hours, 4 hours.

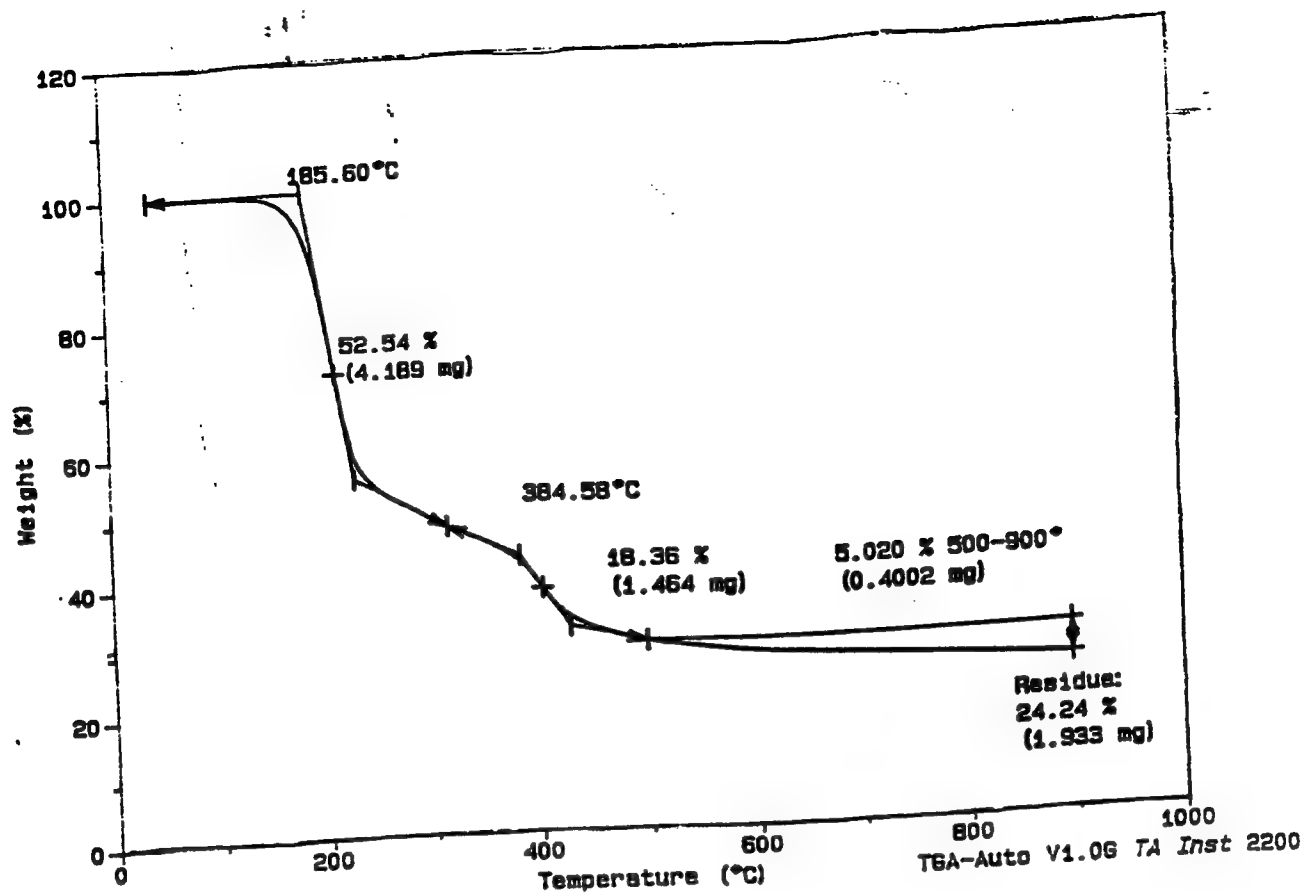


FIGURE 5
TGA of SCPx-781 Clay/ABA Nanocomposite from trial 3.

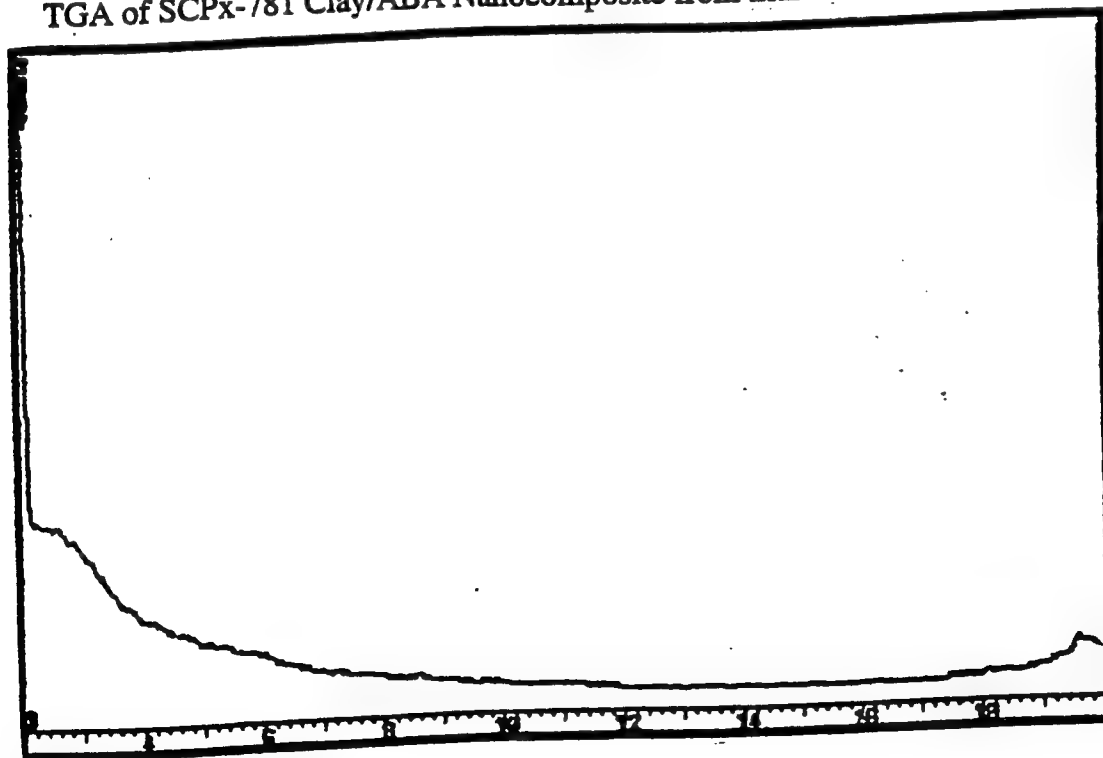


FIGURE 6
XRD scan from trial 3 of SCPx-781 Clay/ABA
Nanocomposite annealed at 200°C for 20 hours.

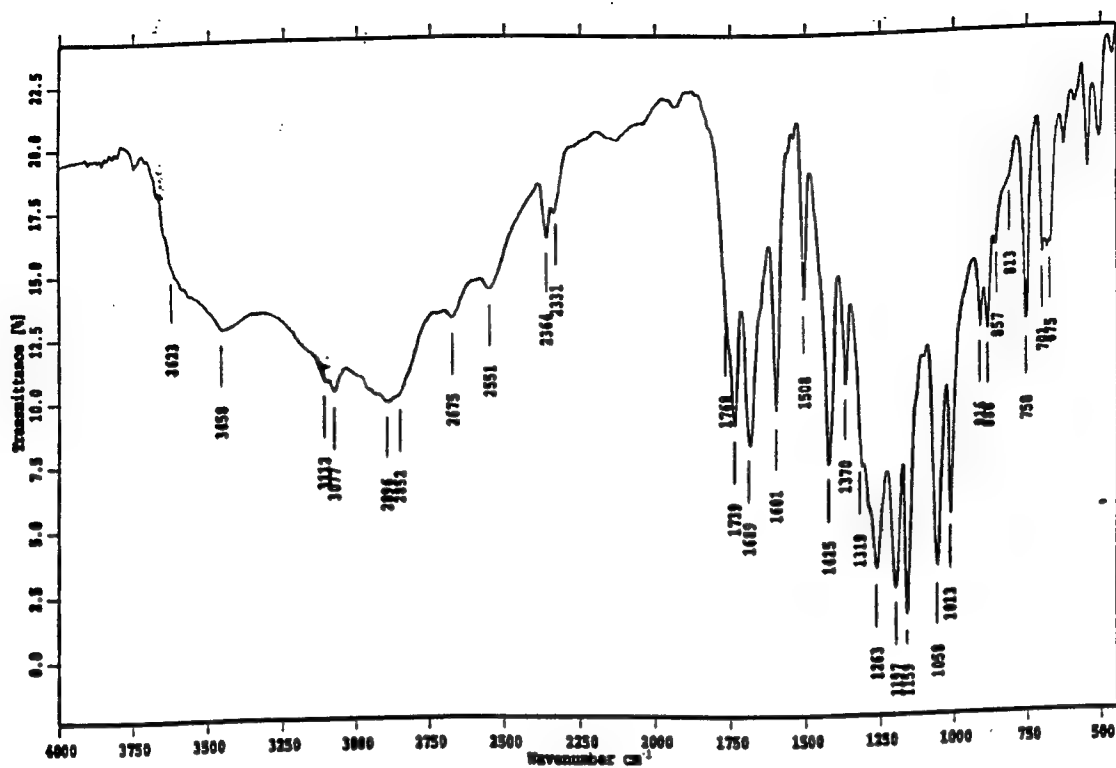


FIGURE 7
IR scan of Montmorillonite/ABA.

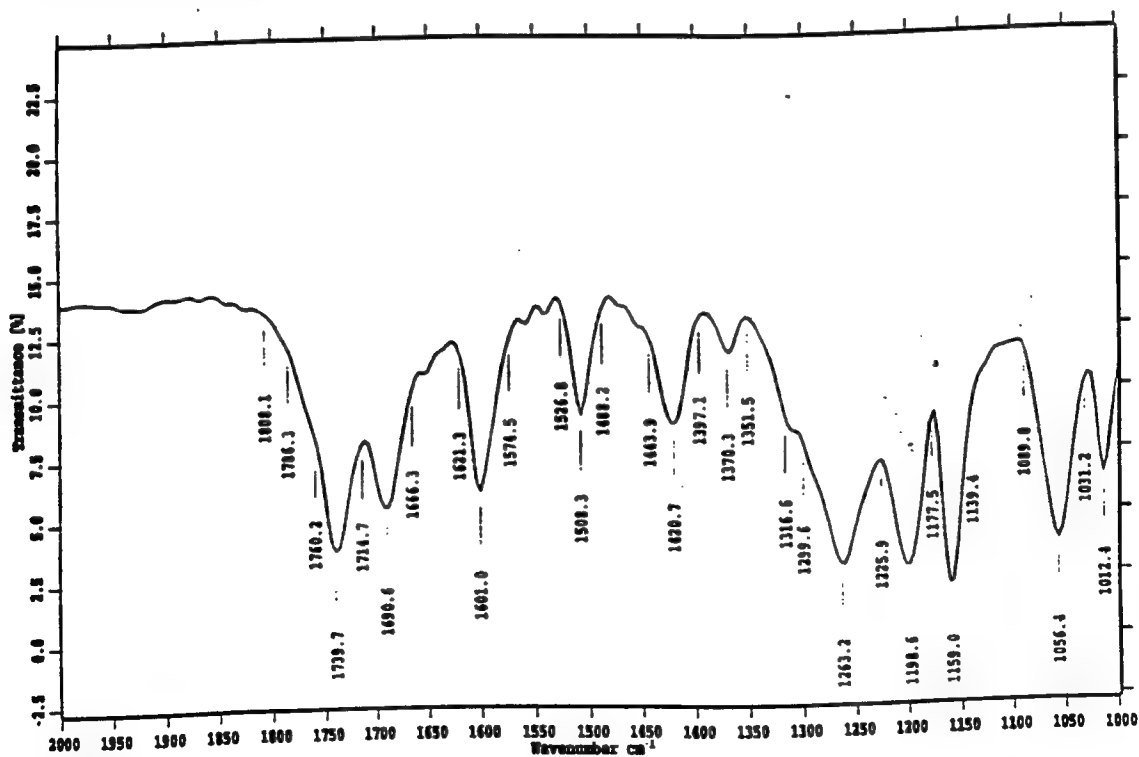


FIGURE 8
IR scan of Montmorillonite/ABA annealed at 200°C for 18 hours.

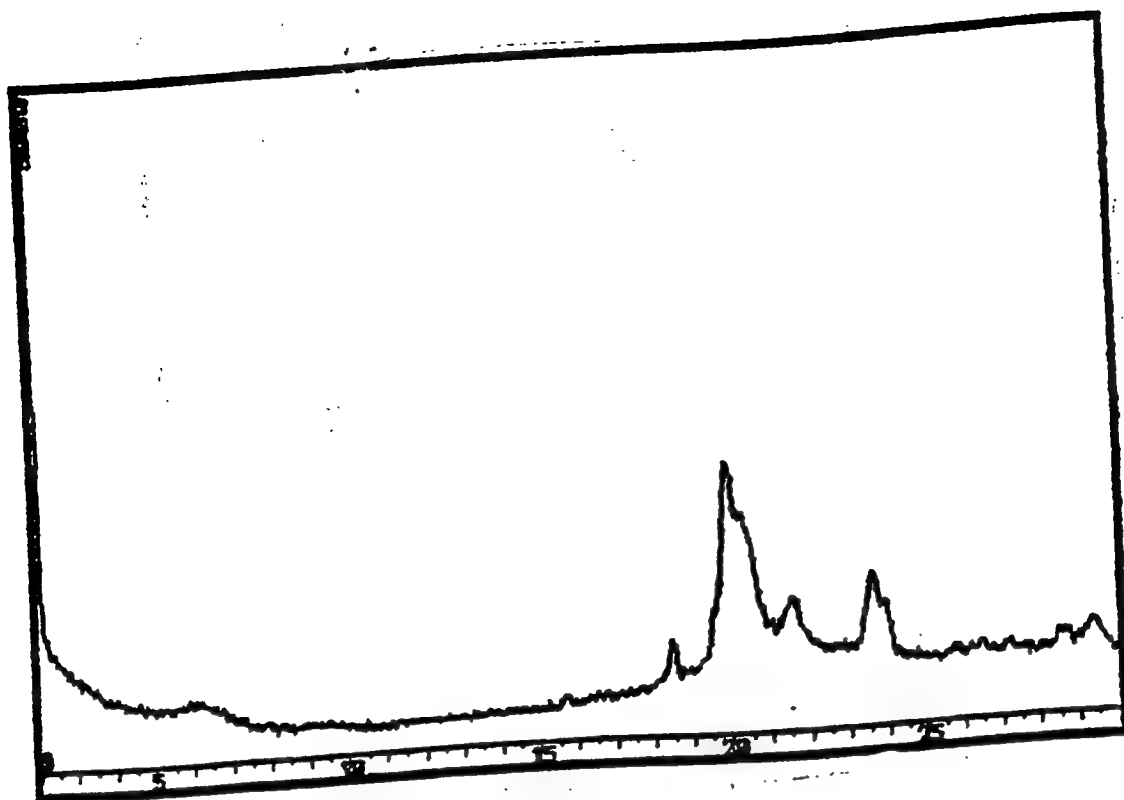


FIGURE 9
XRD scan of Montmorillonite/ABA annealed at 200°C for 18 hours.

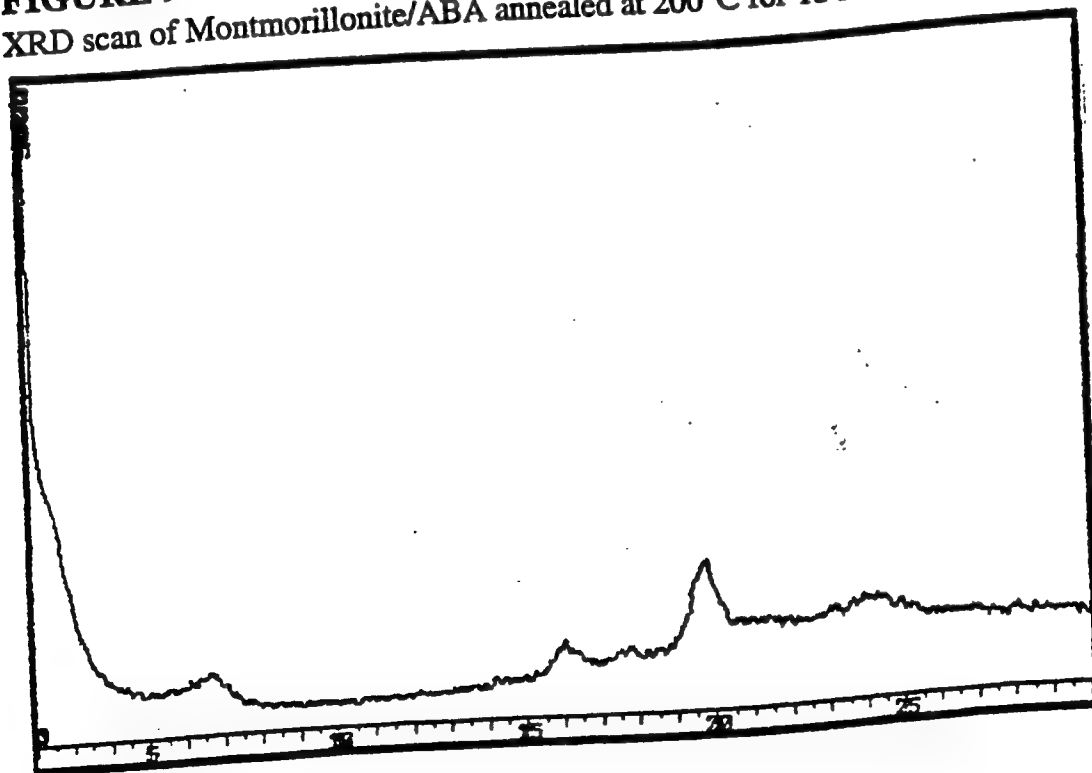


FIGURE 10
XRD scan of Montmorillonite/ABA annealed at 400°C.

**A STUDY OF THE EFFECTS OF VARYING PULSE WIDTH AND DUTY CYCLE ON
POLYMER DISPERSED LIQUID CRYSTAL HOLOGRAPHIC GRATINGS**

Crystal J. Bhagat

**Dayton Christian High School
325 Homewood Avenue
Dayton, OH 45405**

**Final Report for:
High School Apprentice Program
Wright Laboratories, Materials Directorate**

**Sponsored by:
Air Force Office of Scientific Research
Bolling Air Force Base, DC**

and

Wright Laboratory

August 1997

A STUDY OF THE EFFECTS OF VARYING PULSE WIDTH AND DUTY CYCLE ON POLYMER DISPERSED LIQUID CRYSTAL HOLOGRAPHIC GRATINGS

Crystal J. Bhagat
Dayton Christian High School

Abstract

The focus of this investigation was to study the effect of varying pulse width and duty cycle on polymer dispersed liquid crystal (PDLC) holographic gratings. This included four duty cycles of 10%, 25%, 50%, and 75%. The pulse widths used were 10 ms and 100 ms. The energy remained constant while the *rate* of energy deposited into the PDLC film varied. Four chopper wheels representing the duty cycles were built, PDLC syrups were formed, and grating samples with correlating duty cycle and pulse width constructed. The gratings were then written with a 514 nm laser and characterized under a 633 HeNe laser at p polarization. Switching voltage was also conducted on the ITO samples. Results from characterizing showed no trend or pattern with diffraction efficiency. A pattern was seen however with the switching voltage showing lower switching voltages for higher duty cycles. Experiments were also conducted with a pulsed nanosecond laser setup to observe the effect of nanosecond laser pulses on a grating formation. Gratings were written and samples characterized at p and s polarizations. Results showed a near linear dependence between total energy and diffraction efficiency.

A STUDY OF THE EFFECTS OF VARYING PULSE WIDTH AND DUTY CYCLE ON POLYMER DISPERSED LIQUID CRYSTAL HOLOGRAPHIC GRATINGS

Crystal J. Bhagat

Introduction & Background

Polymer dispersed liquid crystal conditions have recently been the focus of preparing Bragg gratings used in the area of holography. A hologram is a type of 3D photograph with a visible parallax. It is an exact recording of the light waves from an object. A polymer dispersed liquid crystal (PDLC) based plate records an interference pattern made by a reference beam and an object beam. The effects of two main constituents were studied in this report. They consist of varying pulse width and duty cycle. Their influence on a PDLC syrup was the core of this investigation.

By varying the duty cycle and pulse width we can vary the *rate* of energy being deposited into the PDLC film while the energy itself remains constant. In order to have these two variables we must look at some formulas in order to determine the settings of the exposure times and frequencies.

D.C. = Duty Cycle = .75, .50, .25, .10

T = total time

T_{on} = pulse width = 10 ms, 100ms

N = # of pulses

T_{off} = time between pulses

E = energy

$T_{on} + T_{off}$ = period

E_{cw} = E pulsed

$E = [P(\text{power of laser})][T(\text{total time})]$

$E_{cw} = (P)(T_{on})(N)$

$T_{off} = (T_{on} / \text{D.C.}) - T_{on}$

$N = [E_{cw} / (P)(T_{on})] = (T / T_{on})$

$T_{total} = (T_{on} + T_{off})N$

T_{off}

D.C.	10 ms	100 ms
75%	3.33	33.33
50%	10.0	100.0
25%	30.0	300.0
10%	90.0	900.0

T_{on}	N
100 ms	1800
10 ms	18000

The number of pulses is too much for the laser shutter. The shutter cannot handle this heavy usage and therefore we need to construct chopper wheels for the laser beam to be able to pulse through this many times. A diagram of these wheels can be seen in the *Methodology* section.

A pindiode detects the light. Since it has a fast response time the shape of the light pulse can actually be traced out on the oscilloscope. We set the oscilloscope at the corresponding frequencies in order to get the desired pulse width of 10 ms or 100 ms.

D.C.	10 ms	100 ms
.75	75 Hz	7.5 Hz
.50	50 Hz	5.0 Hz
.25	25 Hz	2.5 Hz
.10	10 Hz	1.0 Hz

Total Exposure Times of D.C. and Correlating Pulse Width

D.C.	10 ms	100 ms
.75	4.0 min.	4.0 min.
.50	6.0 min.	6.0 min.
.25	12.0 min.	12.0 min.
.10	30.0 min.	30.0 min.

For example, in order to get a sample with a 75% D.C. at 100 ms pulse width we put in the 75% chopper wheel in the grating writing setup with the 514 nm laser and set the oscilloscope at 7.5 Hz to reach a 100 ms pulse width.

In the grating spacing (microns) of a sample, a liquid crystal substance resides in the region of deconstructive interference (dark channels), and dense polymer lies in the region of constructive interference (light channels). The morphology of a grating is related to the sample's performance. This is mainly described as the diffraction efficiency and transmission power observed when a laser beam is focused through the sample's grating. Diffraction efficiency is measured by the diffracted power divided by the calibrated factor, and the transmission is calculated by the transmitted power divided by the calibrated factor.

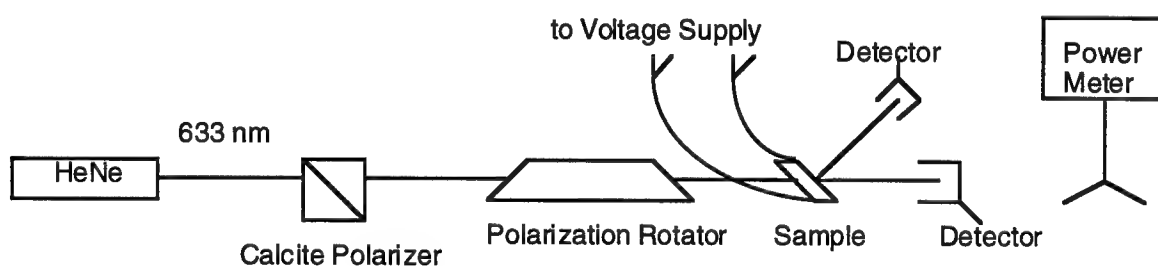
A PDLC syrup contains five main ingredients. The first one is the chain extender N-vinylpyrrolidone (NVP). NVP is a cross-linking monomer and reinforces the grating by assisting in strengthening bonds in the polymer. The next ingredient is the liquid crystal E7. Liquid crystals (LC) exist in a phase between the solid and liquid phases and reserve characteristics of both. They are needed in the syrup's recipe because of their chemical structure and mobile nature. These qualities allow the LC to easily form droplets and travel to regions of low light intensity where less rapid polymerization occurs. Octanoic acid is the surfactant. It is used in the syrup to make the E7 droplets smaller and therefore improving the quality with less scattering of light. Another component used is N-phenylglycine (NPG) which functions as a coinitiator. DPHPA works a another ingredient and stands for the monomer dipentaerythrol hydroxy penta acrylate. The last

constituent is the photo initiator dye, Rose Bengal (RB). Also known as bis(triethylammonium)salt, this dye is used for its display of a broad absorption spectrum. The chemical bond structures of these materials can be found later in this section.

PDLC films can be switched from an opaque (scattering) state to an optically clear state. This is accomplished by applying an electric field to the sample. This method is known as using “switching voltage” on a sample.

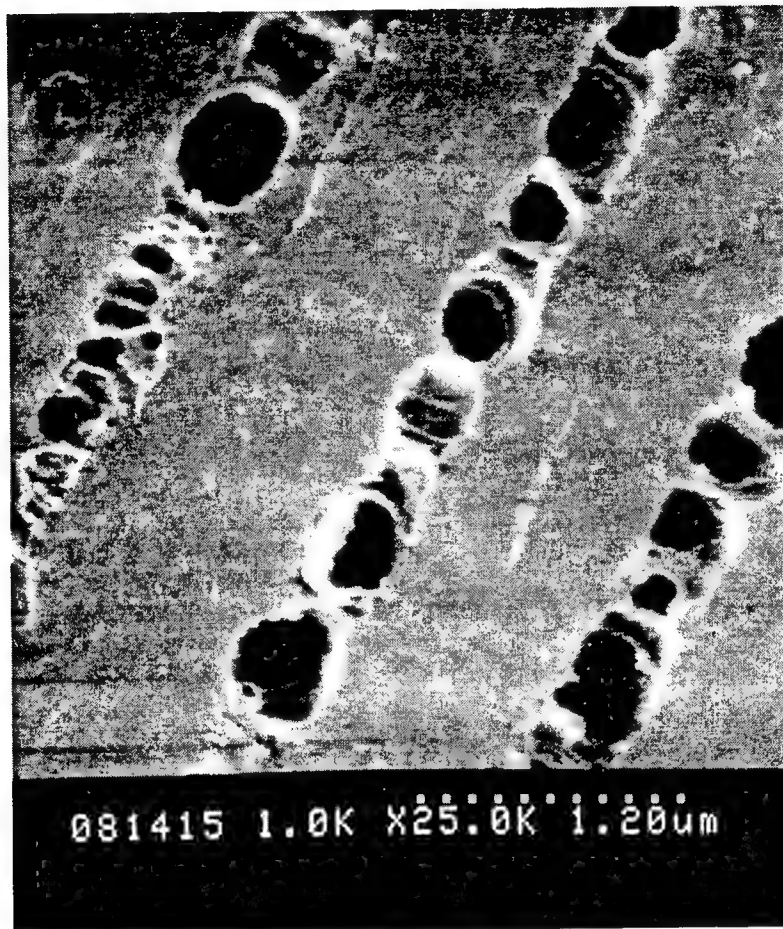
The scanning electron microscope (SEM) can be used to look at the morphology of a grating. The sample film must first be soaked in methanol overnight. This dissolves the liquid crystal. Later it is put in liquid nitrogen in order to fracture it. The sample piece can then be mounted and looked at through the microscope. The SEM works by sending an electron beam which scans the sample in a large chamber. A low voltage SEM shows the morphology of a grating as being made of periodic polymer dispersed liquid crystal planes. E7 microdroplets can be seen confined to the Bragg planes and having the size of about one-half the grating space. These droplets are observed as elongated and coalesced.

“Characterizing” is an essential method of recording diffraction efficiency and transmission as a function of voltage. It is defined as measuring optical properties of an optical material. A setup for characterizing samples looks as follows:



A helium neon laser (HeNe) with the wavelength of 633 nm is used as the coherent light source (unpolarized). Next is the calcite polarizer. This is used to separate horizontal and vertical polarization. The polarization rotator is then used to change the probe beam's polarization from horizontal to vertical. The sample comes next in line. It contains the PDLC holographic gratings. Silicon detectors connected to a power meter are then used to measure the power of the light

diffracted or transmitted. Alligator clips can be attached to the electrodes on the sample to conduct switching voltage. This characterization setup is the main one which we used for characterizing the PDLC holographic gratings.

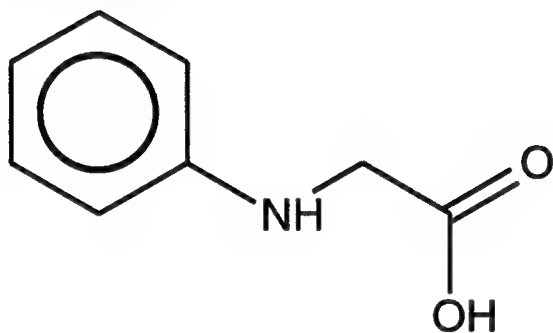


The picture above shows an in-plane view of a typical PDLC grating (SEM). The light channels are the regions of constructive interference where the dense polymer lies. The dark channels are the regions of deconstructive interference where the liquid crystal substance resided. A methanol soak dissolved the E7 which was then sucked out before the sample film was mounted on the SEM for further study.

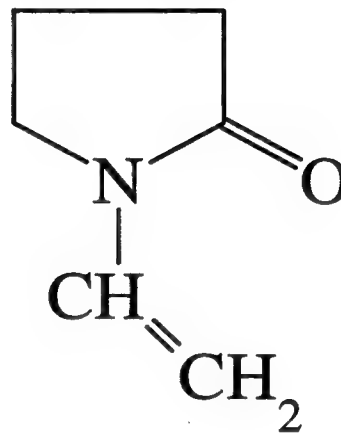
PDLC Syrup Ingredients (not including E7)

N-phenylglycine

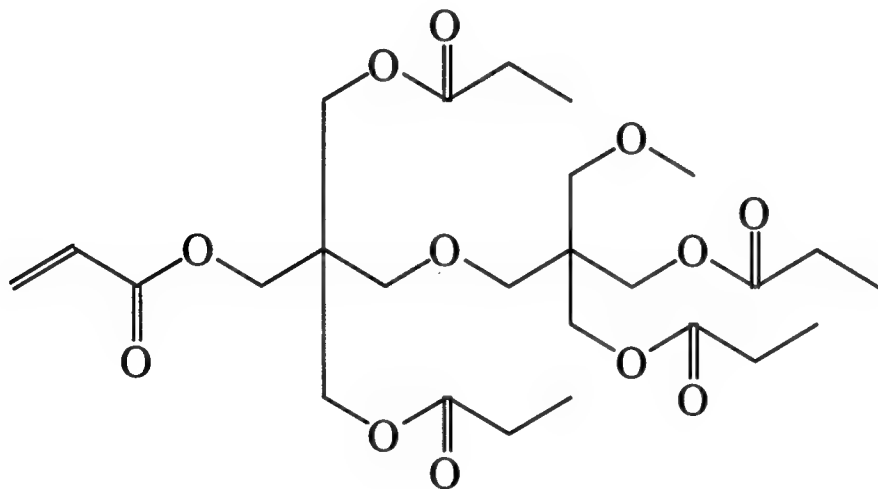
$C_8H_9NO_2$



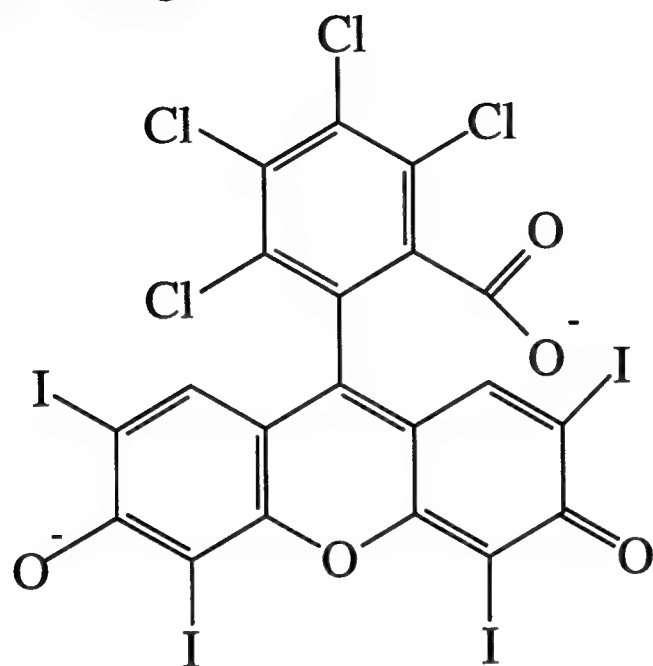
N-vinyl Pyrrolidone



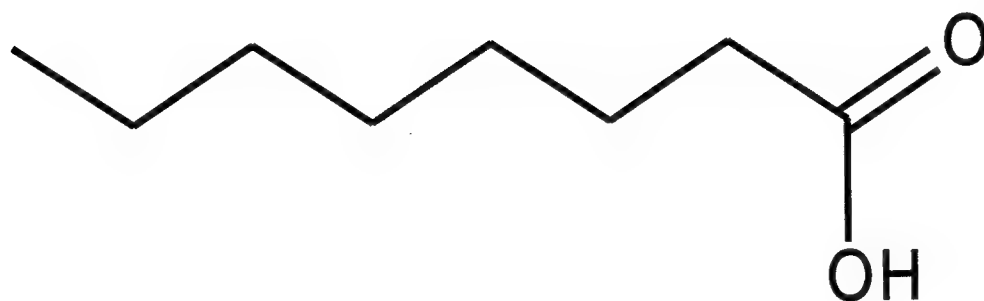
Dipentaerythrol Hydroxypenta Acrylate (DPHPA)



Rose Bengal

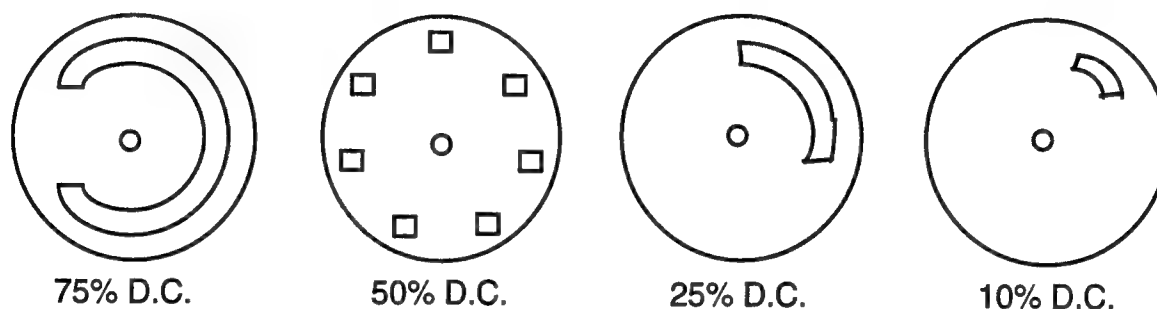


Octanoic Acid



Methodology

The first step was to construct the four chopper wheels representing the duty cycles of 10%, 25%, 50%, and 75%. The wheels were drawn and cut out of strong cardboard. Aluminum foil was then attached with glue over each wheel to reflect the laser light. Otherwise the cardboard would catch on fire from the laser. Actual size was 4.75 inches in diameter for each wheel.



A PDLC syrup with an octanoic acid surfactant was formed with the following recipe.

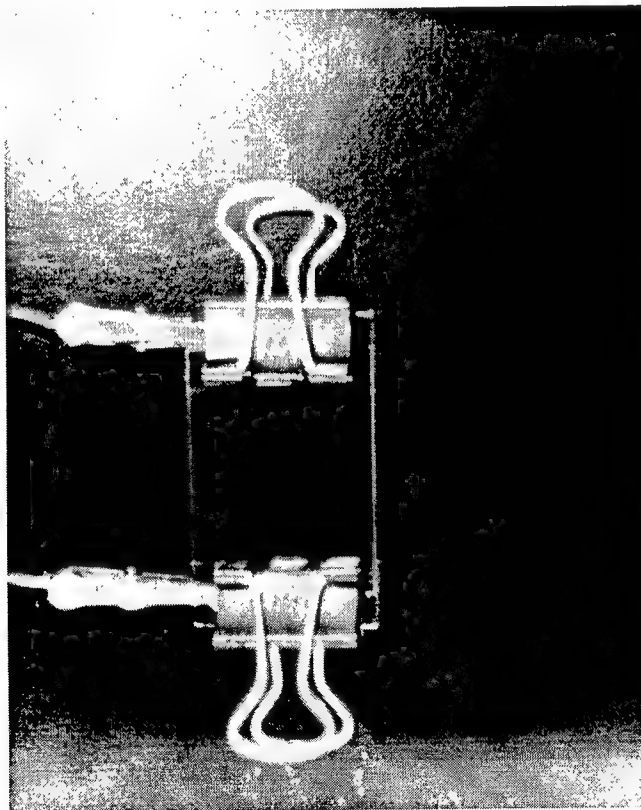
	WEIGHT (g)	% AMOUNT
1) NVP -	0.2	10%
2) E7 -	0.7	35%
3) OA -	0.13	6.5%
4) NPG -	0.045	2.25%
5) DPHPA -	0.92	46%
6) RB -	0.005	.25%
	2.0 grams	

The syrup was then sonicated to ensure a well mixture. It was contained in a glass vile and wrapped with aluminum foil because of the photo sensitive rose bengal dye. Samples were constructed using glass and ITO (Indium Tin Oxide) slides. Spacers 15 μm thick and a circular drop of the syrup were put in between the slides. OD filters were then placed on the sample using refractive index liquid. The sample was mounted and exposed to a bright green laser at 514 nm for

whatever the corresponding exposure time was for that sample. The laser power used was 1 mW/cm² per beam. Three syrups were used for making the samples due to early polymerization of the syrup.

After the grating was written the sample was taken out, OD filters removed, and then put under an incandescent lamp to postcure. The preparing, mixing, and transferring of syrup onto the slides and the actual writing of the sample were all done in the dark with a dim red light due to the photosensitivity of the syrup. Two glass and one ITO sample were made for each of the different conditions and the same procedures were followed as before.

Constructed sample



The next step was to measure the diffraction efficiency and transmission of all the samples. The characterization setup diagram displayed in the *Introduction & Background* section of this report was used in the process using a helium neon laser at 633nm. The formulas used were:

Calibration Data:

Transmitted # - x

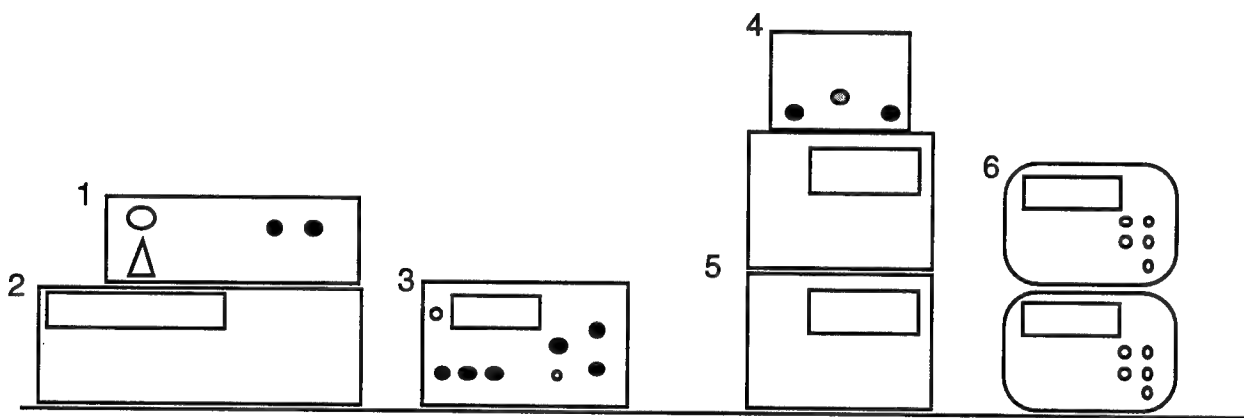
Incident # - y

DIFFRACTION EFFICIENCY = $[(\text{diffracted \# of sample})y]/[(\text{incident \# of sample})x]$

TRANSMISSION = $[(\text{transmitted \# of sample})y]/[(\text{incident \# of sample})x]$

The grating samples were characterized in *p* polarization. Switching voltage data was also collected on several samples. This was done on the ITO samples by attaching electrode clips to the edges of the sample. The clips were then connected to a voltage supply. This applied an electric field to the sample which caused the PDLC films to switch from an opaque state to an optically clear state. Switching voltage was conducted in the characterization setup (*Intro. & Bg.*).

Instruments involved were as follows:



- 1) The *amplifier* reaching up to 400 volts
- 2) The *HEWLETT PACKARD 325A UNIVERSAL SOURCE* is a *function generator* which produced a square wave voltage plus a programmable amplitude.
- 3) The *HMS Light Beam Chopper 220* was the frequency control. It controlled the speed of the chopper.
- 4) The *SYSTRON DONNER PULSE GENERATOR* is a *pulse generator* or *pulse conditioner* which conditioned the pulse from the chopper so the meter could recognize when to read the energy. It synched the energy meters with the light pulses.

5) The *Molelectron JD2000 Joulemeter Ratiometers* were *energy meters*.

6) The *KIETHLEY 195 SYSTEM DMM* was an *ammeter* used to measure current.

A good grating sample was defined as having high diffraction efficiency, low transmission, and a low switching voltage. Diffraction efficiency, transmission, and switching voltage were all recorded and the results made accordingly.

Experiments with the Nanosecond Pulsed Laser:

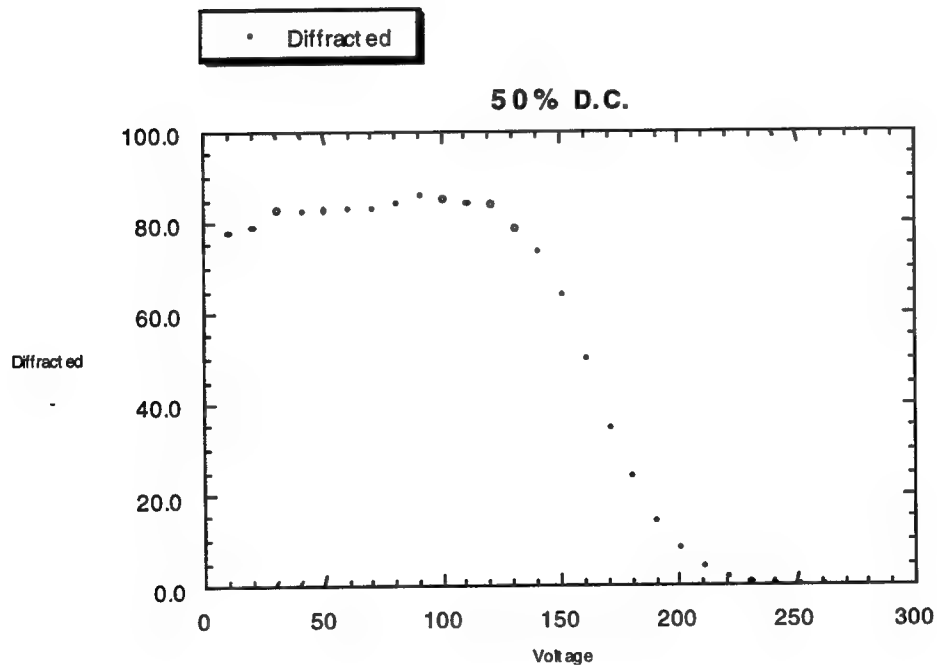
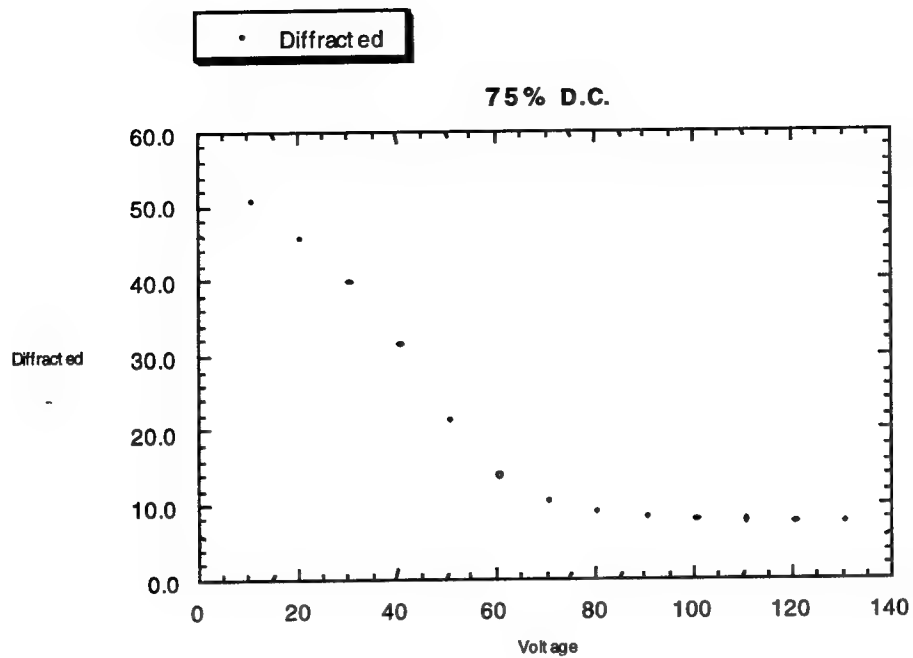
Experiments were also done using a nanosecond laser pulse from a Neodymium: YAG laser using a 532 nm output. One pulse width was 7.0 nanoseconds. The sample was exposed for 3.0 minutes and a 8.0 nanosecond pulse was used to write the holographic Bragg gratings. The beam was expanded and incident on the prism attached to the sample. Overlap of the beams occurred on the sample. Samples were constructed the same way as before with glass slides. The gratings were written and postcured for five minutes. They were later characterized in s and p polarizations with the HeNe laser at 633nm.

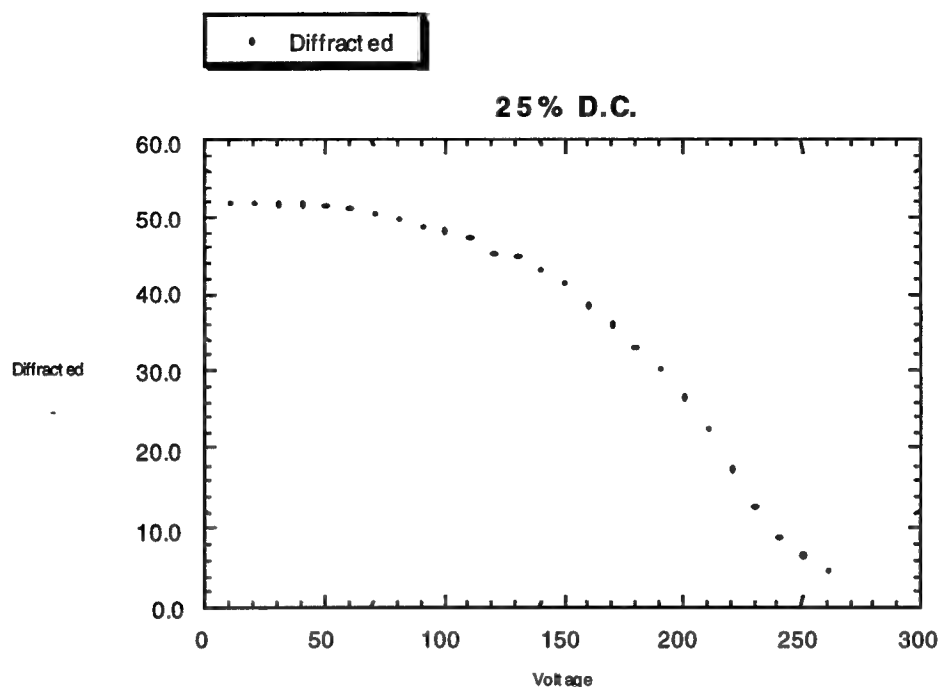
With experiments one and two the repetitions rates and other conditions were the same except for the laser pulse energy which was reduced ten times in the second experiment. With experiments three and four we varied the repetition rate. Experiment five had a ten minute exposure time instead of three minutes. A table in the results section show the conditions of each experiment as well as characterization results.

Results & Conclusions

Results from characterizing the samples of varying duty cycle and pulse width showed no trend or pattern when comparing diffraction efficiencies. We did however see something when conducting switching voltage. Not all the samples switched, but of those that did show a switching voltage a pattern was observed. From the following table and graphs we see that a higher duty cycle resulted in a lower switching voltage compared to a lower duty cycle which resulted in a higher switching voltage. The 10% duty cycle was not included in the graphs due to no consistency of switching between those samples.

Duty Cycle (D.C.)	Diffraction Efficiency	Onset of Switching	<i>Maximum Switching</i>	Voltage/ μm
75%	60%	1.0 V	80.0 V	5.33 V
50%	85%	120.0 V	225.0 V	15.0 V
25%	52%	50.0 V	260.0 V	17.33 V



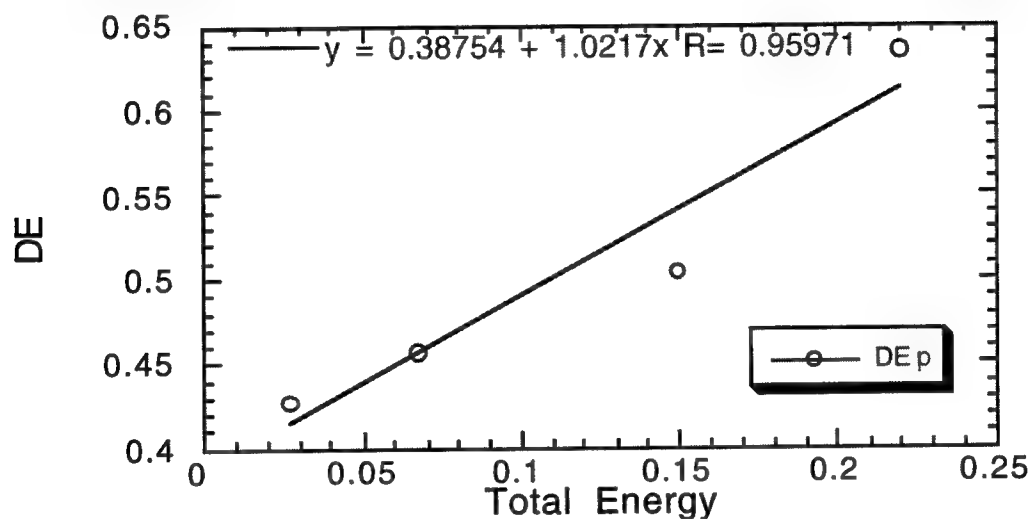


Results were also taken from the nanosecond laser pulse experiments. Experiments one and two had different energies with the second decreased ten times. We can see a drop in diffraction efficiency when looking at experiment two. Between experiments three and four we changed the rep. rate and did not see a big difference due to this. With experiment five we simply increased the exposure time to ten minutes rather than three and did not see much. Overall, the p polarization had a much higher diffraction efficiency and a lower transmission than the s polarization which had very high transmission and much lower diffraction efficiency. This tends to be typical between the p and s polarizations with the p giving us higher diffraction efficiency compared to the s. Results also showed us a near linear dependence between total pulse energy and diffraction efficiency (p) with diffraction efficiency increasing as total energy increased.

Experiment #	Rep. Rate	Pulse Energy ($\mu\text{J}/\text{cm}^2$)	Total Energy (J)	Diffraction Efficiency (p)	Diffraction Efficiency (s)	Transmis. (p)	Transmis. (s)
--------------	-----------	--	------------------	----------------------------	----------------------------	---------------	---------------

1	10 Hz	122.5	0.2208	.6356	.1301	.0458	.7350
2	10 Hz	14.96	0.02694	.4271	.1459	.4015	.8370
3	2 Hz	185.5	0.06678	.4575	.0974	.3347	.8642
4	5 Hz	165.8	0.14922	.5033	.1291	.0308	.7573
5	10 Hz	126.4	0.7584	.4271	.0996	.0174	.7125

Dependence of Diffraction Efficiency on Total Pulse Energy



Suggestions for Future Research

Further experimentation is suggested in testing the effects of varying duty cycle and pulse width on PDLC holographic gratings. The bad samples should be redone and a constant syrup should be used. Several more ITO samples could also be constructed, characterized, and conducted with switching voltage. Morphology should also be studied through the SEM. Concerning the nanosecond laser pulse holographic grating experiment, further experimentation with constant energy and varying repetition rate is suggested. Overall, a further study dealing with the two variables is recommended, one that will be thorough and given more time.

Acknowledgments

Special thanks to Vince Tondiglia, Dr. L. V. Natarajan, Bob Neal, and Dr. Richard Sutherland for all their guidance and support. I am also grateful to Wright Laboratories which made this experience for two summers possible.

References

- Aldrich Catalog Handbook of Fine Chemicals*. Milwaukee: Aldrich Chemical Company, Inc., 1994.
- Bhagat, Crystal. "A Study of the Effects of Varying Chain Length Surfactants on Polymer Dispersed Liquid Crystal Holographic Gratings." Report, Wright Labs: 1996.
- Caulfield, H. John. "The Wonder of Holography." *National Geographic* March 1984: 365-377.
- Green, Floyd J. The Sigma-Aldrich Handbook of Stains, Dyes, and Indicators. Milwaukee: Aldrich Chemical Company, Inc., 1990.
- R.L. Sutherland, L.V. Natarajan, V.P. Tondiglia, and T.J. Bunning, Chem. Mater. 5, 1533 (1993).
"Bragg Gratings in an Acrylate Polymer Consisting of Periodic Polymer-Dispersed Liquid-Crystal Planes."
- R.L. Sutherland, V.P. Tondiglia, L.V. Natarajan, T.J. Bunning, and W.W. Adams, Appl. Phys. Lett. 64, 1074 (1994). "Electrically Switchable Volume Gratings in Polymer-Dispersed Liquid Crystals."
- T.J. Bunning, L.V. Natarajan, V. Tondiglia, R.L. Sutherland, D.L. Veziat, and W.W. Adams, Polymer 36, 2699 (1995). "The morphology and performance of holographic transmission gratings recorded in polymer dispersed liquid crystals."
- V.P. Tondiglia, L.V. Natarajan, R.L. Sutherland, T.J. Bunning, and W.W. Adams, Opt. Lett. 20, 1325 (1995). "Volume holographic image storage and electro-optical readout in a polymer-dispersed liquid-crystal film."

**SURFACE STRUCTURE AND OPTICAL PROPERTIES OF A SENSITIVE
SNAKE INFRARED DETECTOR**

Margaret A. Burns

**Dixie High School
300 South Fuls Road
New Lebanon, OH 45345**

**Final Report for;
High School Apprentice Program
Wright Laboratory**

**Sponsored by:
Air Force Office of Scientific Research
Bolling Air Force Base, Washington, DC**

And

Wright Laboratory

August 1997

SURFACE STRUCTURE AND OPTICAL PROPERTIES OF A SENSITIVE SNAKE INFRARED DETECTOR

Margaret A. Bruns

Abstract

Snakes of the families Boidae and Crotalidae possess highly sensitive image-forming IR sensors used for prey detection. These natural IR sensors have several distinct advantages over artificial IR imaging systems: (1) they have the highest sensitivity known, (2) they are microscopic, (3) they do not require cooling for sensitive operation, and (4) they repair themselves. Using scanning electron microscopy and atomic force microscopy, we found that the tissue overlying the snake infrared receptor terminals has an unusual structure. This surface consists of a series of parallel plates, each of which is covered by an array of "micropits." We tested whether this surface structure may play a role in letting IR radiation through the skin by performing infrared spectroscopy on samples of tissue from the infrared-sensitive organ and from elsewhere on the snake's body. We found that the degree of pigmentation has essentially no effect on infrared transmission through the skin over the spectral range of 2-25 μ m. More importantly, neither pit nor eye tissue show any significant difference from body skin in infrared transmission. However, we found that the outer epidermis effectively transmits wavelengths from about 3-5 μ m and 8-12 μ m. We tested isolated intact pit organs for infrared transmission and reflection, and found that they have very low infrared reflectivity and are highly absorptive over the range of 2-15 μ m. These results show that the tissue overlying infrared-sensitive nerve terminals is transmissive and absorptive at both 3-5 μ m and 8-12 μ m, both atmospheric transmission windows. One of these bands, 8-12 μ m, includes the maximal emission, 10 μ m, of the snakes.

The facts that this surface structure is unique to the infrared-sensing organ and similar to that of the eye, but distinct from that elsewhere on the snake's body, suggest that it may play a role in spectral filtering. Therefore, the goals of this project are to determine the surface structure of the pit organ and the optical properties that this surface imparts to the infrared-sensitive pit.

SURFACE STRUCTURE AND OPTICAL PROPERTIES OF A SENSITIVE SNAKE INFRARED DETECTOR

Margaret Bruns

Introduction

Overview Of (IR)-Sensing Technology:

Infrared energy is electromagnetic radiation, the wavelength of which is longer than that in the red portion of the visible spectrum; the infrared portion of the electromagnetic spectrum lies between about 700nm and 25 μ m. There are currently four different types of thermal detectors used in infrared-sensing technology:

1. **microbolometer:** Infrared energy-induced temperature changes in a bolometer cause changes in electrical resistance. In one type of bolometer, two detectors are used. A window to one of the two detectors allows IR radiation to change resistance in that detector only. The difference in resistance between the two detectors results in detectable current flow in the system.
2. **thermocouples and thermopiles:** These devices contain two dissimilar materials which, when heated, produce a voltage across two open leads. When more than one thermocouples is combined in a single element it is called a thermopile.
3. **thermopneumatics:** In this device, a gas-filled chamber has an IR-transparent window. Incident IR radiation causes the gas to expand, producing a deflection in a deformable membrane attached to the chamber. This deflection is measured using an optical system consisting of a light source aimed at the deformable membrane, and a light sensor.
4. **pyroelectrics:** Pyroelectric devices are based upon materials which, when heated, generate a detectable electric charge.

Artificial IR sensors may also be built upon photon detectors, in which absorption of incident IR photons produces free charge carriers that in turn change the electrical properties of a responsive element. Photon detectors operate without detectable changes in temperature of the sensing material. There are four photic processes currently used:

1. **photoconductivity:** Photoconductive elements produce free charge carriers upon absorption of IR photons. These charge carriers cause measurable changes in the conductivity, and hence, the resistance of the responsive element.
2. **photovoltaic effect:** In this process a junction is formed in a semiconductor. Incident IR photons absorbed at or near this junction produce a measurable voltage, the magnitude of which is proportional to the number of absorbed photons.
3. **photoelectromagnetism:** Here, a semiconductor in a magnetic field absorbs incident IR photons. The magnetic field produces a separation of charge, resulting in a measurable voltage.

4. photoemissivity: In this process, all of a photon's energy is transferred to kinetic energy of an electron. Excited electrons escape from the surface and generate a current in an attached circuit.

Limitations of Artificial (IR)- Sensors:

The technology behind the artificial (IR)-sensing devices is highly advanced, but still has significant limitations. First, many modern IR-sensing devices are bulky and therefore difficult and costly to transport. They often require repairs or modification which increase cost and decrease usefulness. Finally, in order to work at maximal sensitivity, IR-sensing devices often require super-cooling, adding still more to their bulk, cost, and increasing the risk of failure.

Biological IR Detectors:

At least three different types of organisms use infrared detectors. Vampire bats appear to have infrared detectors located in the snout. These blood-drinking bats probably use their IR detectors to locate host blood vessels from which they can feed. Essentially, nothing is known about this IR-sensing system. Better understood is the IR detector in beetles of the genus *Melanophila*. Their IR detector system is located in patches on the ventral surface where the leg joins the body. A single detector consists of a receptor cell that terminates in a fine mechanoreceptive ending, and an onion-like shell of cells around this mechanoreceptor terminal. Incident infrared radiation causes heating of the onion-like shell, which in turn deforms the tip of the mechanoreceptor. This system is used following forest fires to sense the temperature of recently-burned trees which the beetles lay their eggs. Because of the short-range usage, and the anatomy of this system, it is almost certainly not an image-forming infrared detector. On the other hand, certain snakes possess very sensitive image-forming infrared detectors that are relatively well-understood.

Snake IR Detectors:

Boid snakes (family Boidae: boas and pythons) and pit vipers (family Crotalidae: rattlesnakes and their kin) locate prey and perhaps avoid predators and locate basking sites with a highly sensitive and directional array of infrared-receptive organs. Rattlesnakes and other pit vipers have one infrared sensory pit organ on each side of the face, located on the snout between the lateral eye and the nostril. In boas and pythons, the sensory pits are located on the edges of the upper and lower jaws. Unlike pit vipers, boid snakes often have an array of many pits on both upper and lower jaws. Each pit in boid snakes is an indentation

in or between scales, and infrared receptors are located just under the surface of the skin at the bottom of the pit. The pit organ of pit vipers consists of a depression between facial scales. Within this depression lies a suspended membrane that is inside by IR-sensitive nerve fibers. In both types of snakes, infrared radiation is converted into a signal which is then relayed to the brain, where infrared information merges with visible light information coming from the eyes. Thus, snakes "see" the world using both reflected visible light and emitted infrared energy. (See figure 1)

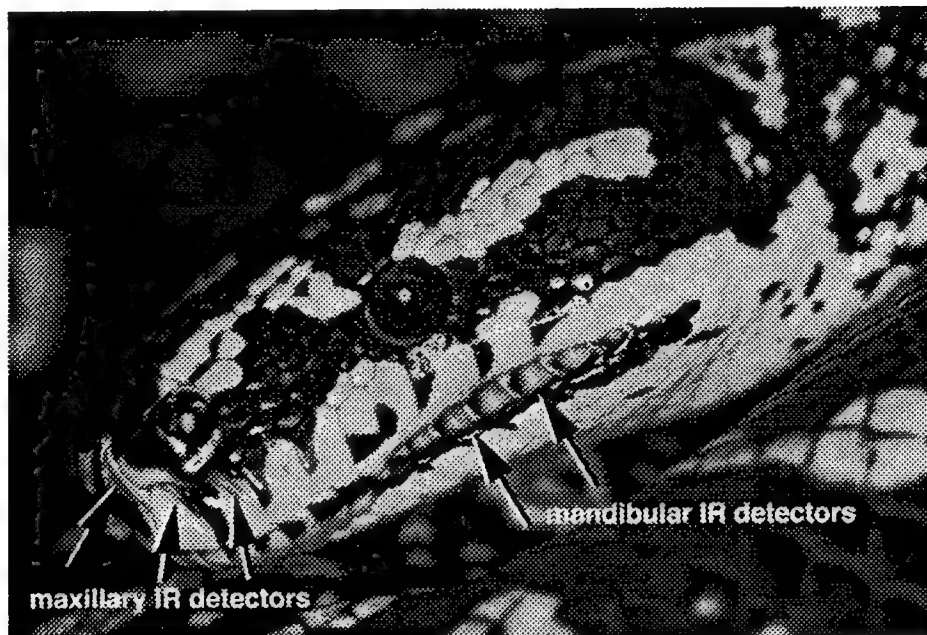


Fig 1:

Why are snake IR detectors better than artificial ones?:

The biological infrared sensors used by boid and crotalid snakes have several distinct advantages over artificial infrared imaging systems. First, they have the highest sensitivity known; experiments on pit vipers indicate that their infrared-sensitive pit organs can detect temperature changes as small as 0.003°C . Second, the receptive units of the pit organ are microscopic. A single pit organ contains thousands of infrared-sensitive nerve terminals, each of which may be only $10\mu\text{m}$ in diameter. Third, snake infrared detectors operate at normal ambient temperatures. That is, they do not require cooling for sensitive operation. Finally, like all biological tissues, they have the capacity of self-repair.

Despite our detailed knowledge of the gross structure of IR-sensing pits and the neural pathway by which infrared information reaches the brain, we know essentially nothing about the spectral sensitivity and biochemistry of snake infrared receptors. We do not know, for example, whether the snake pit IR sensor is responsive over a broad range of

electromagnetic radiation, or whether it is "tuned" to a certain range of wavelengths. Since the infrared-sensitive nerve terminals underlie the outer layer of skin, it is possible that this epidermal layer acts as a spectral filter or perhaps as an antireflective coating. Therefore, the goals of this project were to determine the surface structure of the pit organ and the optical properties that this surface structure imparts to the infrared-sensitive pit.

Methodology:

Scanning Electron Microscopy (SEM):

Samples of living tissues (IR-sensing pit, and dorsal skin) were fixed in a mixture of 2% paraformaldehyde and 2% glutaraldehyde in 0.1M phosphate buffer. Samples were then rinsed in 0.1M phosphate buffer, dehydrated through increasing concentrations of ethanol, and critical point dried in hexamethyldisilazine (HMDS). These samples and samples of shed skins (from IR-sensing pit, dorsal skin, and ocular spectacle) were prepared for scanning electron microscopy by mounting on zinc specimen holders. Electron microscopy was performed by Dr. Tim Bunning of the Materials Directorate, Wright-Patterson AFB, and by Don Church of the University of Virginia.

Atomic Force Microscopy (AFM):

Samples of shed snake skin were mounted onto metallic disks with either cyanoacrylate glue or with adhesive designed for AFM sample preparation. After initial trials, cyanoacrylate glue was the usual method, since AFM adhesive allowed significant motion in samples while collecting AFM images. Samples were imaged in tapping mode or contact mode, both of which produced detailed 3-dimensional images of surface structure. AFM operation was performed by Dr. Angela Campbell of Materials Directorate, Wright-Patterson AFB, and by John Hazel of Western Michigan University.

Infrared Spectrometry :

Shed snake skins from a boa constrictor, ball python, carpet python, rainbow boa, and grey-banded kingsnake were flattened and dried. Areas of interest were removed with scissors and placed in a homemade cardboard mount, which was then placed in a specimen holder.

The infrared spectrum of each sample was measured twenty times in a infrared spectrometer (Perkin-Elmer FTIR 1725x); these measurements were then averaged to produce the final data. Infrared transmission was measured over the range of 5000 to 400

wave numbers (2.0 μm to 25 μm wavelength). All measurements were performed after a 5-minute equilibration time to allow complete purge of the sample chamber atmosphere with dry nitrogen. An initial back ground check was run and stored in computer memory each day.

Python regius pits were isolated intact. Snakes were deeply anesthetized around the stomach area by injection of 100mg ketamine HCl per kg body weight. Pits from the maxilla (upper jaw) were isolated under a dissecting microscope, and stored briefly in a humidified petri dish. Clusters of 5 pits were then mounted onto either aluminum foil or Krylon black-painted cardboard, covered with Glad brand plastic wrap, and subjected to direct hemispheric reflectance infrared spectrometry (DHR) over the wavelength range of 2-15 μm .

Samples tested:

1. *Boa constrictor* maxillary (upper jaw) shed skin, non-pigmented
2. *Boa constrictor* maxillary shed skin, pigmented
3. *Boa constrictor* mandibular (lower jaw) shed skin, non-pigmented
4. *Boa constrictor* mandibular shed skin, scales only
5. *Boa constrictor* mandibular shed skin, interscale skin only
6. *Boa constrictor* spectacle (skin shield covering eye)
7. *Python regius* dorsal pigmented shed skin
8. *Python regius* ventral non-pigmented shed skin
9. *Morelia spilotes* dorsal pigmented shed skin
10. *Morelia spilotes* ventral non-pigmented shed skin
11. *Morelia spilotes* shed skin from labial scale containing pits
12. *Epicrates cenchria* dorsal non-pigmented shed skin
13. *Epicrates cenchria* ventral non-pigmented shed skin
14. *Lampropeltis alterna* dorsal pigmented shed skin
15. *Lampropeltis alterna* ventral non-pigmented shed skin
16. *Python regius* dorsal skin
17. *Python regius* ventral skin
18. *Python regius* isolated intact pit

Results:

Scanning Electron Microscopy:

SEM of the surfaces of isolated infrared-sensitive pits from *Python regius* revealed a series of very long parallel plate-like structures with a width of 2-3 μm . These plates were joined at the long edges. The surface of each of the plates was covered by a regular array of "micropits" of less than 0.5 μm diameter. Similarly, the spectacle overlying the eye was made up of a parallel array of plates, each covered by micropits. Here, though, the width of the plates and the diameter of the micropits are both less than in the pit organ. In addition, micropits on the spectacle appear less regular in arrangement than those in the pit organ.

The microstructure of the pit organ and spectacle are markedly different that of skin elsewhere on the snake's body. Python skin, for example, is covered by parallel rows of short parallel ridges. Boa skin is similar, covered by long parallel strands of material.

All of the results from the scanning electron microscopy were very similar to those from the atomic force microscopy studies (see below).

Atomic Force Microscopy:

AFM images of snake samples revealed structure essentially identical to that seen by SEM. IR-sensing pit samples exhibited an array of surface plates each covered with an array of micropits. The spectacle was also covered by plates containing micropits, but the plates on the spectacle were longer and more narrow than those from the pit, and the micropits were smaller in both diameter and depth than those from the pit. (See figures 3&4).

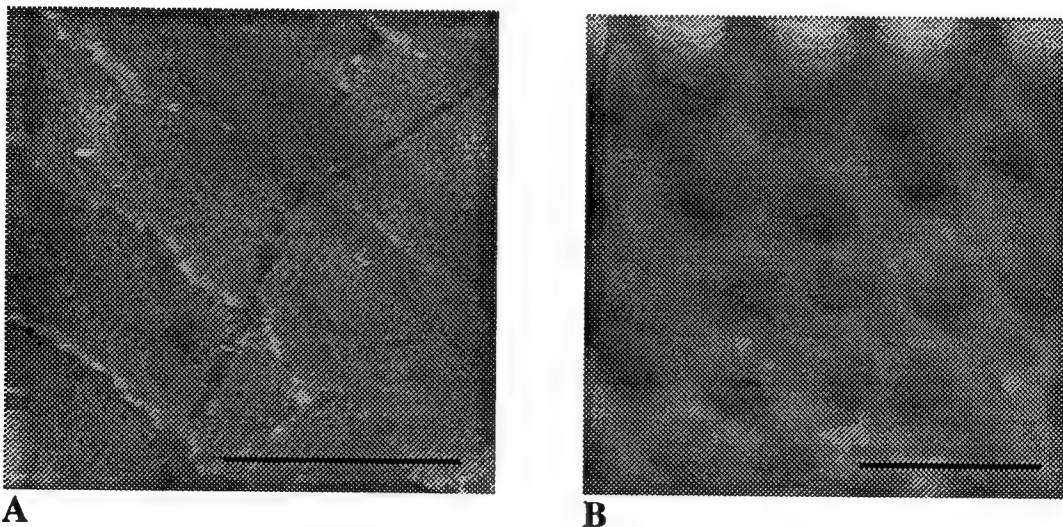


Fig.3: Atomic force micrographs of *Boa* labial scale material. Even though it does not contain the pit structure, IR receptors are located under the skin surface of labial scales. **A:** low power micrograph of labial scale structure. Note the large plate-like formations. The diagonal line is a scratch on the surface of the sample. Scale bar = 10 μ m. **B:** High power micrograph showing the micropits that cover the surface of each plate-like structure. Scale bar = 1 μ m.

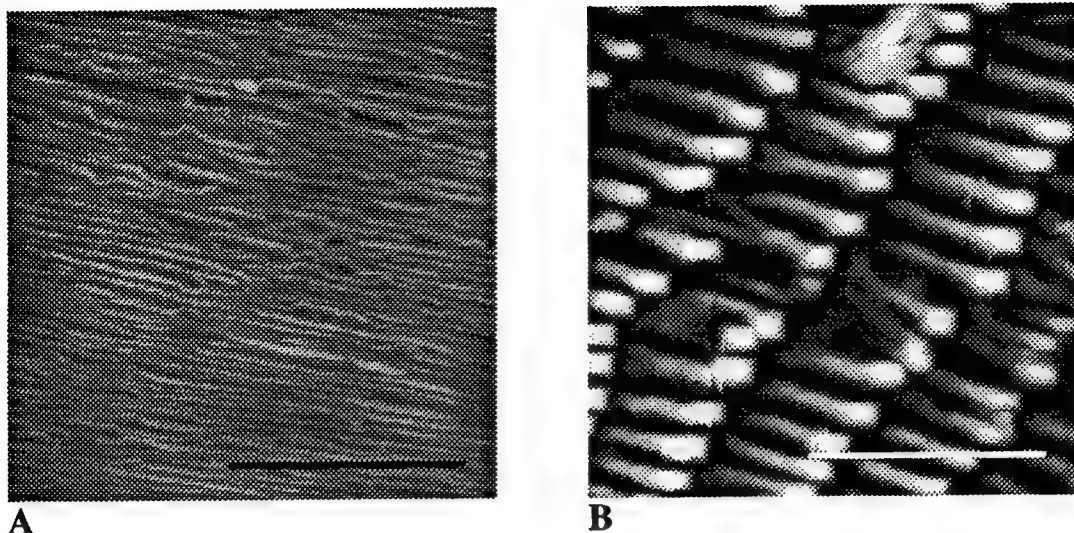


Fig.4: Atomic force micrograph of scale material isolated from regions outside infrared-sensitive pit organs or scales. **A:** *Boa* scale material from the top of the head. Non-labial scales are covered by a parallel arrangement of very long strands. Note the lack of plate-like structures and micropits. Scale bar = 10 μ m. **B:** Scale surface of the Australian carpet python *Morelia spilotes variegata*. Note the lack of micropits and the presence of parallel arrays of short ridges or cylinders. Scale bar = 5 μ m.

Infrared Spectrometry:

The outer layer of the epidermis overlies the infrared receptors, so its optical properties must influence the spectral properties of incident radiation reaching the infrared receptor nerve terminals. Since this layer of skin is periodically shed intact from the snake, and since the structure of these shed epidermal layers faithfully represents the structure in the intact living animal, we investigated the optical properties of shed skin samples.

Since the structure of the outer surface of the shed skin is markedly different from that of the inner surface, we measured the infrared transmission of shed skins by placing the radiant source on the outer surface side or on the inner surface side of the skin. Results of these measurements were essentially identical with all skin samples tested.

Infrared-sensitive pits in some species of snakes (*Python molurus*, for example) contain large amounts of melanin pigment granules, while those in other species (*Python regius*, for example) apparently contain no melanin. We therefore measured the infrared transmission in samples of pigmented vs. non-pigmented skin. IR transmission spectra over the range of 2-25 μ m were again essentially identical. The only observed differences were in the range of 1-2 μ m. Magnification of this portion of the IR transmission spectrum shows that the two peaks (1.5 μ m) and one trough (1.7 μ m) observed in the sample may be present in the sample as well, but with much lower amplitude.

Once everything was set up, I ran boa constrictor skin scans eight different times. I took a look at the top of the jaw region maxilla and compared it to the the underside of the snake around the jaw region mandible. Then, I looked at pigmented vs. non pigmented, plus the inside which is dull vs. the outside of the skin which appears very shine .The last place I took a sample from was the scale vs. the interscale.

When skin came from the same area like the maxilla non-pigmented outside and the maxilla non-pigmented inside, they were quite similar. (See figure 4)

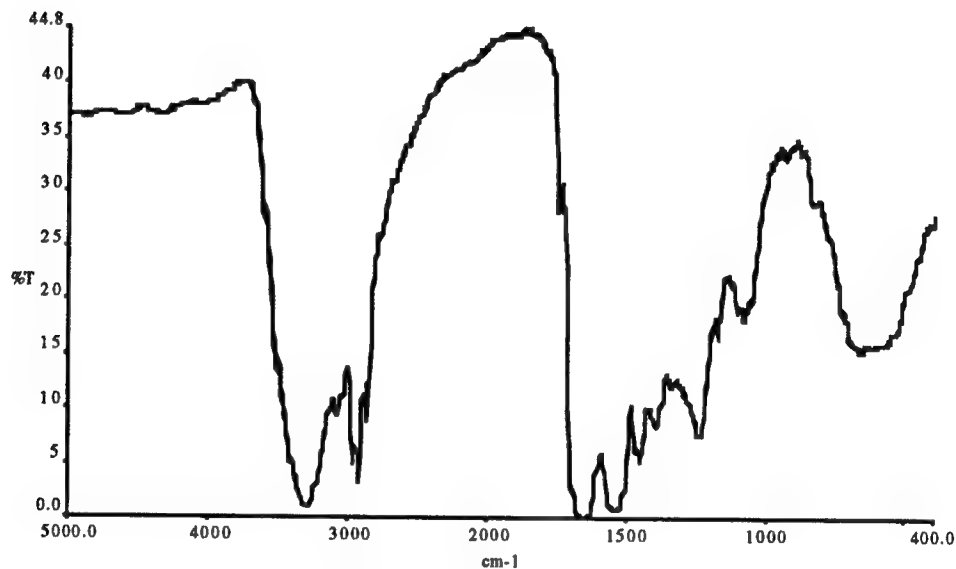


Fig. 4: Comparison of non-pigmented *Boa* epidermis from the maxilla with infrared source on outer side of sample vs. inner side of sample. (Note that their are two lines above however, they are extremely indential which makes it look like their is only one line.)

The results from the mandible non-pigmented outside vs. the mandible non-pigmented inside are similar figure 4.

The maxilla pigmented inside to and the maxilla pigmented outside are also similar. The only noticeable difference is in the height of the spectra. The difference in heights can be located between 1500 and 400 wavelength. (See figure 5)

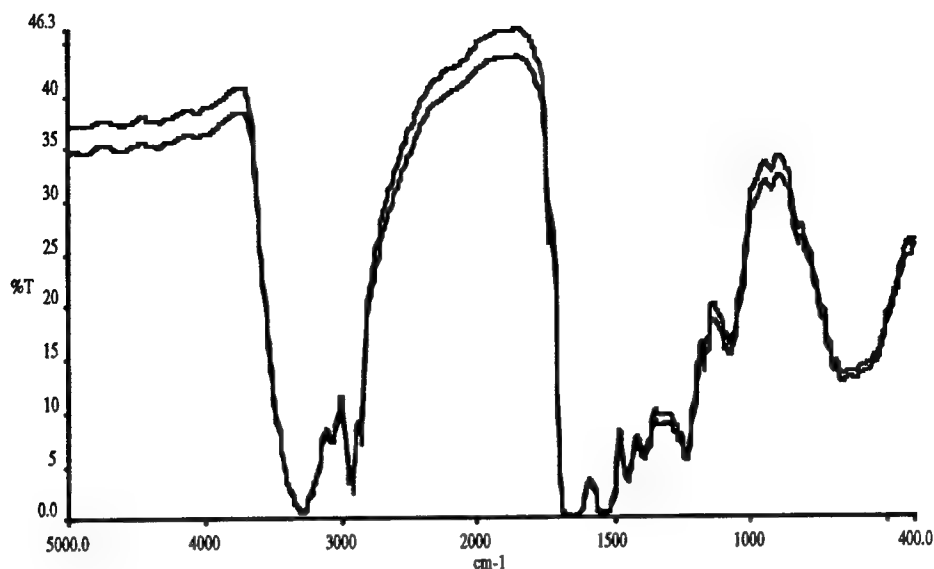


Fig. 5: Comparison of pigmented *Boa* epidermis from the maxilla with infrared source on outer side of sample vs. inner side of sample.

When comparing maxilla pigmented outside to maxilla non-pigmented outside there is little change in the readings. This might suggest pigment (melanin) interferes with the IR transmission to the receptors. The data obtained says this is not true. We thought that there might be one difference in the area of 1700 and 1600 wavelength. However, when we magnified that area it matched up to each other exactly. (See figure 6)

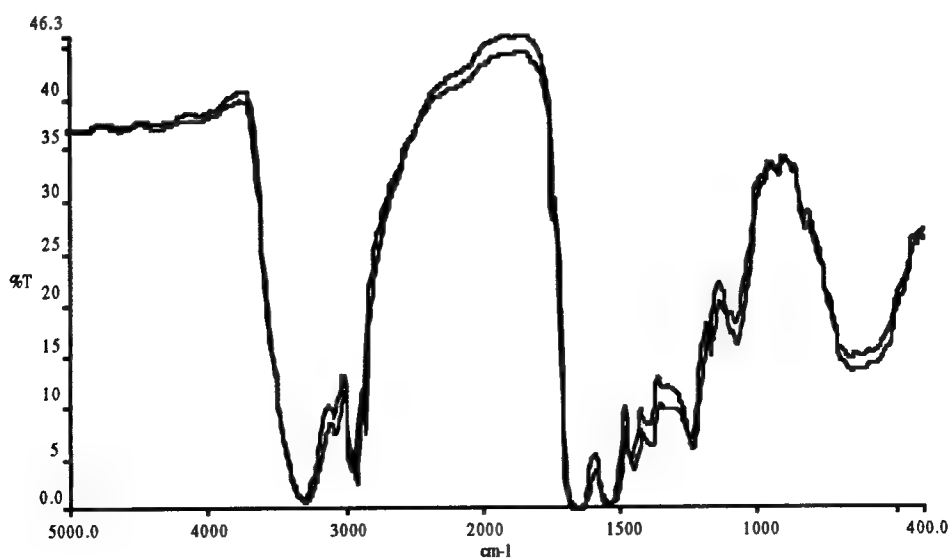


Fig. 6: Comparison of pigmented vs. non-pigmented *Boa* epidermis from the maxilla with infrared source on outer side of sample.

Because the structure of the interscale skin was found to be significantly different from the scale material, we measured the IR transmission spectra of whole skin vs. scales vs. interscales. We found that the scale and interscale are different in many areas of the spectra. The scale material seems to have a higher transmission and less reflectance or absorbency. The interscale has lower transmission and higher reflectance or absorbence. (See figure 7)

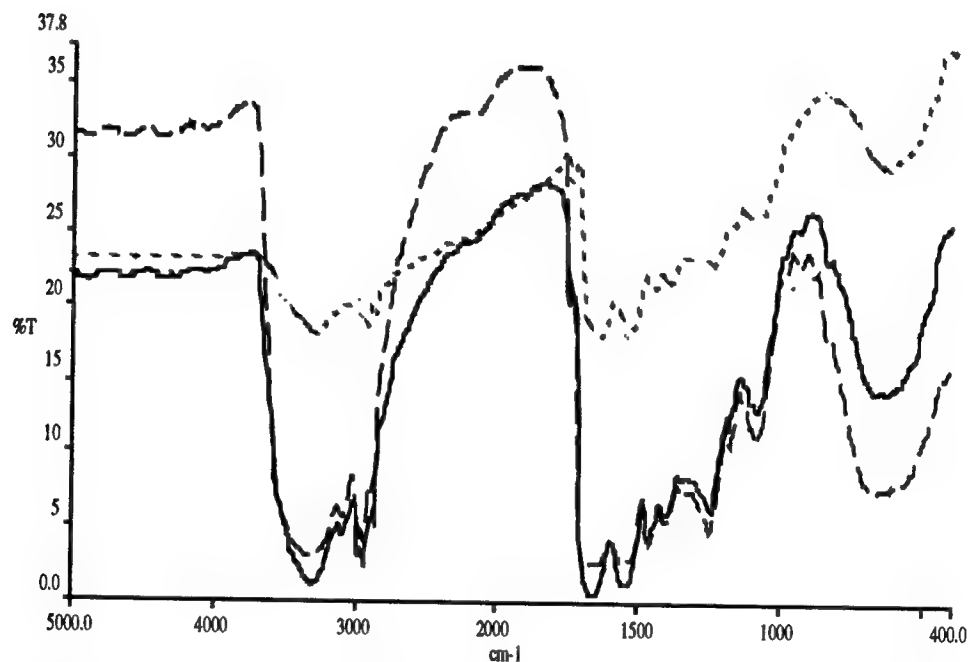


Fig. 7: Comparison of *Boa* mandibular non-pigmented whole skin sample (scale and interscale material, solid line) with scale material only (dashed line) and interscale skin material (dotted line).

The scale samples used to generate the previous data included some interscale material. In order to better determine the spectra of scale vs. interscale material, we completely isolated scales from interscale material. This required that individual scales be isolated, and since there was no way to hold them in the cardboard mount previously used, we mounted them between two potassium bromide (KBr) plates which should be transparent in the infrared region of the electromagnetic spectrum. I prepared scales from the lower jaw (mandible)

completely free of interscale skin. This was compared to samples of interscale skin completely free of scale material. All of the samples were non-pigmented and measured with an IR source from outside. After running a background spectrum on the KBr plates, samples were tested over the range of 5000 to 400 wavenumbers, and I ran 20 scans which were averaged together to get the results. (See figure 8)

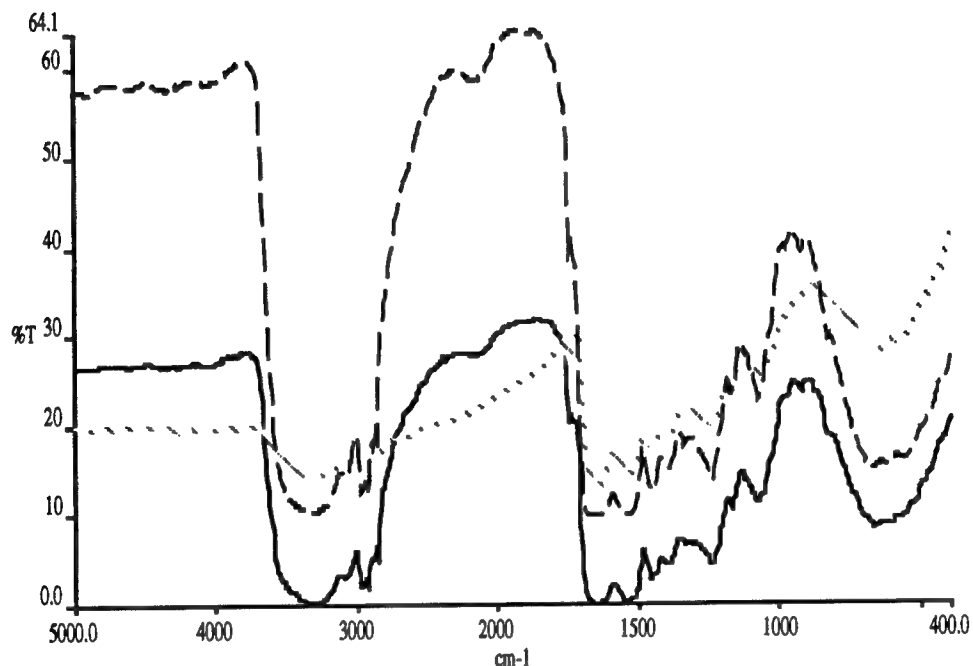


Fig 8: Comparison of *Boa* mandibular non-pigmented whole skin sample (scale and interscale material, solid line) with scale material completely isolated from interscale (dashed line) and interscale skin material completely isolated from scale (dotted line).

The differences between the spectra are summarized below:

1. Interscale much more transmissive from 5000 to 1700 wave numbers
2. From 1700 to 400 wave numbers transmission similar
3. Interscale lacks scale peaks between 5000 to 3700 wave numbers
4. Interscale lacks scale peaks between 2700 to 1800 wave numbers
5. Interscale: unique peaks at 1758 to 1717 wave numbers
6. Other potential differences 1400 to 1200 wave numbers
7. Waviness in interscale sample 1500 to 1400 wave numbers dose not correspond to KBr.

Conclusion

The snake program has come a long way over this summer. The goals of this project were reached with flying colors. We are discovering new areas to study each and everyday. Even though the results may be similar, each sample plays an important part in discovering the key behind this wonderful infrared-sensory system that the snakes possess.

The SEM (Scanning Electron Microscopy) and AFM (Atomic Force Microscopy) results are essentially identical. Each test showed that the isolated infrared-sensitive pits from the *Python regius* revealed a series of very long parallel plate-like structures with a width of 2-3 μ m. The same is true for the *Boa* skin. The surface of each plate was covered with an array of "micropits" less than 0.5 μ m diameter. The spectacle overlying the eye was made up of a parallel array of plates, each covered with micropits. However, the width of the plates and the diameter of the micropits are both less than in the pit organ. The arrangement of the micropits also appeared less regular in the spectacle.

The data from the Infrared Spectrometry was so similar that you would have thought we were testing the same peice of skin material over and over again. It seemed that when the samples came from the same region the results were identical. Example of this is in figure 4: maxilla non-pigmented outside and maxilla non-pigmented inside. Both samples are from the maxilla and are both non-pigmented. However, the only difference is that one is on the inside and the other is on the outside. The same holds true for the rest of the skin material samples, when it comes from the same region of skin.

The only significant difference was between scale material. We found that the scale and the interscale are different in many areas of the spectra. It seemed that the scale had higher transmission and less reflectance or absorbency. The interscale has lower transimission and higher reflectance or absorbance. To better understand the spectra of scale vs. interscale material, we completely isolated scales from interscale material. This required a scale to be isolated, and since there was no way of holding them in the cardboard mount previously used, we mounted them between two potassium bromide (KBr) plates. Through doing this test we found a noticable change in the spectra of the *Boa* mandibular non-pigmented skin samples.

There are still many uncharted paths yet to be taken. However, I have no doubt that the answer behind what makes these animals IR-sensory systems work is within our grasp.

Acknowledgments

Special thanks to Rick Peters, Capt. Gregg M. Caggianelli, and Michael S. Grace, Ph.D. for all of their support and guidance. I would also like to thank Wright Laboratory which made this experience possible.

References

Barrett R., Maderson P.F.A. and Meszler R.M. The Pit Organ of Snakes pg.277-298. In C. Gans and Parsons T.S., Biology of The Reptilia Vol. 2, C. 1970, Academic Press, London.

Molenaar G.J. Anatomy and Physiology of Infrared Sensitivity of Snakes pg. 368-443. In C. Gans and P.S. Winski, Biology of The Reptilia Vol. 17, C. 1992, Univ. Chicago Press, Chicago.

WINDOW DESIGN FOR LASER VELOCIMETER DATA AQUISITION

Shannon M. Campbell

**Carroll High School
4524 Linden Avenue
Dayton, OH 45432**

**Final Report for;
High School Apprentice Program
Wright Laboratory**

**Sponsored by:
Air Force Office of Scientific Research
Bolling Air Force Base, Washington, DC**

And

Wright Laboratory

August 1997

WINDOW DESIGN FOR LASER VELOCIMETER DATA AQUISITION

Shannon M. Campbell
Carroll High School

Abstract

In the project TESCOM, the airflow velocity profile at stage two needed to be measured to find out why the test had failed in the past. A silica window, along with a metal holder, was designed using mechanical engineering techniques. The obstacles to these designs were a flat window had to be placed in a circular compressor case, with the width equal to one blade pitch of stator one, and the length had to be as long as possible given the confinements of the compressor case. Two laser beams will be directed through this window and used to measure the velocity of the airflow between the second rotor and the stator, which is where the problems were in the past. However, the experiment is not complete at this time, due to a September testing date. At that time the suitability of the window designed will be determined.

WINDOW DESIGN FOR LASER VELOCIMETER DATA ACQUISITION

Shannon M. Campbell

Introduction

In order to determine the reason why rotor two did not start in the initial run of TESCOM, a second attempt is scheduled to run in September of 1997. The overall objective of the TESCOM project is to achieve an 8:1 pressure ratio in three stages; to build, design, and test stage-by-stage; and to employ counter-swirl (high reaction) for increased work. In the early eighties a single stage test was completed with two different rotor designs and good performance was demonstrated. In the early nineties a initial stage two test was completed. There was a performance setback with pressure ratio and efficiency; the second stage rotor did not start. This resulted in an investigation into the possible causes of why the second stage rotor did not start.

A laser window is required to allow access into the compressor for the TESCOM measurements. Laser anemometry measurements are used to determine the velocity of small particles (approximately one micron), which are carried by the airflow, and assumed to represent the actual fluid velocity. The window allows two laser beams to measure the velocity of the airflow between the second rotor and stators, as well as between the rotor blades. This measurement is taken by intersecting the two beams at a specific point, where the separate beams form an interference pattern (fringe pattern). As a particle moves through the fringe pattern, the intensity of the light reflected from the particle will vary at a frequency directly related to the particle's velocity.

Discussion of Problem

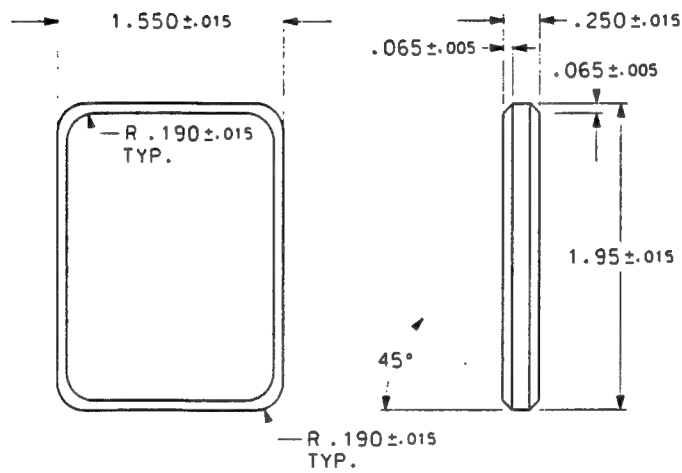
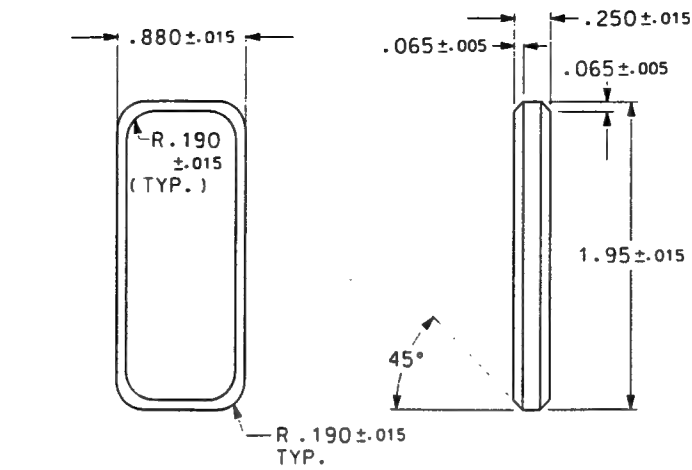
The challenge was to design a window, which consists of a metal holder and the corning 7940 fused silica window. The window had to be flat because the laser beams are rotated around a common axis. If the window was not flat, then the beams would not cross at the planned specific point and the exact position of the measurements would not be accurate. The construction of the window was difficult because it needed to have the largest surface area possible, without affecting the tip flow due to a change in the curvature of the compressor case.

Methodology

First, the compressor case had to be taken apart in order to ensure that accurate measurements of the future window site could be taken. The designated site of the window had to be decided. This was determined by the largest area along the casing that was not obstructed by experimental equipment. Once the site was decided, measurements were taken of the length, width, and the thickness of the case. Using these measurements, an engineering draft of the window was created. This drawing of the window was then sent to Bond Optics to be fabricated.

Next, the window holder was designed to fit securely around the silica window, to ensure that the window would not move during testing. The window will be held in place by the use of teflon tape and rubber "O" rings. This will reduce the amount of friction between the window and the metal holder. To this date, the window drawings have been completed; however, the holder drawings have yet to be finished. Eventually, the drawings will be sent to the machine shop and manufactured for testing in September.

Results



MATERIAL: CORNING 7940 FUSED SILICA

UNLESS OTHERWISE SPECIFIED DIMENSIONS ARE IN INCHES TOLERANCES ARE:				CONTRACT NO.		WRIGHT LABORATORY AERO PROPULSION & POWER DIRECTORATE	
FRACTIONS DECIMALS ANGLES				APPROVALS		TITLE	
0 1 2 3 4 5 6 7 8 9 10 11 12				DATE		TESCOM WINDOW	
DO NOT SCALE DRAWING				DESIGNED BY R. T. McEVY		25JUN97	
FURNISH				CHECKED BY H. LAW		10JUL97	
SIMILAR TO				ENG. BY C. WILLIAMS		25JUN97	
NET WT. GROSS WT.				SCALE 1/1		RELEASE DATE	
				25JUN97		SHEET 1 OF 2	

Conclusion

Due to the scheduling of the test, no conclusions can be drawn at this time. At the completion of testing it will be decided if the window was suitable for the TESCOM procedure. Also, the cause of the initial setback will hopefully be discovered at that time.

References

Battle, G.C. Connolly, Tom. Keesee, Anne M. Laser Window and Mirror Materials. Vol.9. IFI/ Plenum Data Co. New York. 1977

Drain, L.E. The Laser Doppler Technique. John Wiley & Sons. New York. 1980

Durst, F. Melling, A. Whitelaw, J. H. Principles and Practice of Laser-Doppler Anemometry. Academic Press. New York. 1980

Introduction to Lasers. Laser/Electro-Optics Tech. Series. Vol. 1. Second edition. Center for Occupational Research and Development. Waco, TX. 1990

Klein, Claude A. Mirrors and Windows for High Power/High Energy Laser Systems. The Society of Photo-Optical Instrumentation Engineers. Bellingham, WA. 1989

Laser Anemometry Advances and Applications: Proceedings of the Fifth International Conference. The International Society for Optical Engineering. Bellingham, WA. 1993

Percio Castro's report was not available at the time of publication.

**2 PHOTON IONIZATION AND DISASSOCIATIVE ATTACHMENT OF
ELECTRONS TO EXCITED MOLECULES**

Jason R Caudill

East Alton Wood River High School

**Final Report for:
High School Apprentice Program
Wright Laboratories**

**Sponsored by:
Air Force Office of Scientific Research
Bolling Air Force Base, Washington DC**

and

Wright Laboratory

August 1997

2 PHOTON IONIZATION AND DISSOCIATIVE ATTACHMENT OF ELECTRONS TO EXCITED MOLECULES

Jason R Caudill

East Alton Wood River High School

Abstract

An experimental system was prepared to study formation of ions from excited molecular states. An EMG 103 excimer laser using XeCl to excite Sulfur Dioxide molecules. Nanoseconds later an LPX 305i excimer laser using ArF is used to create electrons for attachment to the now excited Sulfur Dioxide molecules forming negative ions. The negative ions could then be counted by a quadrupole mass spectrometer. Preparation of the experimental system proceeded by testing for positive ions via 2-photon ionization.

Two Photon Ionization and Dissociative Attachment of
Electrons to Excited Molecules

Jason R. Caudill

Introduction

No matter how hard you try you cannot get away from pollution. Even when you are in a place that seems to be absent of the presence and influence of man you can find signs of his work, whether it be contaminated water or a polluted forest. Of course impurity such as this is helped by cutting down on the amount of it and by cleaning up even if it is others who tainted the environment. There is also less obvious pollution. Chemicals put in the air from various sources can be very dangerous to both nature and man. These sources could be anything from vehicle emissions, to factory smoke, to large fires. Filters and

chemicals that are used to cut down on the impurities. Dissociative attachment of molecules is an alternative possibility to break up chemical contaminants. In theory if the molecular contaminants are excited with lasers then they may be more ready to dissociatively attach with electrons to ultimately form nonhazardous materials that would be safe to handle. In this partial study Sulfur Dioxide is used.

Methodology

Dissociative attachment of electrons to excited molecules is being studied to measure the difference in attachment rates between the molecules ground and excited states. In this experiment excimer lasers are used to create electrons and also excite the molecules. The first step was to design an experimental vacuum chamber in which this process will occur. The chamber was designed by Dr. Paul Barnes and allows for scans from a quadrupole mass spectrometer. Sulfur Dioxide can flow through pinholes of various sizes which were placed between the chamber and mass spectrometer. Two lasers were used during this experiment (an EMG 103 using XeCl to excite the molecules and an LPX 305i using ArF to create electrons. The lasers were synchronized so that they would arrive at varying times; either before after or simultaneously. The alignment of the lasers was accomplished using a signal generator and pulse delay generator. Using an oscilloscope and photo diode the laser pulses could be seen and adjusted accordingly. Next to confirm the mass spectrometer was operational we created ions internally. Because this was a new

experimental design we tried to count positive ions first because we new tha they should be there. The ions were pushed towards the mass spectrometer by creating an electric field.

Results

Since ions were not initially found we thaught that maybe we weren't creating any electrons . Trying to fix this problem we tweaked the lasers to get as much power as possible out of them. We put new fills in the lasers, we purified the gas, and we cleaned the optics. We were using mirrors to change the path of the laser beam and while measuing the power of the beam we discovered we were losing more than 75% of the energy through the mirrors. To compansate for this we moved the chamber so that the beam would go directly in to the chamber. We still did not detect ions, however there was a peak on the mass spectrometer readout everytime the laser pulsed. Dr. Barnes theorized that this was do to the laser hitting the metal of the chamber and forcing electrons to escape. These electrons were sensed by the mass spectrometer accounting for the spikes.

Conclusion

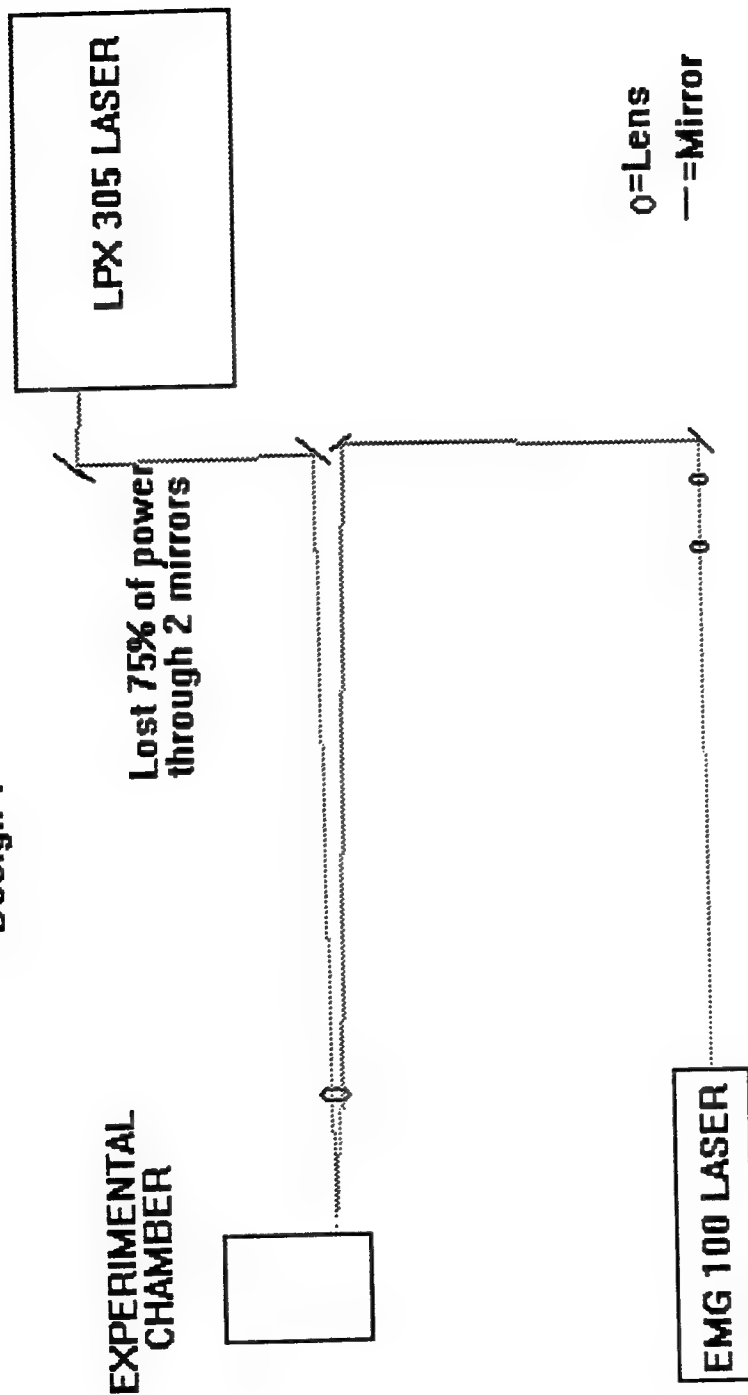
Unfortunately my time was with Dr. Barnes was up before we could see any ions

externally. Because this experiment is in its beginning stages it will take a while before negative ions can be detected. The next steps will be to put plasma in the chamber because we think we are creating ions. With plasma we will know there are ions and if the mass spectrometer doesn't read them then we are possibly creating ions but they are not getting to the mass spectrometer. If ions are found then we are either not creating any ions at all or just not enough to be counted. Even if everything was going fine now (which unfortunately it is not) This experiment would be going on for quite a while. I look forward to perhaps working on it next summer.

Acknowledgments

I would like to acknowledge the Air Force Office of Scientific Research and RDL for giving me the chance to working the High School Apprentice Program. Also I would like to thank Wright Labs for participating in the program. Mostly I need to give credit to Dr. Paul Barnes, (who let me help with the experiment this report is about) Bob Knight, Steve Adams, George Limes (from Wright Connections, another summer program), Dr. Bish Ganguly, (who got me working in Wright Labs) and Dan Danishek for his help and administrative support this summer.

Design 1



This was the first design for the setup of the lasers. We lost 75% of our power from the LPX laser through the mirrors.

DESIGN 2

EXPERIMENTAL
CHAMBER

No power lost through
mirrors

LPX 305 LASER

This was the second design of the setup of the lasers.
We lined the chamber and the LPX laser up to eliminate
the power lost through the mirrors.

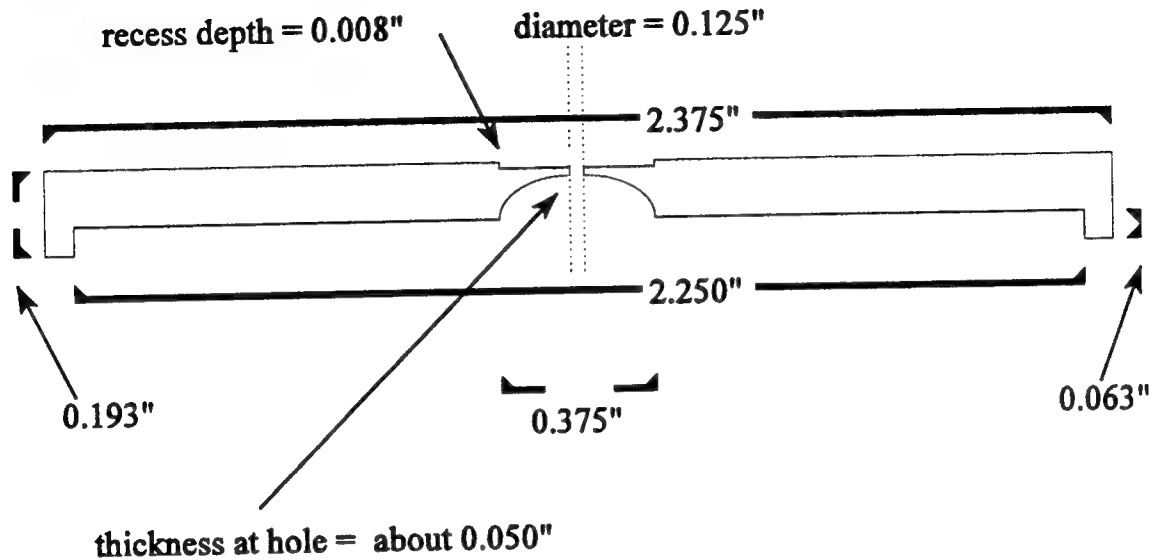
O = Lens

— = Mirror

EMG 100 LASER

7-6

Cross section of 2.375" diameter disc



Stainless Steel disc

This is the design for the pinhole that will be placed in to the experimental vacuum chamber. Other small discs will be placed in the recess at the top of the disc. These will contain the actual pinholes which are in sizes of 1, 2, 5, 10, 50, 100, and 200 micrometers. The original design did not have the recess at the top of the disc but had the pinholes built in. However we discovered that it would be much cheaper and faster if we had made them this way.

HIGH SCHOOL APPRENTICE PROGRAM ACCOMPLISHMENTS

Bernardo V. Cavour

**Kettering-Fairmont High School
3301 Shroyer Road
Kettering, OH 45420**

**Final Report for:
High School Apprentice Program
Wright Patt Laboratory**

**Sponsored by:
Air Force Office of Scientific Research
Bolling Air Force Base, DC**

and

Wright Patt Laboratories

August 1997

HIGH SCHOOL APPRENTICE PROGRAM ACCOMPLISHMENTS

Bernardo V. Cavour
Kettering-Fairmont High School

Abstract

During the Air Force Office of Scientific Research High School Apprentice Program at Wright Laboratory, many tasks were accomplished in both sides of the computer world: The software, and hardware sides. In the software side, most of the time was spent programming an easy-to-use user interface to input and do several tasks with data into a database. The program used for the programming was Microsoft Access. The goal for the user-interface was to let unexperienced people be able to use, and take advantage of the power of Microsoft Access, without making it necessary for people to know how to program, or even use Access. On the other hand, on the hardware side, some of the tasks were: Building computers from scratch, upgrade out-of-date computers, locate and replace bad parts with good ones, and find different ways on how to approach malfunctioning computers.

HIGH SCHOOL APPRENTICE PROGRAM ACCOMPLISHMENTS

Bernardo V. Cavour

During the Air Force Office of Scientific Research High School Apprentice Program at Wright Laboratory, many tasks were accomplished in both sides of the computer world: The software, and hardware sides.

On the software side, most of the time was spent programming an easy-to-use graphic user interface to input data and manage several tasks within data into a database. The program used for the programming was Microsoft Access, using Visual Basic as the programming language. The end-result goal for the user-interface was to allow unexperienced users be able to work, and take advantage of Microsoft Access's tools, without making it necessary for users to know how to program, or even know how to use MS Access. Another percent of the time was spent on configuring computers to the network, and/or find and resolve conflicts with other hardware pieces of the computer. Finally, the remaining part of the time spent on the software part of computers was by collecting characteristic data of each of the computers and input them in a main database, so it can be used as a way of keeping track of what computers will need upgrades, available units, etc.

On the other hand, the hardware side, some of the time was spent on tasks such as: putting computer parts together to make systems, upgrade out-of-date computers with new parts, locate and replace defective parts with working ones, and find different ways on how to approach malfunctioning computers, such as recognizing error messages and what to do with them.

NEURAL NETWORKS AND DIGITAL IMAGE PROCESSING

Christopher R. Clark

**Niceville High School
800 Johns Sims Parkway East
Niceville, FL**

**Final Report for;
High School Apprentice Program
Wright Laboratory**

**Sponsored by:
Air Force Office of Scientific Research
Bolling Air Force Base, Washington, DC**

And

Wright Laboratory

August 1997

Abstract

The areas of study presented are neural networks and digital image processing. These topics are explored using different approaches to determine their potential for use in future military sensor technology. Raw data taken from existing sensors was used to test the ability of conventional digital image processing techniques and neural networks to isolate and recognize potential targets in the input image. The process of finding a target in a scene is known as automatic target recognition.

The first task of the project involved implementing the Filtered Recursive Pulse-Coupled Neural Network in Matlab. The Pulse-Coupled Neural Network had been previously studied and it was determined that research should be continued to learn more about its features¹. The next job was to use the Filtered Recursive Pulse-Coupled Neural Network in conjunction with fuzzy logic and a neural network classifier to develop an automatic target recognition system.

Table of Contents

ABSTRACT	2
TABLE OF CONTENTS	3
FILTERED RECURSIVE PULSE-COUPLED NEURAL NETWORK (FRPCNN).....	4
PCNN THEORY AND BACKGROUND.....	4
PCNN PROCESSING.....	5
FRACTIONAL POWER FILTER (FPF)	5
RECURSION.....	6
MATLAB IMPLEMENTATION	6
AUTOMATIC TARGET RECOGNITION (ATR).....	7
ATR SYSTEM THEORY	7
MATLAB SYSTEM MODEL	8
<i>Pre-Processing</i>	8
<i>Target Classification</i>	9
SUMMARY AND CONCLUSION	10

Filtered Recursive Pulse-Coupled Neural Network (FRPCNN)

PCNN Theory and Background

The Pulse-Coupled Neural Network² (PCNN) is based on recent understandings of the cat's visual system³. It has an inherent ability to perform exceptional segmentation. It is also invariant to all geometrical deformations of an image including size, position, rotation, distortion, and intensity. This means that the network will have the same output for an object no matter what size it is, where it is located in the image, the angle that it is positioned at, and the background that it is located in. These abilities solve some of the most difficult problems in image processing. It has advantages over digital filters because filters require modification for each particular application while the PCNN can be used for many applications with a single implementation. The PCNN is far less computationally intensive than conventional neural networks as well. For these reasons, it is the ideal choice for target recognition and classification.

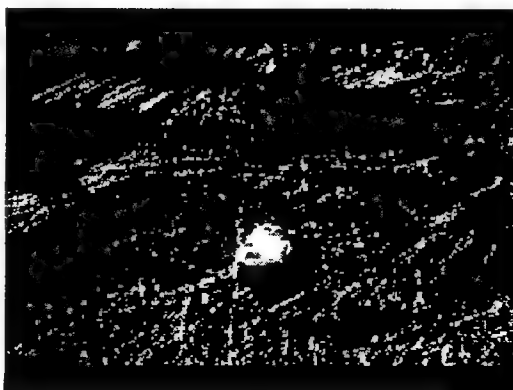
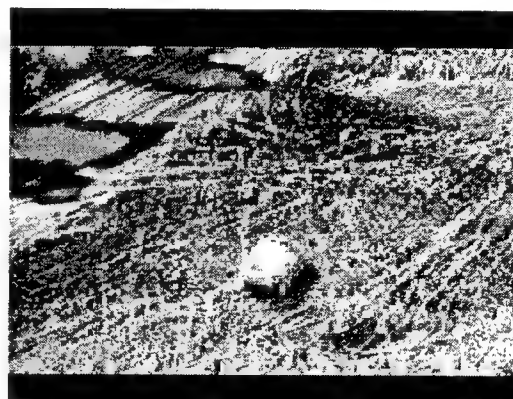


Figure 1 a, b, c: The PCNN Process

PCNN Processing

The PCNN algorithm is an iterative process. Basically, it consists of three steps:

1. Each pixel's intensity is converted to a pulse frequency. (Figure 1a)
2. The pixels are linked, causing similar frequencies to synchronize themselves. (Figure 1b)
3. The time-averaged pulse pattern is reconverted to an intensity image. (Figure 1c)

Fractional Power Filter (FPF)

The FPF⁴ is a first-order composite Fourier filter that has the ability to trade-off generalization and discrimination. This sensitivity parameter is used to tell the filter how close the presented image must be to the target images—full generalization will accept almost anything as being a target while full discrimination requires an almost exact

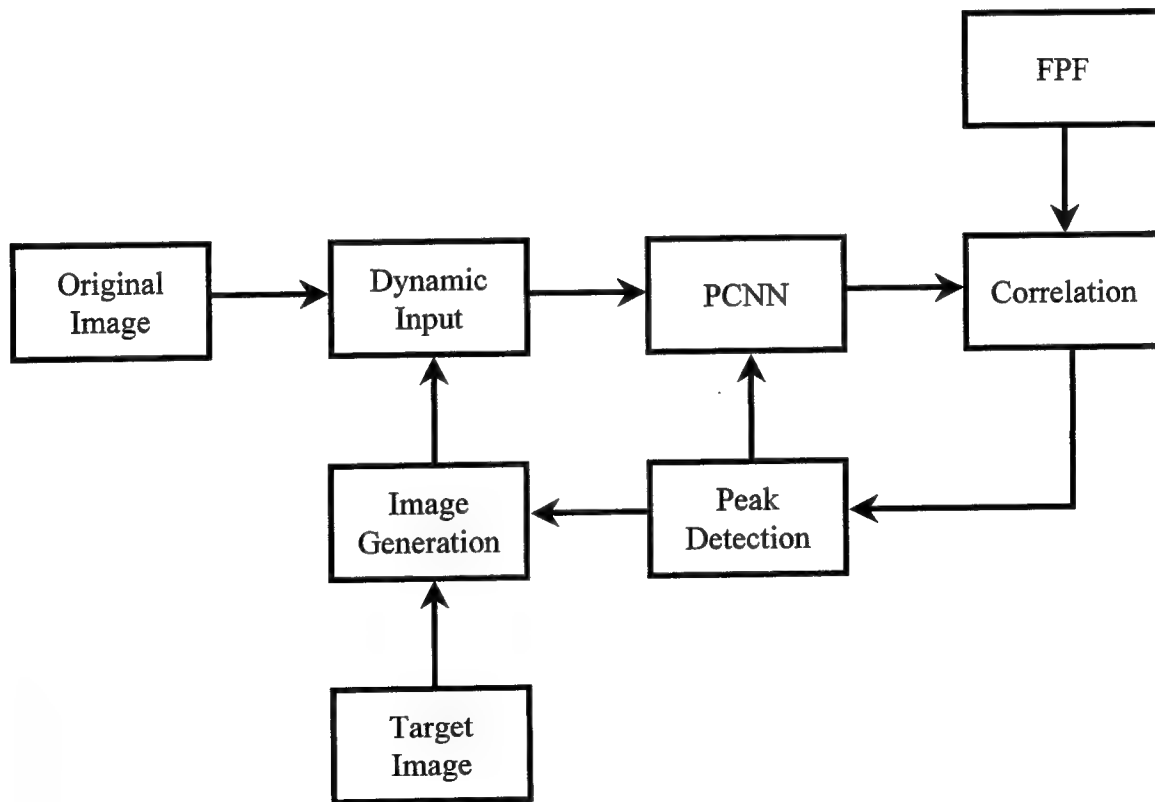


Figure 2: Logic Flow of the FRPCNN

match. The composite nature of the filter allows it to still be used when the exact presentation of a target cannot be predicted. Also, a single FPF can be used to detect multiple targets. The filter is a correlation built from training images.

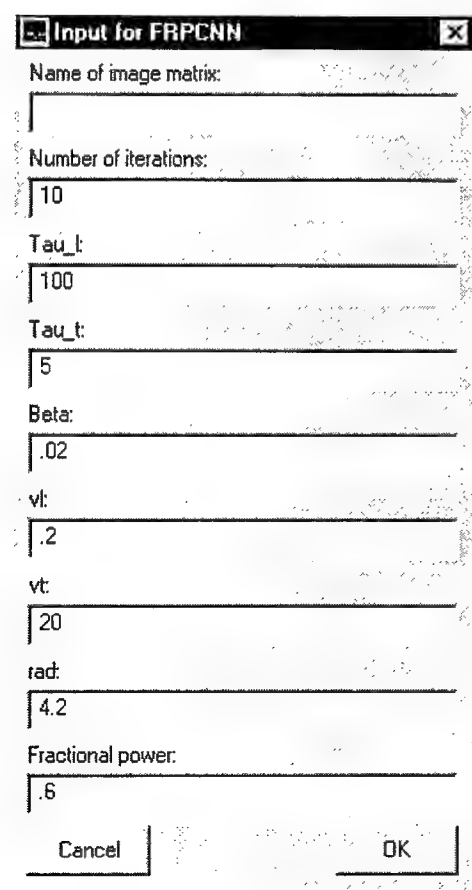
Recursion

The recursive process of the Filtered Recursive Pulse-Coupled Neural Network^{5,6} is shown in Figure 2. Initially, the dynamic input is the same as the original image. The input image is passed to the PCNN. Each pulse output is correlated with the FPF creating a correlation surface. Next, a peak detection algorithm is performed on the surface. If a significant peak is found, meaning that the pulse output is very similar to the filter, control is passed on to the next step. If a strong similarity is not found the PCNN will iterate and produce a different pulse which is again correlated and analyzed. After a successful

peak location, image generation will occur. In this step the image is changed to enhance the target in the scene using the target image and the location of the peak in the correlation surface. This modified image is now the dynamic input and is used for the next repetition of the entire process.

Matlab Implementation

The FRPCNN was implemented in MathWorks' Matlab. This involved writing code for the PCNN, the FPF, and the other steps of the recursion process. The finished system is fully automated and shows progressive output while

A screenshot of a Matlab input dialog box titled "Input for FRPCNN". The dialog contains several input fields with the following values: "Name of image matrix:" (empty), "Number of iterations:" (10), "Tau_t:" (100), "Tau_i:" (5), "Beta:" (.02), "v1:" (.2), "v2:" (20), "rad:" (4.2), and "Fractional power:" (.6). At the bottom, there are "Cancel" and "OK" buttons.

Input for FRPCNN	
Name of image matrix:	
Number of iterations:	10
Tau_t:	100
Tau_i:	5
Beta:	.02
v1:	.2
v2:	20
rad:	4.2
Fractional power:	.6
Cancel	OK

Figure 3: Matlab Input Dialog

running. The user has full control of input parameters and can set the number of iterations (Figure 3). A typical execution of the system with sufficient iterations can be completed in just a couple minutes. The final output data is of very high quality and is suitable for further processing.

Automatic Target Recognition (ATR)

ATR System Theory

The goal of an ATR system is to be able to find, isolate, and identify a target in a scene. In military context, the target might be an enemy vehicle, weapon, building, bridge or any other strategic item. A self-guided smart munition must have a fast, reliable ATR system on board. Ideally, the target's size, position, and surroundings should not deter the system.

Generally there are three stages in the ATR processing. The first is data collection and pre-processing. This initial stage involves the use of sensors such as infrared detectors to capture information about the area. Usually, some quick calculations are performed on the data in order to improve the speed and performance of the rest of the system. The second step is the target classification step. This part of the system attempts to determine whether or not a target is present in the data reported by the sensors. Finally, the system performs post-processing. This could involve changing some properties of the flight system to cause the munition to home in on the target.

Matlab System Model

The Matlab ATR system developed uses the FRPCNN followed by fuzzy logic processing for its pre-processing elements. The target classification stage employs a neural network classifier.

Pre-Processing

The first step of the pre-processing involves running the FRPCNN as discussed earlier to isolate potential targets. The final dynamic input generated by the FRPCNN is then passed on to a fuzzy logic processor. At this point, the binary data is the same size as the original image, which for a typical sensor is usually well over 75,000 pixels, or data points. A way to reduce the amount of data was desired so that the system could be used in real-time. Therefore, fuzzy logic is used to divide the image into fuzzy sets, or regions. Then each of these regions is assigned a single decimal value in the interval $[0,1]$, which is calculated based on the number of "on" pixels in that region. Using this system, a 256-by-256 element image can be represented by as few as 100 values obtained from 100 fuzzy regions. Although the data size is reduced by at least 700 percent, no significant information is lost.

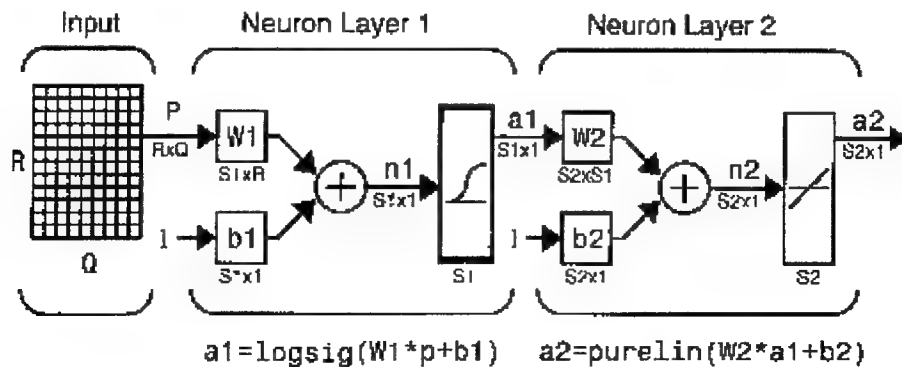


Figure 4: Neural Network Classifier Architecture

Target Classification

A neural network classifier performs the target classification. The network architecture is shown in Figure 4. It is a 2-layer backpropagation neural net, with a 10 neuron log-sigmoid hidden layer and a 2-neuron linear output layer. The input data consists of the fuzzy logic output from three examples of tanks and three examples of mines. The trained system was able to correctly identify all of the training images. In addition, it is able to accurately classify images produced by tanks and mines that have not previously been shown to the network.

Summary and Conclusion

A Filtered Recursive Pulse-Coupled Neural Network was successfully implemented in Matlab. The system was given input images from different sources and produced quality output in which the target was significantly enhanced and background clutter was subdued. The FRPCNN was used in conjunction with a fuzzy logic processor and a neural network classifier to create an Automatic Target Recognition System. The ATR system is able to handle large input due to the data reduction accomplished by the fuzzy logic methods. All of the presented targets were correctly identified by the system.

In conclusion, a robust, high-speed ATR technique was developed that can be used in a wide variety of applications with minimal modifications.

¹ Christopher R. Clark. "Neural Networks and Digital Image Processing – Final Report for 1996 HSAP." (1996).

² J.L. Johnson. "Pulse-Coupled Neural Nets: Translation, rotation, scale, distortion, and intensity signal invariances for images." Applied Optics. 33(26), 6239-6253 (1994).

³ R. Eckhorn, H.J. Reitboek, M. Arndt, P. Dickie. "Feature Linking via Synchronization among Distributed Assemblies: Simulations of Results from Cat Visual Cortex." Neural Computation. 4, 93-102 (1992).

⁴ J. Brasher and J.M. Kinser. "Fractional-Power Synthetic Discriminant Functions." Pattern Recognition. 27(4), 577-585 (1994).

⁵ J.M. Kinser, J.L. Johnson. "Stabilized Input with a Pulse-Coupled Neural Network." Submitted to Optical Engineering. (1996).

⁶ J.M. Kinser. "Object Isolation." Submitted to Optical Memories and Neural Networks. (1996).

**ELECTRONIC STUDIES OF POLYPYRROL FILMS GROWN ON
SEMICONDUCTOR WAFERS**

Aaron Davis

**Niceville High School
800 Johns Sims Parkway East
Niceville, FL**

**Final Report for;
High School Apprentice Program
Wright Laboratory**

**Sponsored by:
Air Force Office of Scientific Research
Bolling Air Force Base, Washington, DC**

And

Wright Laboratory

August 1997

**Electronic Studies of Polypyrrole Films
Grown on Semiconductor Wafers**

Aaron Davis
High School Apprentice
Fuzes Branch
Wright Laboratory Armament Directorate

Abstract

Conventional polymers have been viewed purely as insulators. Since more research and development has been targeted toward polymers, now they are considered a future source of electronic materials [1]. Polymers first developed as non-conductive hydrocarbons because they were tailored for applications which demand low cost, light weight, and flexibility. Inherently conductive polymers [2] can also exhibit these characteristics. It is foreseen that someday conductive polymers will replace conventional materials in numerous applications ranging from electronic circuits and components to power transmission lines.

Experiments were performed to form a functional hybrid polymer/semiconductor bilayer. Factors considered in the formation of a diode include the dopant parameters, substrate parameters, and corrosion. Conventional semiconductor wafer material (such as silicon or gallium arsenide) was used as substrates for polypyrrole growth. Zener diodes and Schottky diodes were made through use of semiconductor wafer material coated with lightly doped semiconducting polymer material.

Electronic Studies of Polypyrrole Films Grown on Semiconductor Wafers

Aaron Davis

Introduction

Conventional polymers have been viewed purely as insulators. Since more research and development has been targeted toward polymers, now they are considered a future source of electronic materials [1]. Polymers first developed as non-conductive hydrocarbons because they were tailored for applications which demand low cost, light weight, and flexibility. Inherently conductive polymers [2] can also exhibit these characteristics. It is foreseen that someday conductive polymers will replace conventional materials in numerous applications ranging from electronic circuits and components to power transmission lines.

As a first step to the development of all-polymer electronic junction devices, it is logical to begin with fabrication of hybrid polymer/semiconductor bilayers. In order to accomplish this, conventional semiconductor wafer material (such as silicon or gallium arsenide) can be used as a substrate upon which the conducting polymer is grown. In the ideal sense, either p-n junction diodes or Schottky diodes can be made through use of semiconductor wafer material coated with lightly doped semiconducting or heavily doped metallic polymer films, respectively.

Discussion of Problem

To form a functional hybrid polymer/semiconductor bilayer, one must select an appropriate dopant at the proper concentration to make the conducting polymer portion of the bilayer. A considerable

variety of counterions have been used in the deposition of polypyrrole; units include toluene sulfonate, dodecylbenzenesulfonate and perchlorate [3]. The substrate used as the film support also plays a factor in the formation of a useful electronic diode. The purpose of this project is to gain insight into the combination of conducting polymer characteristics and semiconducting wafers that produce either p-n junction or Schottky diodes.

Methodology

Preliminary measurements were performed to determine the doping concentration of silicon and gallium arsenide wafers. A Signatone (model S-301-4) four-point probe and a Hewlett Packard (model HP 34401A) multimeter were used to measure the sheet resistance, resistivity and dopant concentration according to the four-point probe method (see fig 1). Wafer thickness was measured via calipers.

Basic measurements now out of the way, experiments were conducted to determine the best possible choice of doping parameters. Dodecylbenzenesulfonate (DBS), lithium perchlorate (LPC) and toluenesulfonic acid (TSA) dopants were tried in both water and acetonitrile solvents. Molarity concentrations between 10^{-4} M and .15 M were used. These investigations helped to resolve the problem of how to make the polymer semiconducting or semimetallic. Free standing polypyrrole (PPY) films were removed following deposition upon stainless steel strips. Their conductivities were measured by the four-point probe method previously mentioned.

After determining the best dopant parameters, p-type PPY films were electrochemically deposited onto semiconducting silicon wafers. Heavily doped (Russian, Yury Vasiliev, vasil@ropnet.ru) and lightly doped (Wafernet, San Jose CA) semiconductor material of both p-type and n-type silicon wafers was used. PPY was deposited in water based solutions (.05 M PPY/.02 M TSA) and also in acetonitrile based solutions (.05 M PPY/.02 M TSA). N-type gallium arsenide (GaAs) wafer material also supported PPY growth but deposition was limited to acetonitrile based solutions due to the corrosion caused by water based solutions. In order to help the polymer formation onto the GaAs, a colloidal suspension (Nyacol

Products, Ashland MA) of tin oxide nanoparticles was sprayed and dried on the substrate before deposition.

Electronic behavior tests were carried out on a Tektronix type 576 curve tracer and a Signatone S-1160 1-micron analytical probe station. The hybrid polymer/semiconductor bilayers were examined for diode behavior.

Results

Refer to table 1 for results on sheet resistance, resistivity and dopant concentration of semiconductor wafers.

DBS is an excellent dopant for electrochemical polymerization of smooth PPY films. DBS doped PPY films grown in water based solutions were readily removed from their stainless steel substrates. Conductivity measurements of PPY/DBS films proved them to be semimetallic with conductivities above 1 siemen. While good films were deposited in water based solutions, problems arose with attempts to form films from acetonitrile based solutions due to the limited solubility of DBS in acetonitrile. An attempt to dissolve 10^{-4} M DBS in acetonitrile still resulted with DBS flakes floating around in the solution after 1 hour on the magnetic stirrer.

Next, LPC was tested because of its ability to dissolve in acetonitrile. The LPC had worse effects than the DBS. It would dissolve in solution but upon electrochemical deposition, the cathode would be attacked. Lead, stainless steel and even gold electrodes were corroded. This dopant was discarded.

The final dopant tested proved to be the ideal dopant for this project. TSA dissolved in both acetonitrile and water based solutions. Use of this dopant resulted in relatively rough films but they were still usable. The conductivity of the PPY/TSA films at .05 M PPY/.02 M TSA (solution U) were just under 1 siemen which lent themselves to semiconductor behavior, a necessity in the formation of semiconductor junctions.

Trials first involved n-type and p-type silicon wafers. PPY deposited from solution U onto the anode (silicon substrate) was performed with an estimated current density of 1 mA/cm^2 . Due to the irregular shape of each substrate the estimated area of any given one could only be determined within an accuracy of plus or minus 5 percent. PPY/TSA films grown on p-type Wafernet, n-type and p-type Russian wafers exhibited nearly linear current versus voltage behavior (see Fig 2) similar to that of a resistor. The desired effect began to show with films grown on the n-type wafernet substrates, namely Schottky diode behavior.

Still with no true p-n junction diode, tests were begun on the GaAs substrates. No PPY films were deposited on GaAs from aqueous solution since corrosion of the anode occurred faster than the polymerization of pyrrole. Conductive polymer film material was deposited on GaAs from acetonitrile solutions but looked very rough and discontinuous. The drying of a colloidal nanoparticulate tin oxide film sprayed onto the wafer assisted the deposition process and allowed an even layer of PPY to be deposited. Current versus voltage data showed this to be the hybrid junction device sought. Upon comparison with commercially available diodes it was found that the p-n junction of PPY/GaAs (see Fig 3) produces electronic behavior comparable to that of a standard Zener diode (see Fig 4).

Conclusion

The type of counterion used in the electrochemical preparation of conducting films of PPY has a significant impact upon the resultant molecular configuration and bulk polymer properties, including the level of electrical conductivity [3]. In order to produce the desired effect, it was necessary to obtain a polymer with semiconductive rather than a semimetallic behavior. TSA was the most effective dopant utilized both for its solubility and the electrical conductivity it would provide to the polymer film. TSA produced conductivities below 1 siemen, resulting in semiconductive films. DBS produced conductivities greater than 1 siemen, resulting in semimetallic films.

References

1. J. Mort, "Conductive Polymers," Science 208, (1980) 819.
2. M. Aldissi, Inherently Conducting Polymers, Noyes Data Corporation (Parkridge NJ) 1993.
3. G. R. Mitchell, F. J. Davis and C. H. Legge, Synthetic Metals 26 (1988) 247.
4. G. Nagasubramanian, S. DiStefano, and J. Moacanin, J. Electrochem. Soc. 133, No.2 (1986) 305.
5. G. Horowitz and F. Garnier, Solar Energy Materials 13, (1986) 47.

$$R_s = \frac{V}{I} \cdot CF \quad \Omega/\text{square}$$

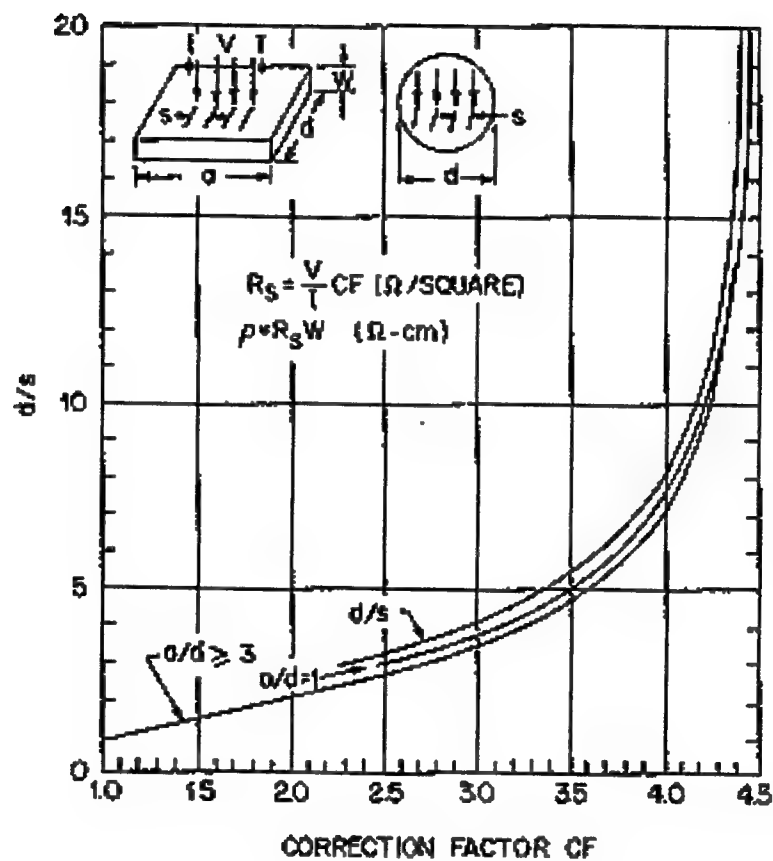


Figure 1. The Four-Point Probe Method.

Semiconductor Wafer	Sheet Resistance (Ω/square)	Resistivity ($\Omega\text{-cm}$)	Impurity Concentration (cm^{-3})
N-Type Si/As [Russian]	.063	.0022	2×10^{19}
P-Type Si/B [Russian]	.1485	.0055	1.5×10^{19}
N-Type Si/As [Wafernet]	14.76	.0375	1.2×10^{17}
P-Type Si/B [Wafernet]	3.937	.01	2.0×10^{18}
N-Type GaAs	.0045	2.34×10^{-4}	1.0×10^{19}

Table 1. Results on sheet resistance, resistivity and dopant concentration.

P-Type Russian

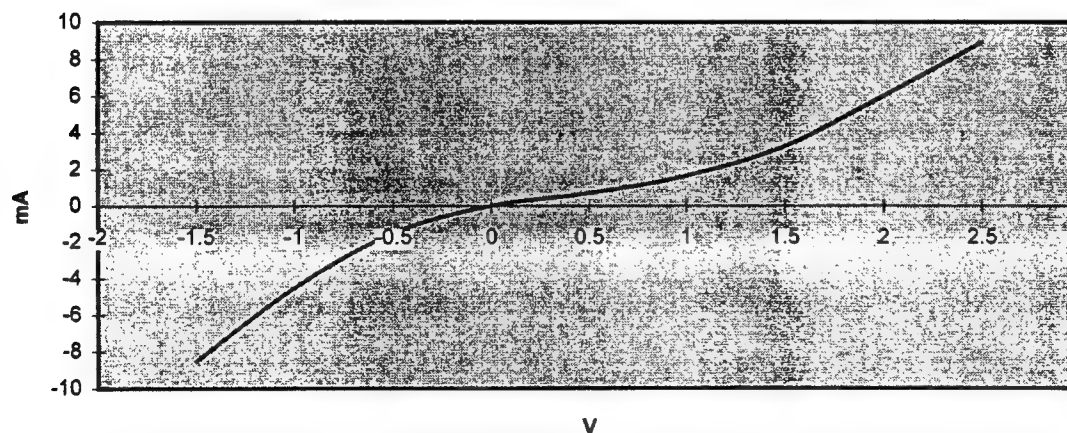


Figure 2. Curve Trace of a P-P junction grown on P-Type Russian.

Gallium Arsenide

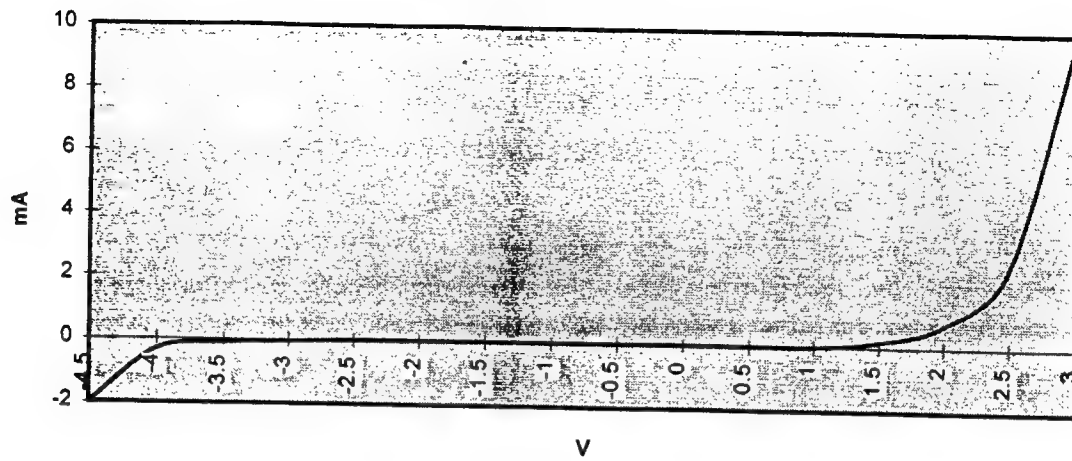


Figure 3. Curve Trace of a P-N junction grown on Gallium Arsenide.

Zener Diode

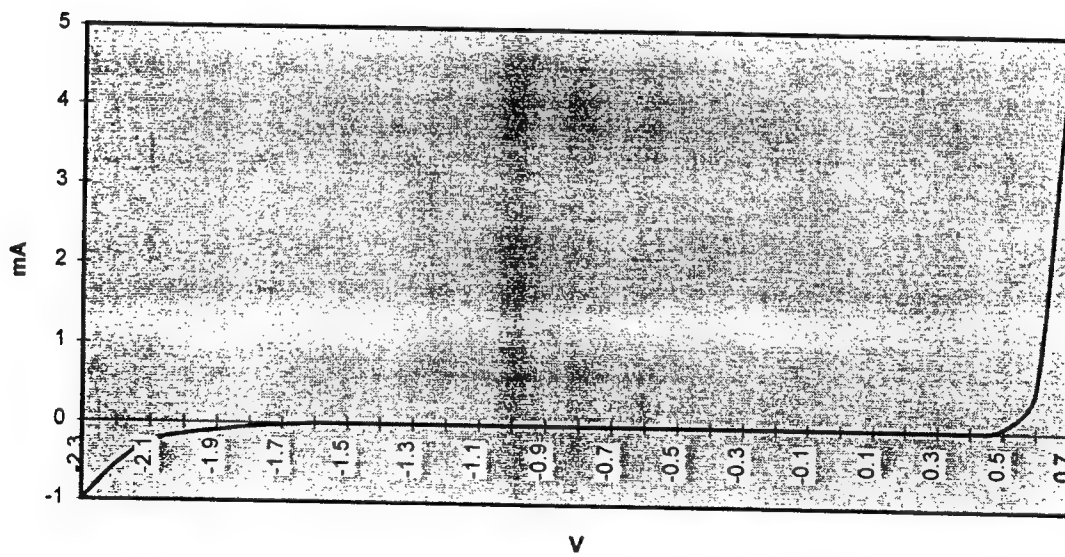


Figure 4. Curve Trace of a True Zener Diode.

TRACTION MODELS

Debbie L. Dressler

**Centerville High School
500 East Franklin Street
Centerville, OH 45458**

**Final Report for:
High School Apprentice Program
Wright Laboratory**

**Sponsored by:
Air Force Office of Scientific Research
Bolling Air Force Base, Washington, DC**

And

Wright Laboratory

August 1997

TRACTION MODELS

Debbie L. Dressler

Centerville High School

ABSTRACT

The viscosity of various lubricants used in an engine, specifically for bearings, was examined to produce models for reference for each lubricant as well as examine the effects of testing conditions. Friction data was plotted as a function of pressure, temperature, engine speed, and slip and this data allows us to predict the amount of heat generated and the power lost by the mechanical components. We found that when the data was plotted as friction versus slip it formed a curve that could be modeled. After we obtained the needed constants for each curve we could predict how the lubricant would behave for different conditions. Transforming the graphs from slip (x-values) and friction (y-values) to shear strain rate and shear stress respectively produces a graph of essentially the same shape. These graphs were interpreted to develop a model to fit all traction models and help predict lubricant behaviors.

TRACTION MODELS

Debbie L. Dressler

I. INTRODUCTION

We studied the effects and behavior of two lubricants, Mil-l-7808K and Mil-L-23699 on nonconformal surfaces. The lubrication at these conditions is called elastohydrodynamic lubrication.

Newton's Law of Viscosity says that the shear stress in a fluid is proportional to the rate of change of velocity with respect to y ,

$$\tau = \mu * \frac{du}{dy} \quad (1)$$

where $\frac{du}{dy}$ = *shear strain rate* and μ = *absolute viscosity*.

Thus for a Newtonian fluid, a plot of shear stress versus shear strain rate gives a straight line.

In elastohydrodynamic lubrication the shear stress is not proportional to the shear strain rate and consequently a plot of shear stress as a function of shear strain rate produces a curve. This non-ideal or non-Newtonian behavior results in part because the high pressures encountered change the contact area due to elastic deformation of the metal. Another source of the non-Newtonian behavior is the pressure-viscosity effects of the lubricant.

The goal of this project is to develop a model for the stress curves when there is elastohydrodynamic lubrication.

II. APPARATUS

The apparatus consists of a metal ball, rotated by a shaft and placed in contact with a rotating disk four inches in diameter. The contact between the ball and the disk was

lubricated. The pressure/load between the ball and the disk was controlled by a pneumatic piston. The temperature was measured by a thermocouple and this temperature reading was used to control the temperature by means of eight 500 watt cartridge heaters. The rotation speeds of the ball and disk were controlled by two independent stepper motors. These speeds were used to calculate the slip which is the percentage of slide to roll by the following equation:

$$x = \frac{\Delta U}{\bar{U}} = \frac{(\text{speed of ball} - \text{speed of disk})}{\frac{1}{2}(\text{speed of ball} + \text{speed of disk})} \quad (2)$$

The torque was measured with a strain gauge transducer and the following two equations were used to obtain the traction coefficient:

$$T = F_f * r \quad (3)$$

$$TC = \frac{F_f}{L} \quad (4)$$

where T = measured torque, F_f = frictional force, r = radius of the ball, TC = traction coefficient, and L = load applied to transducer.

III. METHODOLOGY

Sigma Plot, a commercially available program, was used to fit curves to the collected data. Three different basic equations were used to model the data that we had collected. The traction coefficient data and slip data was imported into Sigma Plot and the curves (Graphs 1 -14) were generated. Using Sigma Plot's "curve fit" feature, which fits nonlinear curves, three different equations were solved for each data set.

A. MODEL 1

The first equation used to model the data sets was obtained from the Handbook of Nonlinear Regression. It is:

$$TC = \frac{-k_{max} + 2k_{max}s}{1 + e^{-(2 \cdot m \cdot x)/overk_{max}}} \quad (5)$$

where TC = traction coefficient, k_{max} = maximum function value, m = slope @ (0,0), and x = slip.

The k_{max} and m values were recorded in Table I.

B. HAMROCK MODEL

The second equation used was from Fundamentals of Fluid Film Mechanics by Hamrock.

$$TC = \frac{a x}{[1 + (b x)^c]^{1/c}} \quad (6)$$

where TC = traction coefficient and x = slip.

The constants a , b , and c for the Hamrock Model were recorded in Table III.

C. PKG MODEL

The third equation used, obtained from the computer program manual ADORE, was:

$$TC = [(a + b x) * e^{(c x)}] + d \quad (7)$$

where TC = traction coefficient and x = slip.

The constants a , b , c , and d were recorded in Table II.

IV. DISCUSSION

The two models, Model 1 and Hamrock Model, fit most of the graphs with the exception of graphs 5, 9, and 13. Plots 5, 9, and 13 hit a maximum coefficient and then decrease slightly approaching a limit for large values of x . The reasons for this decrease in shear stress have not been explained although it is agreed that the lubricant behaves as a plastic solid at low temperatures and high pressures as the strain rate increases. Model I and the Hamrock Model are incapable of adequately fitting the recorded data when there is a maximum value at an interior point on the x axis..

The PKG Model was found to produce an adequate fit to the data. The superiority of the PKG Model is probably related to the fact that it has four constants that can be adjusted and the other models have two and three. Now that a good fit has been established the coefficients a, b, c , and d should be related to physical properties. So far we have not been able to relate these constants to the physical but we can make the following determinations.

- By looking at the shape of the graph it is apparent that c must be negative.
- The graph must go through $0,0$ so therefore: $a = -d$.
- At $0,0$ the slope of the function is the initial viscosity of the lubricant. Evaluating the derivative of the function at $x = 0$ gives us: $(a * c) + b = \text{initial viscosity}$.
- Taking the limit of the PKG function as $x \rightarrow \infty$ gives $\lim_{x \rightarrow \infty} PKG = d$ so you know that d equals the limiting traction coefficient, which if graphed as physical properties would be the limiting shear stress.
- The data has a peak at a certain of value of x , which at this time is not related to any physical properties. You still have to take a range of data to find that peak.

V. CONCLUSION

Three different models were used to describe the data that was collected during this project. The first model had two constants that could be solved, the second model had three constants, and the third model, the PKG model, had four constants. It was found that the PKG Model, with four constants, was the only model that could adequately model the data. The Sigma Plot program was used to find the four values for the constants that best reproduced the data. The goal was to relate the coefficients a, b, c , and d to the lubricant's physical properties but due to the nonlinear behavior there is a peak that must be determines experimentally. This PKG model fits all the data but you still must take many data points to determine the coefficients.

BIBLIOGRAPHY

- Hamrock, Bernard J. Fundamentals of Fluid Film Lubrication. McGraw-Hill Ser. In Mechanical Engineering. New York: McGraw-Hill, 1994: Chps. 1, 4, 14, & 16.
- Shigley, Joseph E. Mechanical Engineering Design. McGraw-Hill Ser. In Mechanical Engineering. ed. B.J. Clark and J.W. Maisel. New York: McGraw-Hill, 1972: Chp. 10.
- Ratowsky, David A. Handbook of Nonlinear Regression Models. New York: New York and Baisel, 1935.
- Gupta, Pradeep K. inc. ADORE. Vers. 2.4. Computer software. SpringerVerlag, 1984.
- Box, George E.P., et al. An Introduction to Design, Data Analysis, and Model Building. Statistics for Experimenters. New York: John Wiley and Sons inc., 1978: chp. 16.
- Johnson, K.L. and J.L. Tevaarwerk. Shear Behavior of Elastohydrodynamic Oil Films. 1976.

TABLE I

TEST CONDITIONS

MODEL 1

Lubricant	Speed	Temperature	Pressure	m	kmax
Mil-L-7808K	5 m/s	100°C	1.00 GPa	9.672e-4	.015604
			1.25 GPa	2.314e-3	.020421
			1.50 GPa	4.476e-3	.026470
	10 m/s	100°C	1.00 GPa	1.1840e-3	0.0149
			1.25 GPa	2.6682e-3	0.0190
			1.50 GPa	4.7403e-3	0.0232
		125°C	1.00 GPa	7.0411e-4	0.0102
			1.25 GPa	1.9711e-3	0.0168
			1.50 GPa	3.3597e-3	0.0201
		175°C	1.00 GPa	4.2931e-4	3.9062e-3
			1.25 GPa	1.0334e-3	0.0132
			1.50 GPa	1.9867e-3	0.0163
	15 m/s	30°C	1.25 GPa	0.0167	0.0287
			1.50 GPa	0.0288	0.0338
			1.00 GPa	1.4262e-3	0.0161
		100°C	1.25 GPa	2.7158e-3	0.0183
			1.50 GPa	5.1252e-3	0.0219
			1.00 GPa	7.8967e-4	9.8430e-3
		125°C	1.25 GPa	1.6438e-3	0.0151
			1.50 GPa	3.2501e-3	0.0177
			1.00 GPa	2.6339e-4	8.4369e-3
		175°C	1.25 GPa	1.3129e-3	0.0148
			1.50 GPa	2.7254e-3	0.0201
			1.00 GPa	9.0435e-3	0.0235
Mil-l-23699	20 m/s	30°C	1.25 GPa	0.0215	0.0270
			1.50 GPa	0.0388	0.0292
			1.00 GPa	1.3383e-3	0.0127
		100°C	1.25 GPa	2.9720e-3	0.0169
			1.50 GPa	5.9885e-3	0.0212
			1.00 GPa	5.7590e-4	0.0101
		125°C	1.25 GPa	1.1272e-3	0.0127
			1.50 GPa	1.9620e-3	0.0153
			1.00 GPa	5.3988e-4	7.0708e-3
		150°C	1.25 GPa	8.1184e-4	0.0105
			1.50 GPa	1.2692e-3	0.0129
			1.00 GPa	4.1866e-3	0.0260
	5 m/s	30°C	1.25 GPa	7.1630e-3	0.0328
			1.50 GPa	0.0167	0.0381
			1.00 GPa	1.9586e-3	0.0168
		100°C	1.25 GPa	2.3995e-3	0.0228
			1.50 GPa	8.4949e-3	0.0371

TABLE II

TEST CONDITIONS

PKG MODEL

Lubricant	Speed	Temperature	Pressure	a	b	c	d
Mil-L-7808K	5 m/s	100°C	1.00 GPa	-0.01920	1.2656e-14	-0.06179	0.01890
			1.25 GPa	-0.02113	6.632e-14	-0.1270	0.02209
			1.50 GPa	-0.0243	1.504e-13	-0.1834	0.0278
	10 m/s	100°C	1.00 GPa	-0.01707	7.353e-15	-0.08578	0.01697
			1.25 GPa	-0.0194	1.138e-6	-0.1661	0.0201
			1.50 GPa	-0.0227	3.222e-14	-0.2515	0.0239
		125°C	1.00 GPa	-0.0119	6.093e-15	-0.0762	0.0116
			1.25 GPa	-0.0177	7.985e-15	-0.1311	0.0183
			1.50 GPa	-0.0198	4.179e-14	-0.1967	0.0210
		175°C	1.00 GPa	-4.131e-3	2.616e-14	-0.1066	4.432e-3
			1.25 GPa	-0.0159	1.102e-14	-0.0678	0.0165
			1.50 GPa	-0.0169	4.747e-15	-0.1381	0.0175
	15 m/s	30°C	1.25 GPa	-0.0257	7.4549e-3	-0.3577	0.0277
			1.50 GPa	-0.0240	0.0112	-0.3126	0.0306
			1.00 GPa	-0.0180	9.261e-15	-0.0894	0.0185
		100°C	1.25 GPa	-0.0187	7.6766e-7	-0.1795	0.0192
			1.50 GPa	-0.0213	2.989e-11	-0.2909	0.0224
			1.00 GPa	-0.0110	7.458e-15	-0.0947	0.0108
		125°C	1.25 GPa	-0.0162	8.376e-15	-0.1251	0.0164
			1.50 GPa	-0.0178	1.854e-14	-0.2319	0.0182
			1.00 GPa	-0.0208	6.596e-15	-0.0126	0.0209
		175°C	1.25 GPa	-0.0166	1.718e-14	-0.1013	0.0164
			1.50 GPa	-0.0203	5.728e-14	-0.1453	0.0217
			1.00 GPa	-0.0236	1.6651e-3	-0.4485	0.0237
Mil-l-23699	5 m/s	30°C	1.25 GPa	-0.0204	0.0104	-0.3041	0.0236
			1.50 GPa	-0.0203	0.0137	-0.3713	0.0261
			1.00 GPa	-0.0138	8.986e-15	-0.1208	0.0138
		100°C	1.25 GPa	-0.0170	1.948e-14	-0.2179	0.0175
			1.50 GPa	-0.0207	2.248e-11	-0.3652	0.0215
			1.00 GPa	-0.0127	1.540e-14	-0.0555	0.0125
		125°C	1.25 GPa	-0.0143	2.943e-15	-0.0981	0.0143
			1.50 GPa	-0.0161	2.944e-14	-0.1518	0.0163
			1.00 GPa	-8.2677e-3	3.165e-14	-0.1020	7.5458e-3
		150°C	1.25 GPa	-0.0121	4.969e-15	-0.0856	0.0119
			1.50 GPa	-0.0142	1.328e-14	-0.1139	0.0141
			1.00 GPa	-0.0259	6.822e-14	-0.2029	0.0269
	10 m/s	30°C	1.25 GPa	-0.0330	5.035e-14	-0.3012	0.0332
			1.50 GPa	-0.0316	5.034e-14	-0.4455	0.0388
			1.00 GPa	-0.0172	1.159e-13	-0.0859	0.0203
		100°C	1.25 GPa	-0.0228	7.843e-14	-0.1126	0.0248
			1.50 GPa	-0.0302	1.113e-13	-0.2204	0.0387
			1.00 GPa	-0.0172	1.159e-13	-0.0859	0.0203

TABLE III

TEST CONDITIONS

HAMROCK MODEL

Lubricant	Speed	Temperature	Pressure	a	b	c
Mil-L-7808K	5 m/s	100°C	1.00 GPa	9.5773e-4	0.0569	2.2864
			1.25 GPa	2.9873e-3	0.1175	1.3090
			1.50 GPa	0.0115	0.3126	0.7735
	10 m/s	100°C	1.00 GPa	1.2665e-3	0.0705	1.7008
			1.25 GPa	3.7958e-3	0.1613	1.2022
			1.50 GPa	6.8491e-3	0.2614	1.3263
		125°C	1.00 GPa	6.8144e-4	0.0649	2.6125
			1.25 GPa	2.7822e-3	0.1213	1.1023
			1.50 GPa	5.1027e-3	0.2104	1.1756
		175°C	1.00 GPa	2.0465e-3	0.1161	0.3720
			1.25 GPa	2.0303e-3	0.0370	0.5255
			1.50 GPa	3.0503e-3	0.1357	1.0274
	15 m/s	30°C	1.25 GPa	0.0160	0.5541	2.9663
			1.50 GPa	0.0257	0.7605	3.5975
			100°C	1.00 GPa	4.9512e-3	0.0460
			1.25 GPa	3.6870e-3	0.1688	1.2978
			1.50 GPa	7.1801e-3	0.2991	1.4055
			125°C	1.00 GPa	0.0419	4.1072e-3
			1.25 GPa	2.1411e-3	0.1081	1.2259
			1.50 GPa	4.2028e-3	0.2135	1.4844
			175°C	1.00 GPa	3.7452e-4	1.3206e-5
			1.25 GPa	1.2850e-3	0.0826	2.4531
			1.50 GPa	7.3684e-3	0.1947	0.6177
			20 m/s	30°C	1.00 GPa	0.0100
	1.25 GPa	0.0177			0.6568	4.2929
	1.50 GPa	0.0266			0.9092	5.3156
		100°C	1.00 GPa	1.5540e-3	0.1001	1.4839
			1.25 GPa	3.8979e-3	0.2041	1.4432
			1.50 GPa	7.6347e-3	0.3427	1.6641
		125°C	1.00 GPa	5.4185e-4	0.0591	3.6926
			1.25 GPa	1.4224e-3	0.0751	1.1223
			1.50 GPa	2.4629e-3	0.1332	1.3826
		150°C	1.00 GPa	1.3876e-3	0.0108	0.3306
			1.25 GPa	2.0389e-3	0.0222	0.3892
			1.50 GPa	1.4189e-3	0.0914	1.5923
Mil-I-23699	5 m/s	30°C	1.00 GPa	5.1641e-3	0.1807	1.6204
			1.25 GPa	6.3025e-3	0.1921	3.5676
			1.50 GPa	0.0553	1.3024	0.8645
		100°C	1.00 GPa	8.9301e-3	0.1707	0.4210
			1.25 GPa	6.7747e-3	0.1457	0.5887
		1.50 GPa	0.0351	0.6958	0.6553	

SIGMA PLOT CURVE FIT

MODEL 1

PKG MODEL

HAMROCK MODEL

<pre> [Parameters] kmax=.04m=.01 [Variables] x=col(1)y=col(2) [Equations] f=-kmax + 2*kmax/(1+exp(- 2*m*x/kmax))fit f to y [Constraints] [Options]</pre>	<pre> [Parameters] a=-.02b=.02c=-.5d=.02 [Variables] x=abs(col(5))y=abs(col(6)) [Equations] f=((a+b*x)*exp(c*x))+dfit f to y [Constraints] b>0 [Options]</pre>	<pre> [Parameters] a=.011b=.3c=3 [Variables] x=abs(col(1)) y=abs(col(2)) [Equations] f=(a*x)/(1+(b*x)^c)^(1/c)f it f to y [Constraints] [Options]</pre>
--	---	--

Graph 1

Mil-L-7808K

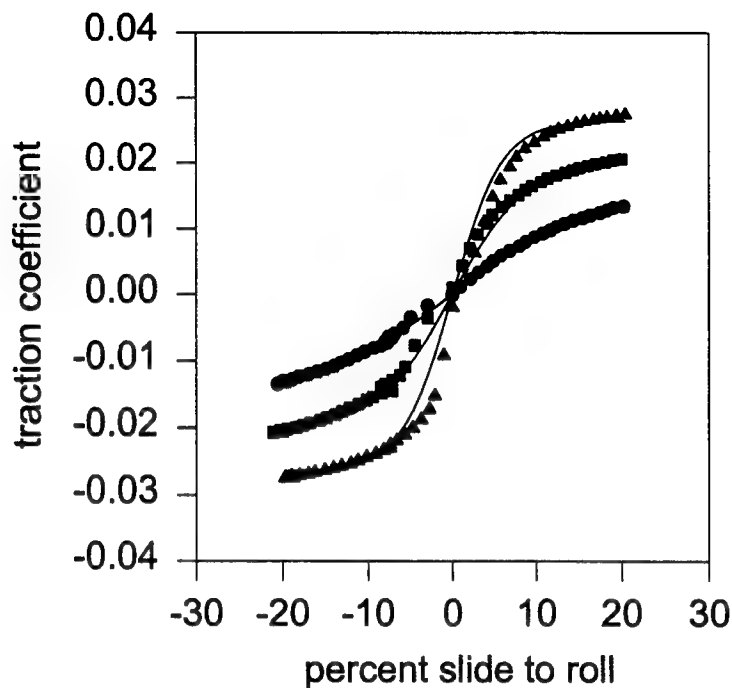
5 m/s

100 deg.C

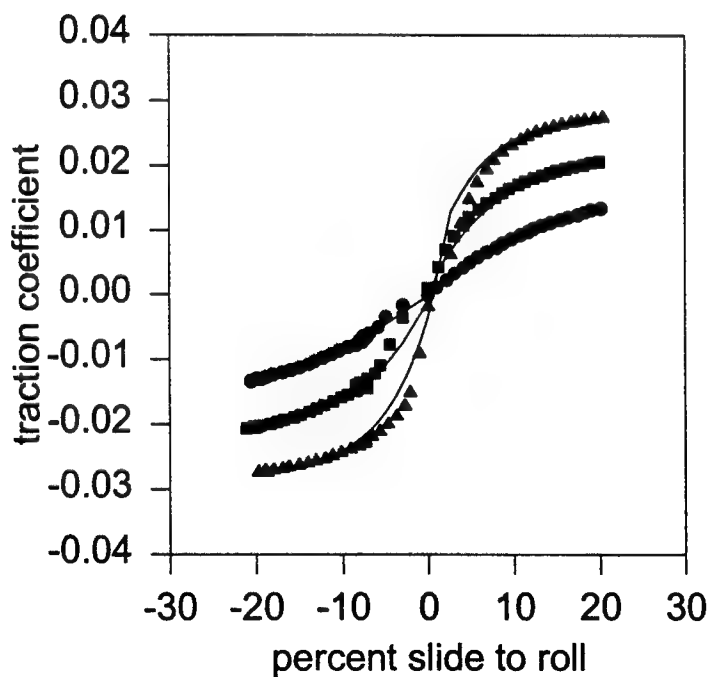
Pressure

- 1.00 GPa
- 1.25 GPa
- ▲ 1.50 GPa

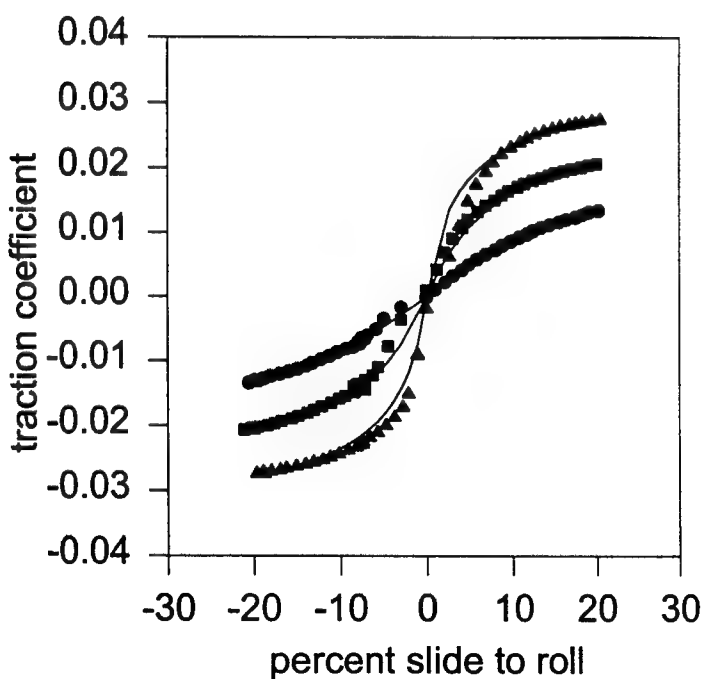
Model 1



PKG Model



Hamrock model

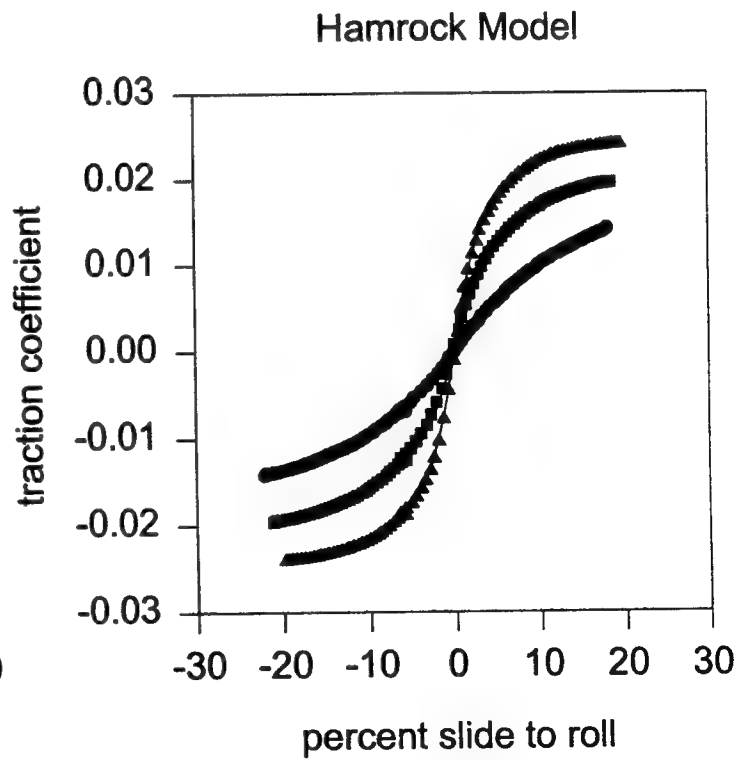
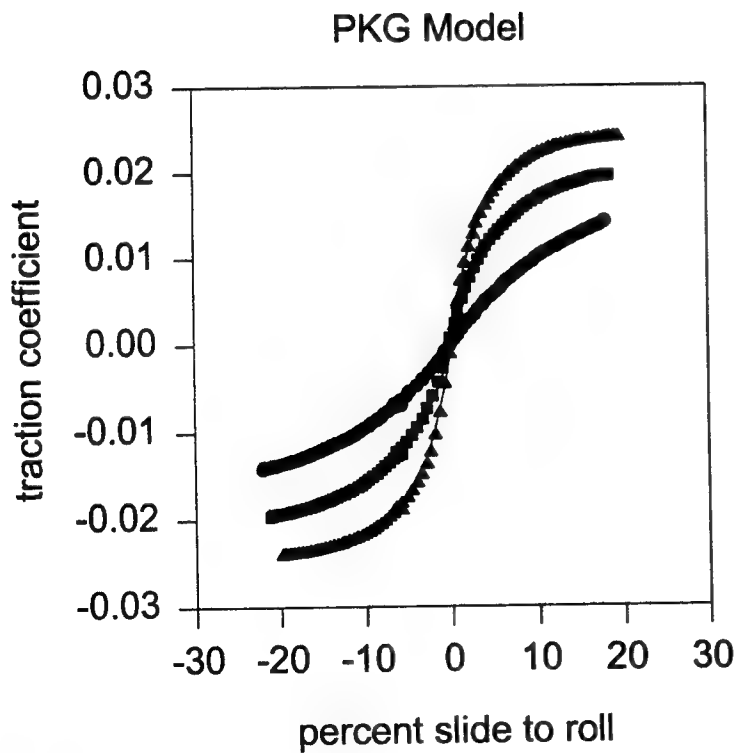
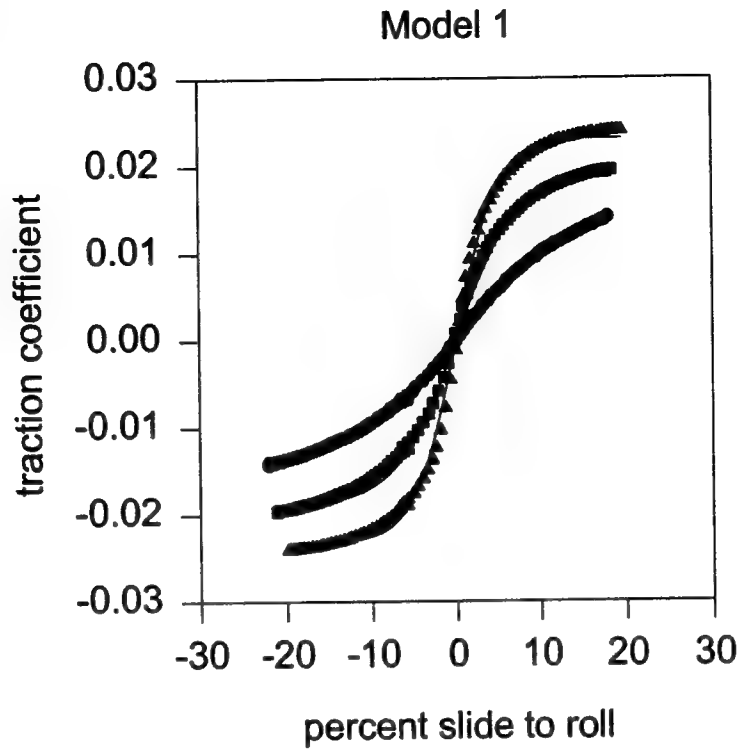


Graph 2

Mil-L-7808K
10 m/s
100 deg.C

Pressure

- 1.00 GPa
- 1.25 GPa
- ▲ 1.50 GPa



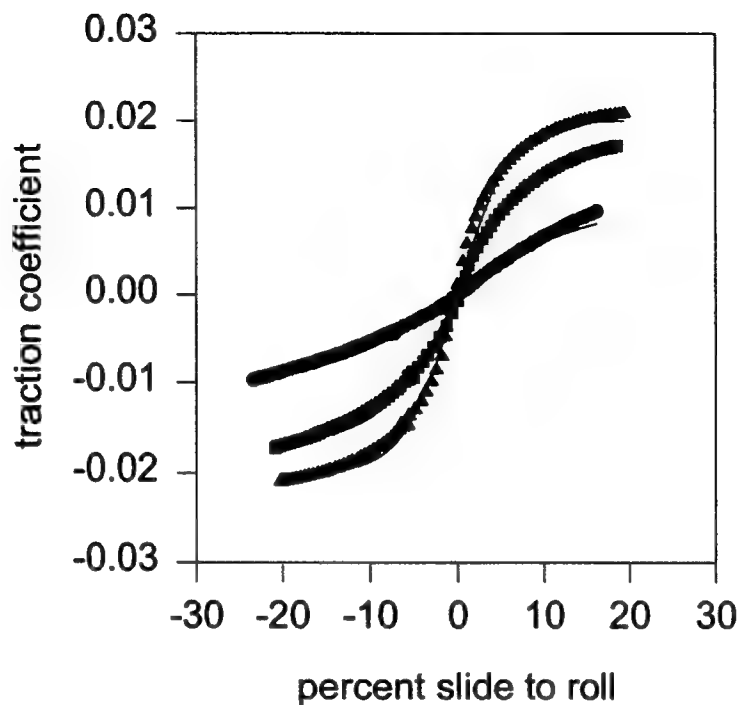
Graph 3

Mil-L-7808K
10 m/s
125 deg.C

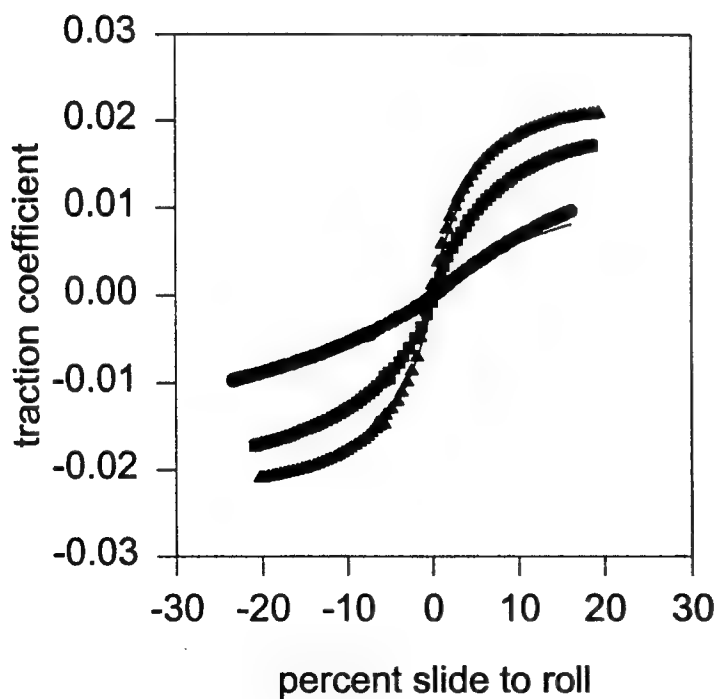
Pressure

- 1.00 GPa
- 1.25 GPa
- ▲ 1.50 GPa

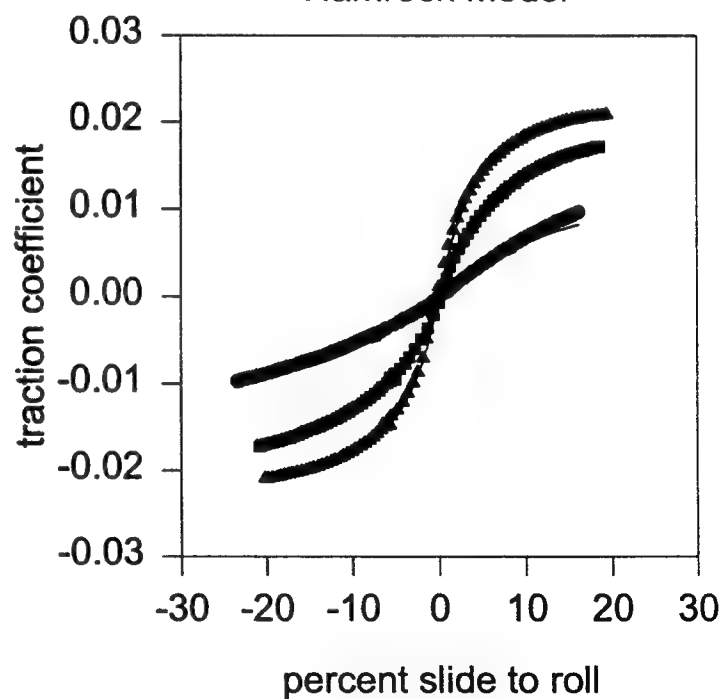
Model 1



PKG Model



Hamrock Model



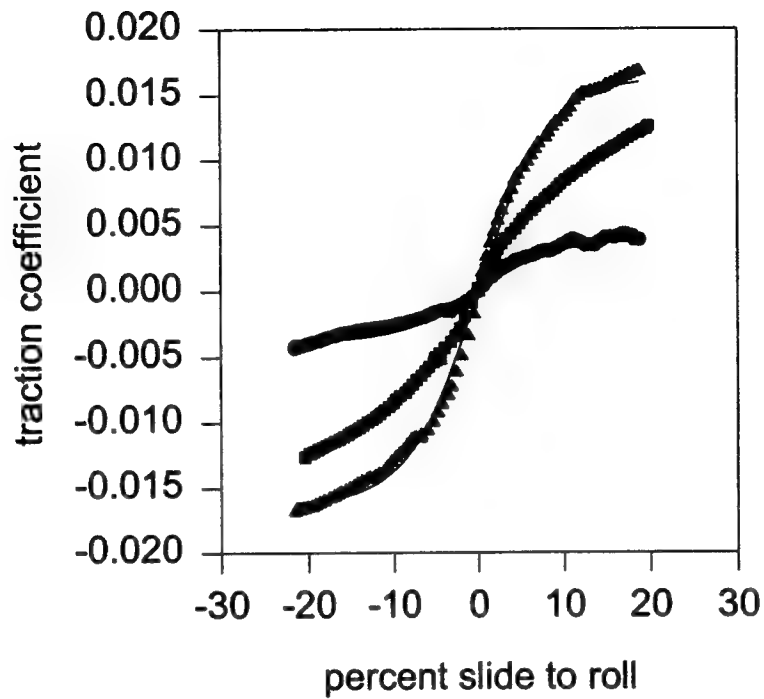
Graph 4

Mil-L-7808K
10 m/s
175 deg.C

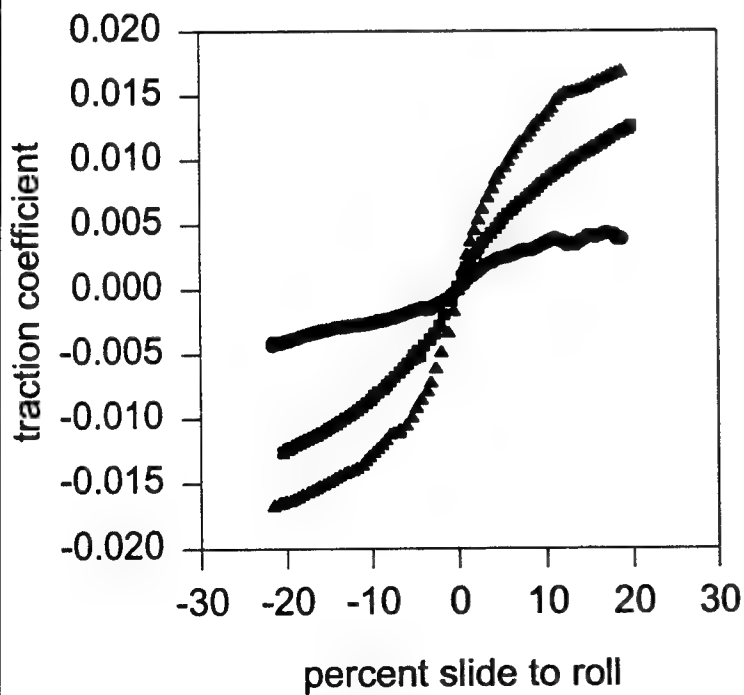
Pressure

- 1.00 GPa
- 1.25 GPa
- ▲ 1.50 GPa

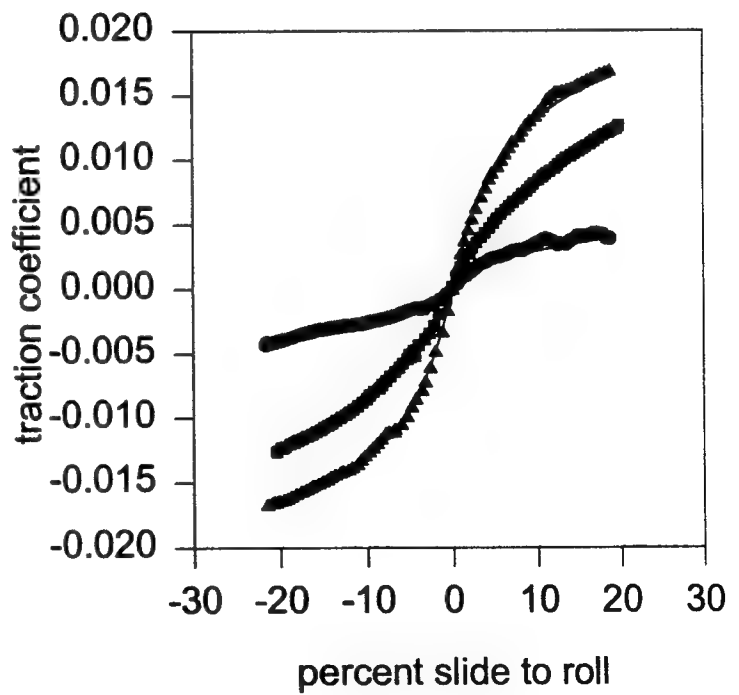
Model 1



PKG Model



Hamrock Model



Graph 5

Mil-L-7808K

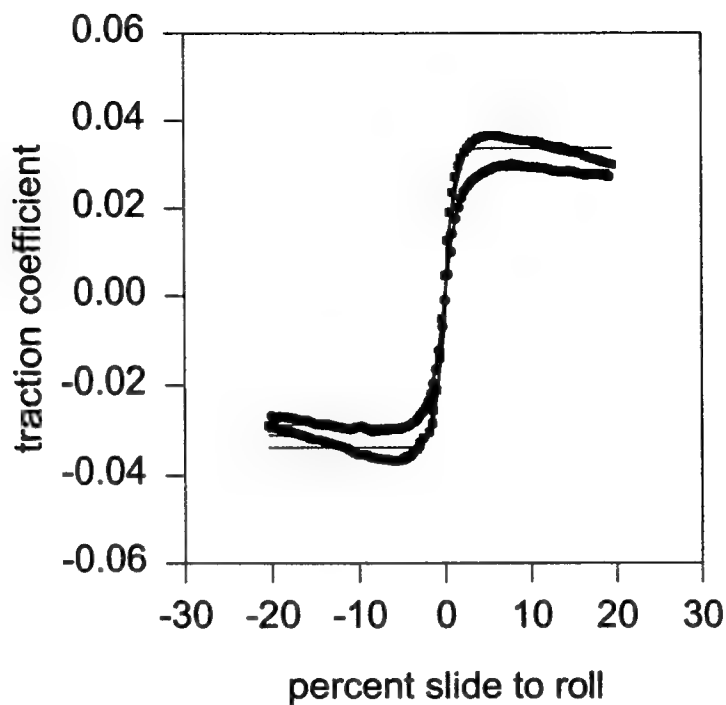
15 m/s

30 deg.C

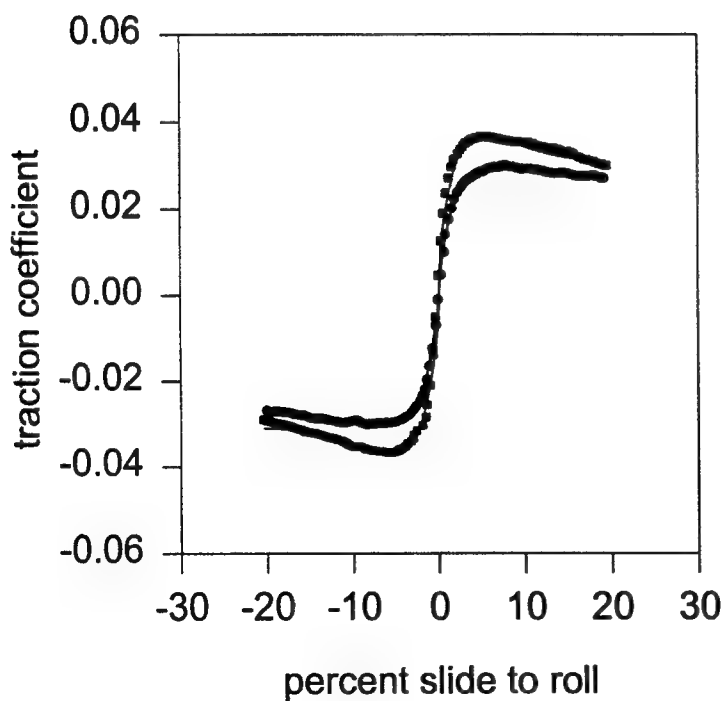
Pressure

- 1.25 GPa
- 1.50 GPa

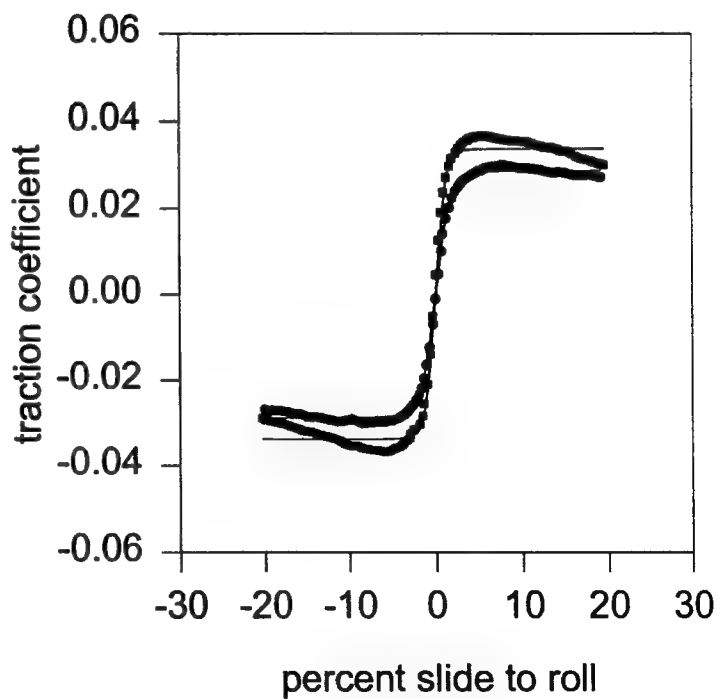
Model 1



PKG Model



Hamrock Model

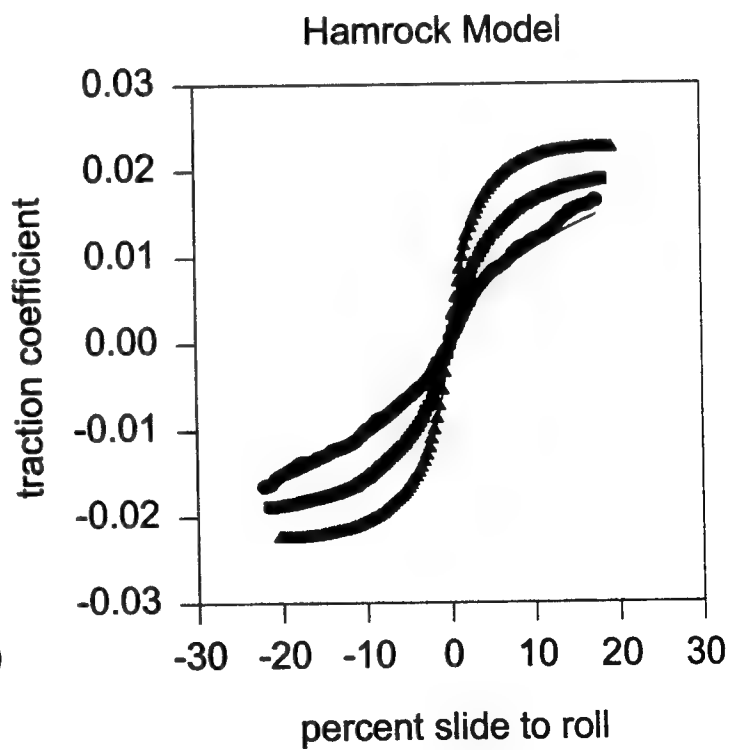
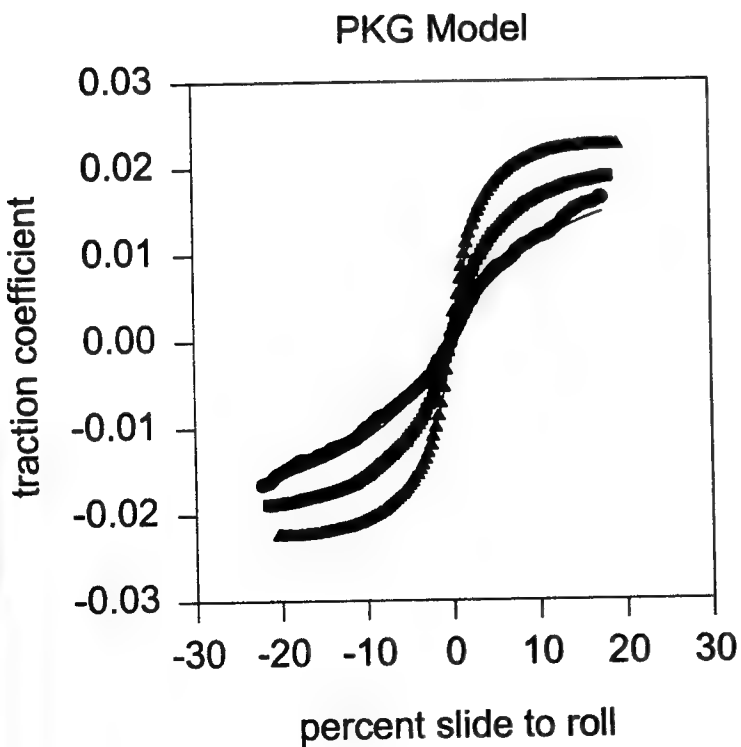
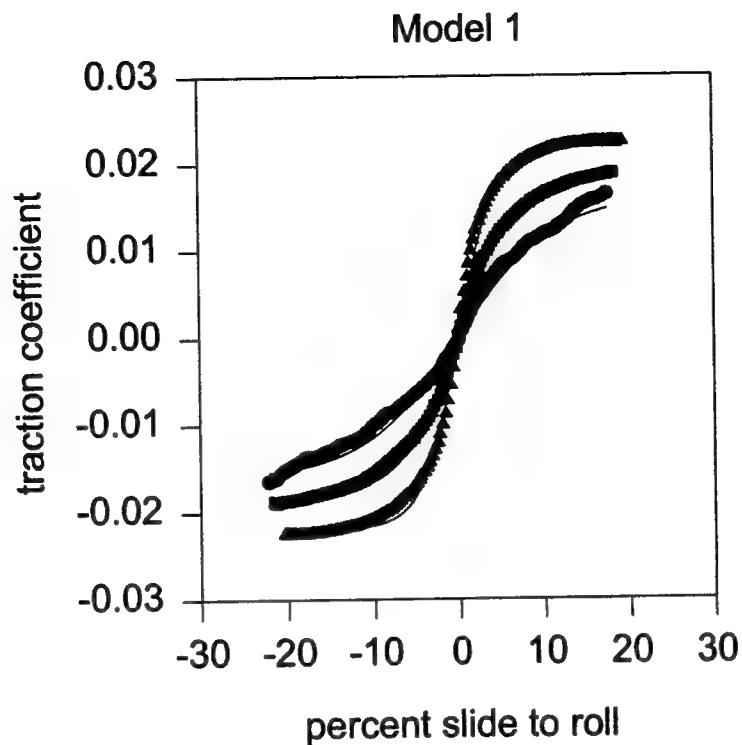


Mil-L-7808K
15 m/s
100 deg.C

Graph 6

Pressure

- 1.00 GPa
- 1.25 GPa
- ▲ 1.50 GPa

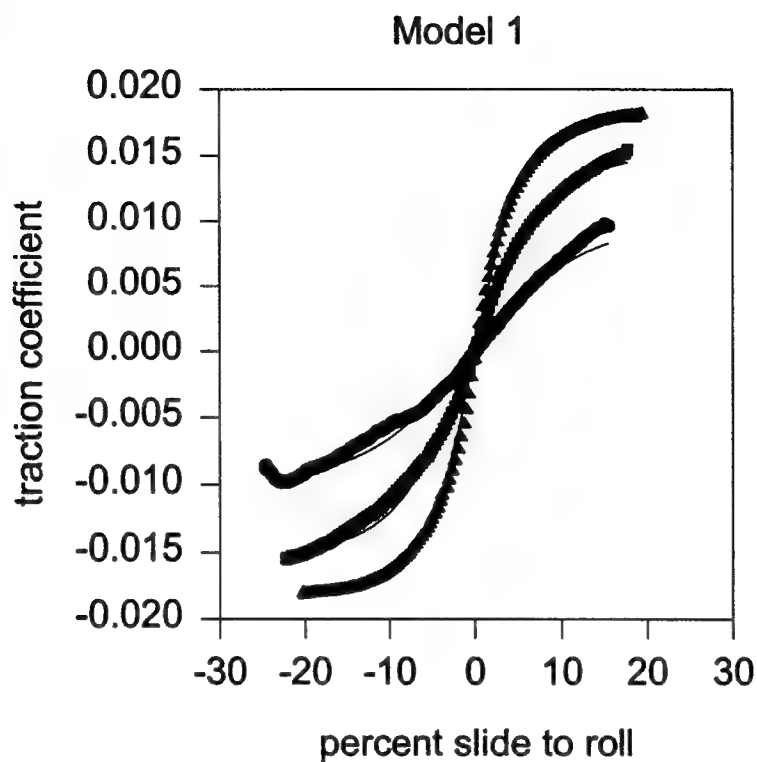


Mil-L-7808K
15 m/s
125 deg.C

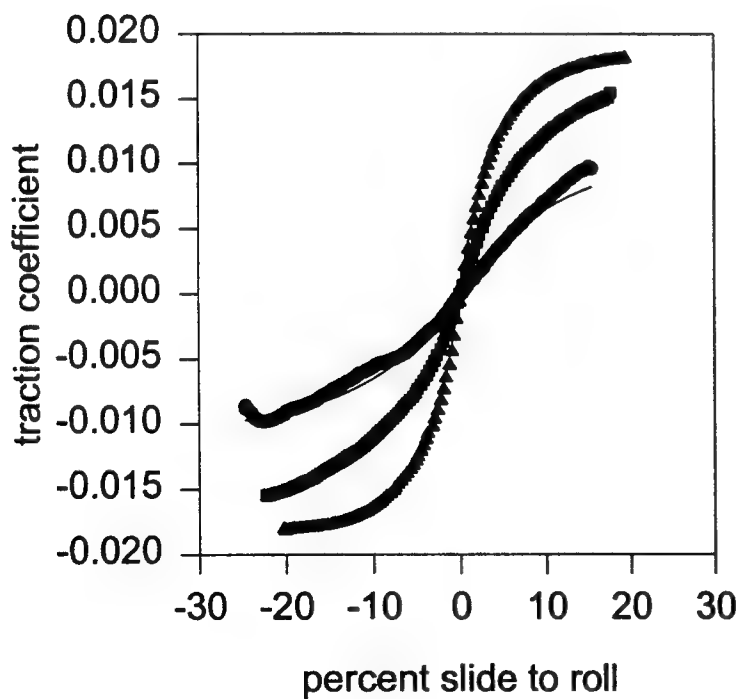
Graph 7

Pressure

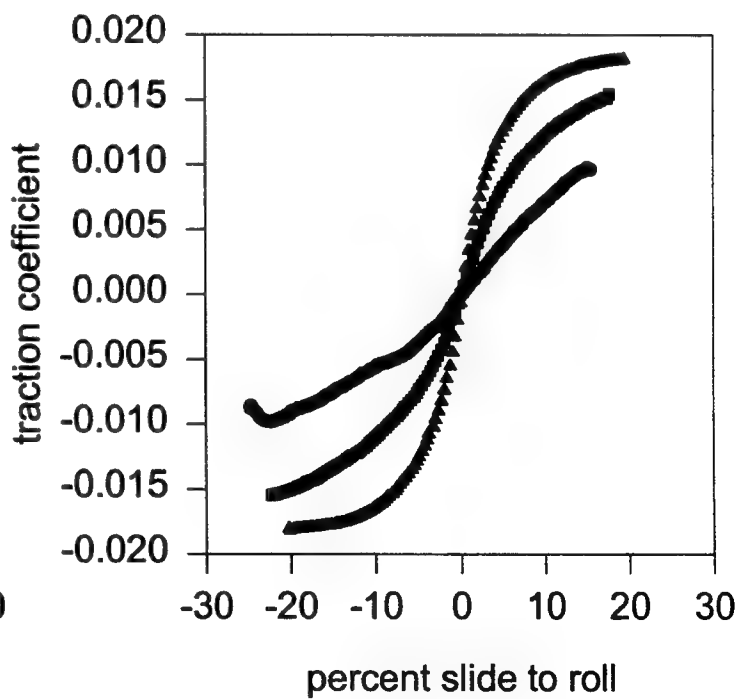
- 1.00 GPa
- 1.25 GPa
- ▲ 1.50 GPa



PKG Model



Hamrock Model

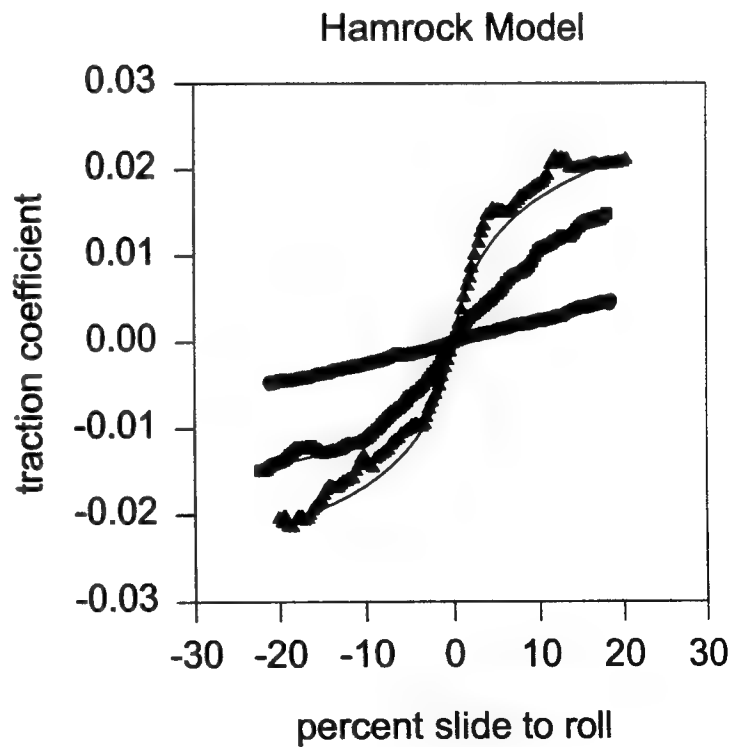
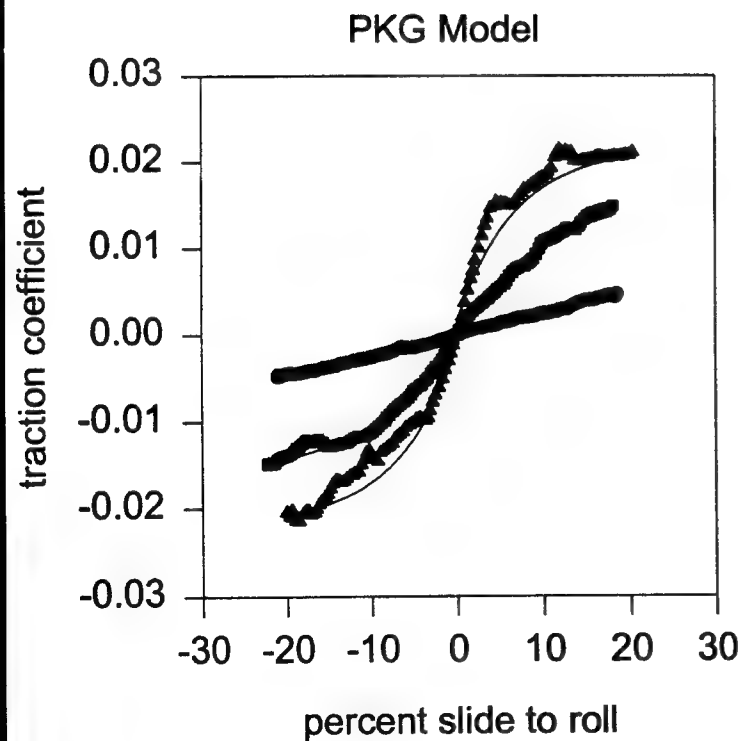
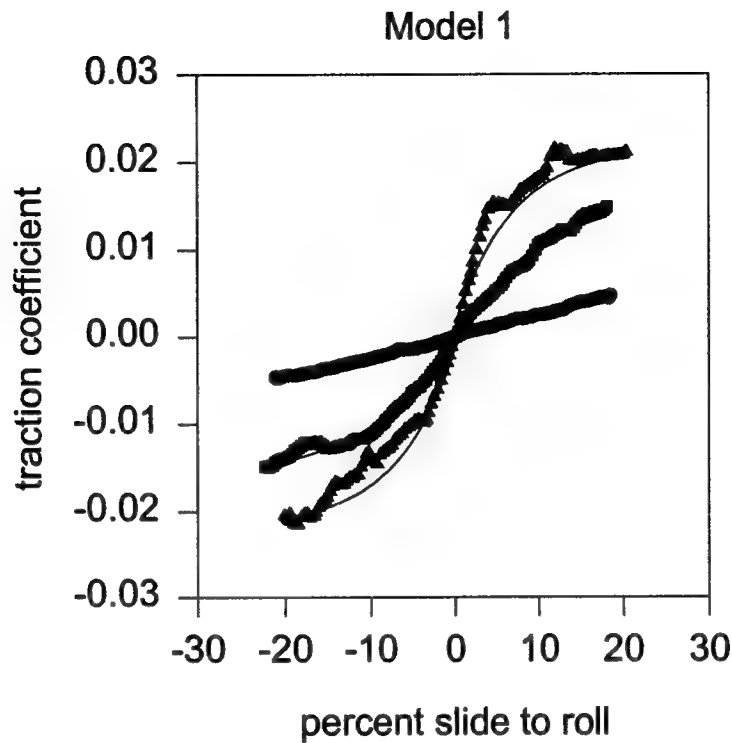


Graph 8

Mil-L-7808L
15 m/s
175 deg.C

Pressure

- 1.00 GPa
- 1.25 GPa
- ▲ 1.50 GPa

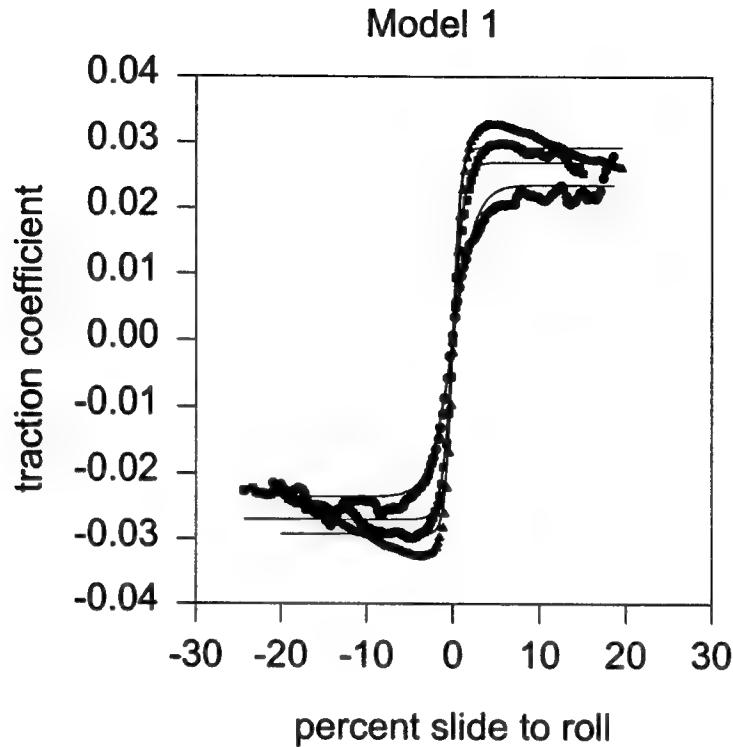


Graph 9

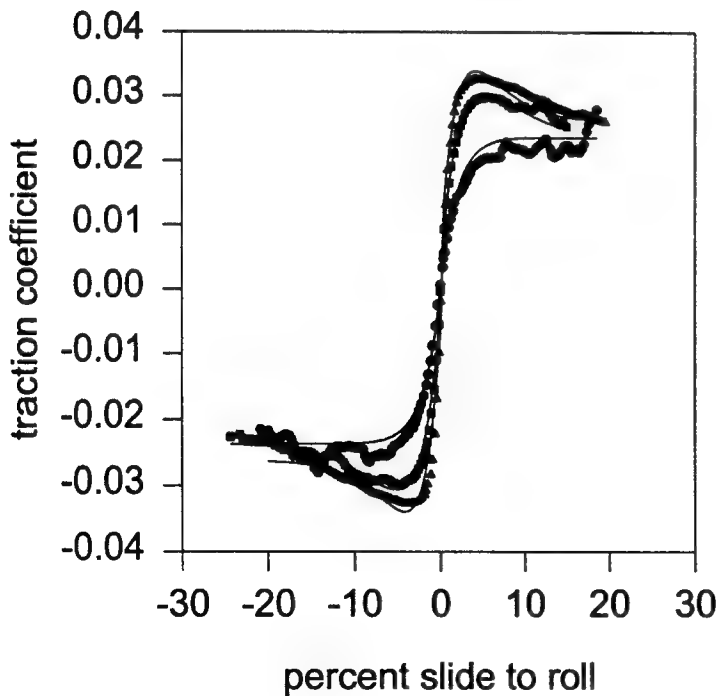
Mil-L-7808K
20 m/s
30 deg.C

Pressure

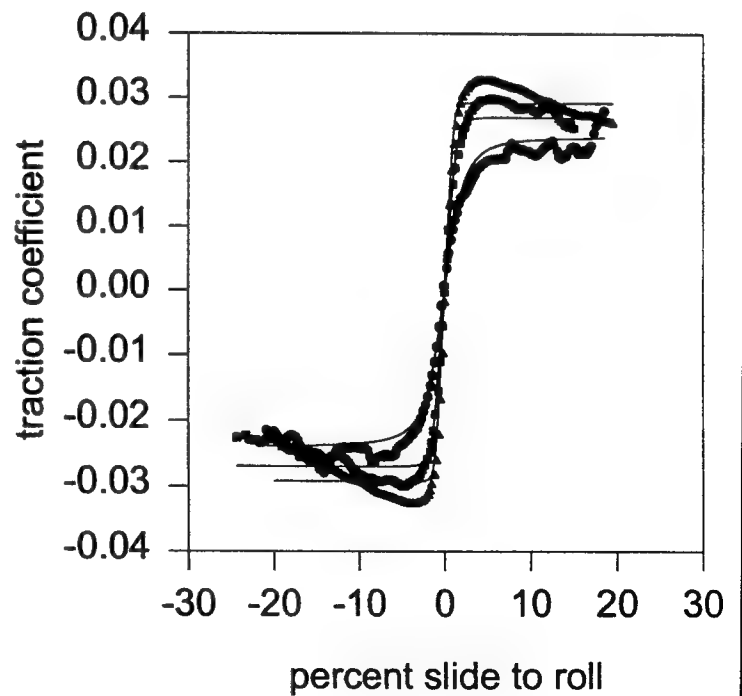
- 1.00 GPa
- 1.25 GPa
- ▲ 1.50 GPa



PKG Model



Hamrock Model



Associate did not participate in the program.

Technical Report Library User's Manual

Landon W. Frymire

**Laurel Hill High School
8078 Fourth Street
Laurel Hill, FL 32567**

**Final Report for:
High School Apprenticeship Program
Wright Laboratory**

**Air Force Office of Scientific Research
Eglin Air Force Base, FL**

and

Wright Laboratory

August 1997

Table of Contents

<u>Title</u>	<u>Page</u>
Introduction	3
Opening the Technical Report Library	4
Beginning a Report Search	5
Editing and Adding New Reports	7
Conclusion	10
References	10

Introduction

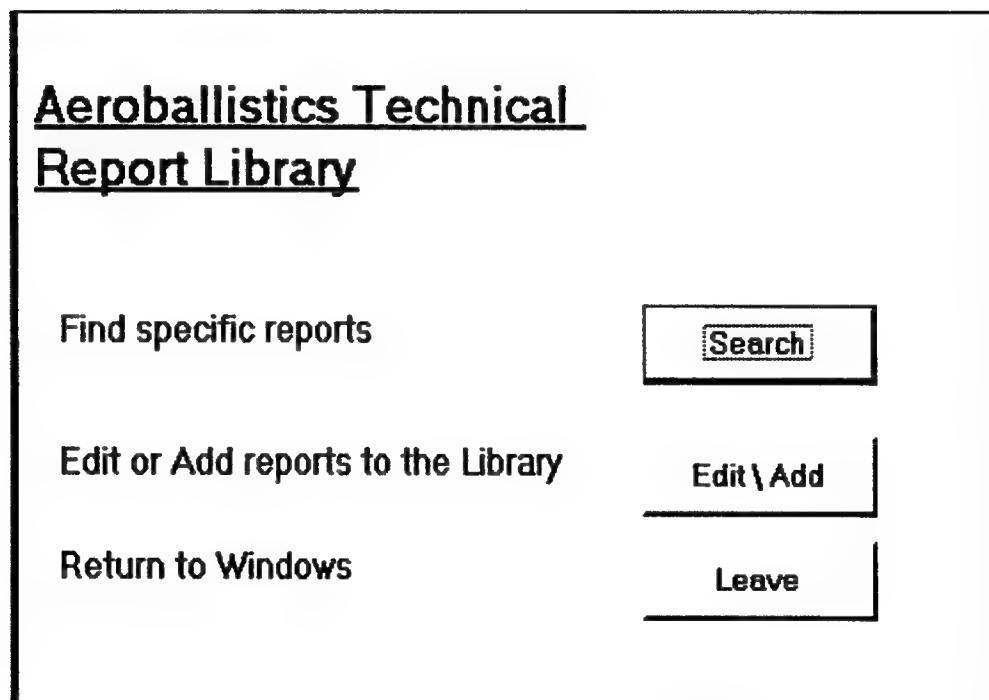
Within the Aeroballistics Section of Wright Laboratory, Armament Directorate, Eglin Air Force Base, FL, there are over five-hundred reports pertinent to the work done by the section. This large amount of unorganized data makes it difficult to find a specific report written on a subject currently being researched. In the past engineers in the section have relied on each other to recall the author and location of the report desired. Therefore, due to the difficulty and possibility of retirement\downsizing in the future, an organized system with search capabilities was needed to simplify and increase the rate at which a report can be found.

With these objectives in mind a technical report library was created using the Microsoft Access database program. An automated database was created using Microsoft Access and the programming language Visual Basic. The basic Microsoft Access objects were customized to receive data from the user. Then Visual Basic code was used to link the objects and run the program. Each report was then entered into a table containing the report title, author's name, keywords pertaining to the report, the report number, and date completed. To enable the search system to work, queries were designed that use forms to obtain the necessary information from the user. After the required forms were created a report was formatted to print a hardcopy of the results. Finally, event procedures were created using Visual Basic which in essence is what is responsible for running the database program.

This report therefore is intended to provide the user with information concerning the setup of the database, the capabilities, and procedures.

Opening the Technical Report Library

1. Begin Microsoft Access.
2. Open the file named **Technical Report Library**. Once you have selected the above file the Main Menu (Figure 1) will appear.



**Aeroballistics Technical
Report Library**

Find specific reports	<input type="button" value="Search"/>
Edit or Add reports to the Library	<input type="button" value="Edit \ Add"/>
Return to Windows	<input type="button" value="Leave"/>

Figure 1 Main Menu

Beginning a Report Search

Using the report search option is like using the card catalog in a library. The database is setup using several fields which all contain data about the report. Each field can be searched using specific information using a query. A query is an object that receives information from the user and applies it to the database. The Technical Report Library is setup in such a way that the user is given a dialog box which prompts for the criteria it uses to narrow down the results. The Technical Report Library also has the capability of searching through the database using more than one criteria.

To begin a search of the Technical Report Library using one set of criteria

1. On the Main Menu click the Search Button.
2. Once the Search Dialog box (figure 2) is displayed, enter the information in the appropriate box and click on the check box located directly to the right of the entered text.
3. Click the Ok button to initiate the search.

Report Title:	<input type="text"/>	<input type="checkbox"/>	<input type="button" value="Ok"/>
Author(s):	<input type="text"/>	<input type="checkbox"/>	
Key Words:	<input type="text"/>	<input type="checkbox"/>	<input type="button" value="Close"/>
Report Number:	<input type="text"/>	<input type="checkbox"/>	
Date:	<input type="text"/>	<input type="checkbox"/>	

Figure 2 Search Dialog Box

To search the database using multiple criteria.

1. Click the Search Button on the Main Menu.
2. Enter the first set of criteria in the desired box and click in the check box to the right of the text.
3. Enter the next set of criteria in its box and again click the appropriate check box.
Continue entering data and selecting the check boxes for each set of criteria entered.
4. Click the OK button in order to begin the multiple search.

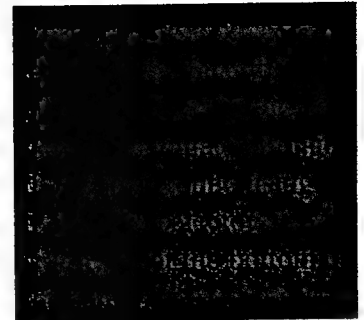
The Technical Report Library also allows to create a hardcopy of your results.

This feature allows anyone to print up a report of the information and take it to the filing system to find each of the reports desired.

To print out the results of a search.

1. Conduct a search for the needed reports. Pg. 2
2. On the Search Results screen (figure 3) click on the **Print button**.
3. Once you have previewed in its formatted form click on the print button

 to beginning printing.







<u>Search Results</u>	
Report Title	Aerodynamic Test Results: Scaled 105-mm XM915/M916
Date	3/1/89
Key Word	Spin-Stabilized Large caliber projectiles, XM915, XM916, M483
Author	Abate, Gregg ; Wong, Brian ; Hathaway, Wayne
Report Number	ATATL-TR-88-161
<div>PrintClose</div>	
Record:  1  of 9	

Figure 3 Search Results

Editing and Adding New Reports

The second option on the Main Menu, the Edit/Add option, is a feature that allows the user to input data, add data, and find reports when only bits and pieces of information are available that would not be sufficient for a complete search.

To add a new report to the library

1. Open the edit screen.
2. Click the new record button ►* in the record selector (figure 4).
3. Type the new data in the appropriate box.
4. Click the close button when finished. The program will automatically insert the report into the table and open the table to enable you to assign it a file number.
5. Use the find button  to locate the new report(s).
6. Once the report has been located assign it a number between the file number directly above it and the one directly below.
7. Close the table by using the close button  in the top right-hand corner.

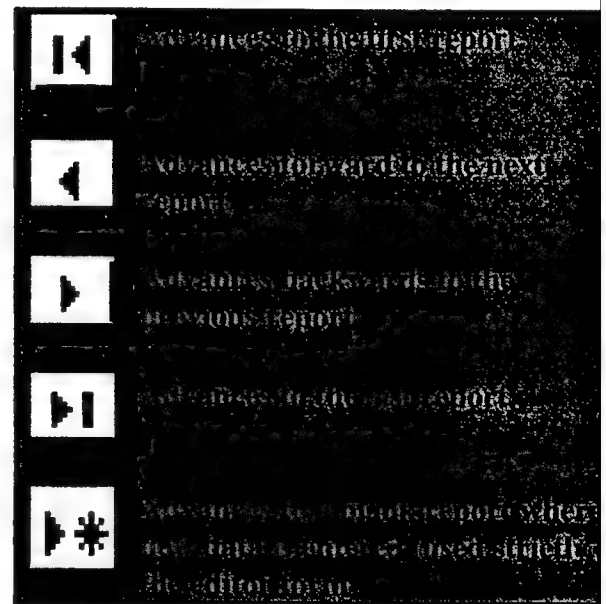
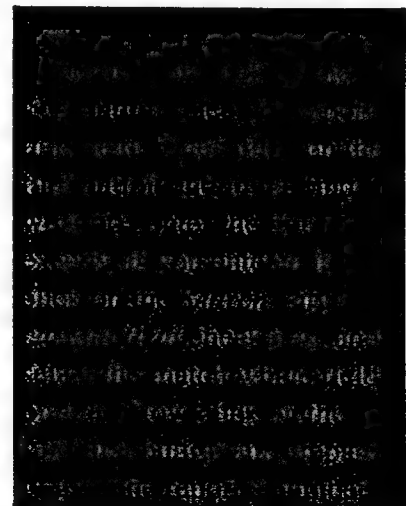



Figure 4

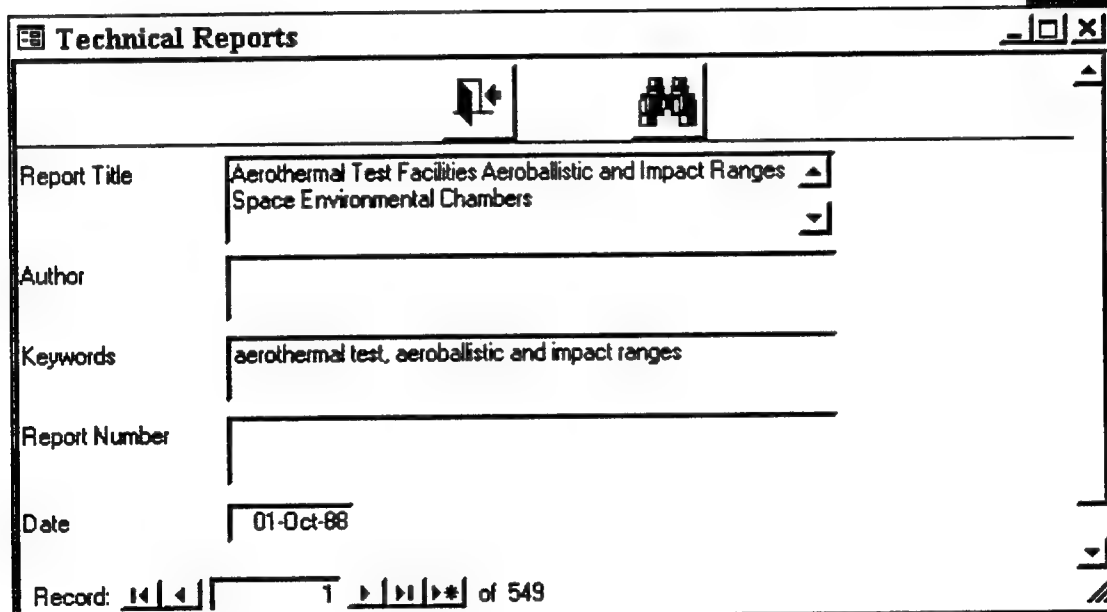


Editing data for old reports.

1. Begin by clicking on the **Edit/Add button** in the Main Menu. This opens the editor form

(figure 5) where all of the changes are made to information in the table's fields.

2. Click on the find button  in order to open the find dialog box.
3. Enter the known data in the box and click the **Find Button**.
4. If the field located is the incorrect one, click the **Find Next button** until the desired field is selected.
5. Enter the new data in the field and when finished click on the **Close button**.



Technical Reports

Report Title: Aerothermal Test Facilities Aeroballistic and Impact Ranges
Space Environmental Chambers

Author:

Keywords: aerothermal test, aeroballistic and impact ranges

Report Number:

Date: 01-Oct-88

Record: 1 of 549

Figure 5 Edit form

Conclusion

With the creation of the Technical Report Library an organized system is now in operation. The system allows easy access to the reports in the Aeroballistics Section of Wright Laboratory, Armament Directorate, Eglin Air Force Base, FL. In the event that information is needed on a subject within the section, anyone would now be able to access the library and find the reports that discuss the desired subject. This system also makes the entry of the new reports coming into the section more accurately filed. Finally, the Technical Report Library ensures that in the future despite the retirement of personnel or the ever present threat of downsizing the knowledge stored will not be over looked.

References

On Line Help, Microsoft Access Version 7.00

Schultz, Gregory, Microsoft Access 2.0 for Windows, Course Technology, Inc. 1994

Allison Gadd's report was not available at the time of publication.

THE STUDY OF THE ELECTRO-OPTIC
COEFFICIENTS OF DR-1 AND DANS

Matthew Gerding

Fairborn High School
900 E. Dayton-Yellow Springs Road
Fairborn, OH 45424

Final Report for:
High School Apprenticeship Program
Materials Directorate, Wright Laboratory

Sponsored by:
Air Force Office of Scientific Research
Bolling Air Force Base
Washington, D.C.

and

Wright Laboratory

August 1997

THE STUDY OF THE ELECTRO-OPTIC COEFFICIENTS OF DR-1 AND DANS

Matthew Gerding

Abstract

The electro-optic coefficients of several important poled polymers were measured and recorded to establish a baseline for future reference. The experiment employed allowed us to electrically pole a sample and measure the material's electro-optic coefficient. The experiment followed the basic reflection ellipsometric technique of Teng and Man¹, but with a few variations. The results of these baseline measurements will aid in the research and discovery of new polymers with the necessary characteristic of high electro-optic coefficients and sufficient thermal stability.

THE STUDY OF THE ELECTRO-OPTIC COEFFICIENTS OF DR-1 AND DANS

Matthew Gerding

Introduction

Poled polymer materials are being studied for many optical applications. One of these applications is their usefulness as optical communication modulators. A poled polymer with the aid of an applied modulating voltage field can vary the phase of propagating through the material. The change in optical phase may then be used in a device as a means of optical communication. Many polymers are available, but we chose to use solutions of DR-1 and DANS in poly(methylmethacrylate) (PMMA) because of their simplicity and wealth of published results. We measured the electro-optic coefficients of these polymers and their stability versus time using a basic experimental setup similar to the one used by Teng and Man¹.

Discussion of Problem

In today's world, advancements in technology and science are being made at an astounding and rapidly increasing rate. One of these advancements is the use of polymers in optical communication systems. As new polymers are being discovered and produced, a systematic comparison of these new materials with the older generation materials is needed to determine material improvements. Therefore, a baseline of the characteristics of older polymers is needed. A basic standardized procedure for measuring new materials, is also essential.

The experimental setup was limited by the need for the following considerations: (1) it had to control the temperature of the sample within a range of $\pm 5^{\circ}\text{C}$; (2) it had to be able to apply a strong DC field to the sample in order to pole the material; (3) access to the samples was not to be hindered by the equipment configuration to allow for easy measurement of many samples. Our setup was designed to meet these standards and remain simple and inexpensive.

Methodology

1. Experimental setup

All of our equipment for the experiment was readily available in the lab. First we assembled the electronic equipment and connected them to a Mac II computer via a GPIB bus to allow for easy computer control and data acquisition. Next, a temperature controller and relay were wired together and installed into an aluminum box. The next step was the construction of a sample holder that would accurately control the surface temperature of the sample. A switch box was also designed and constructed to connect a voltmeter, ammeter, and sample to the other necessary electronic equipment. Finally, a switch was added to control a cooling fan that was needed to rapidly cool the sample. The complete experimental setup is shown schematically in Figure 1.

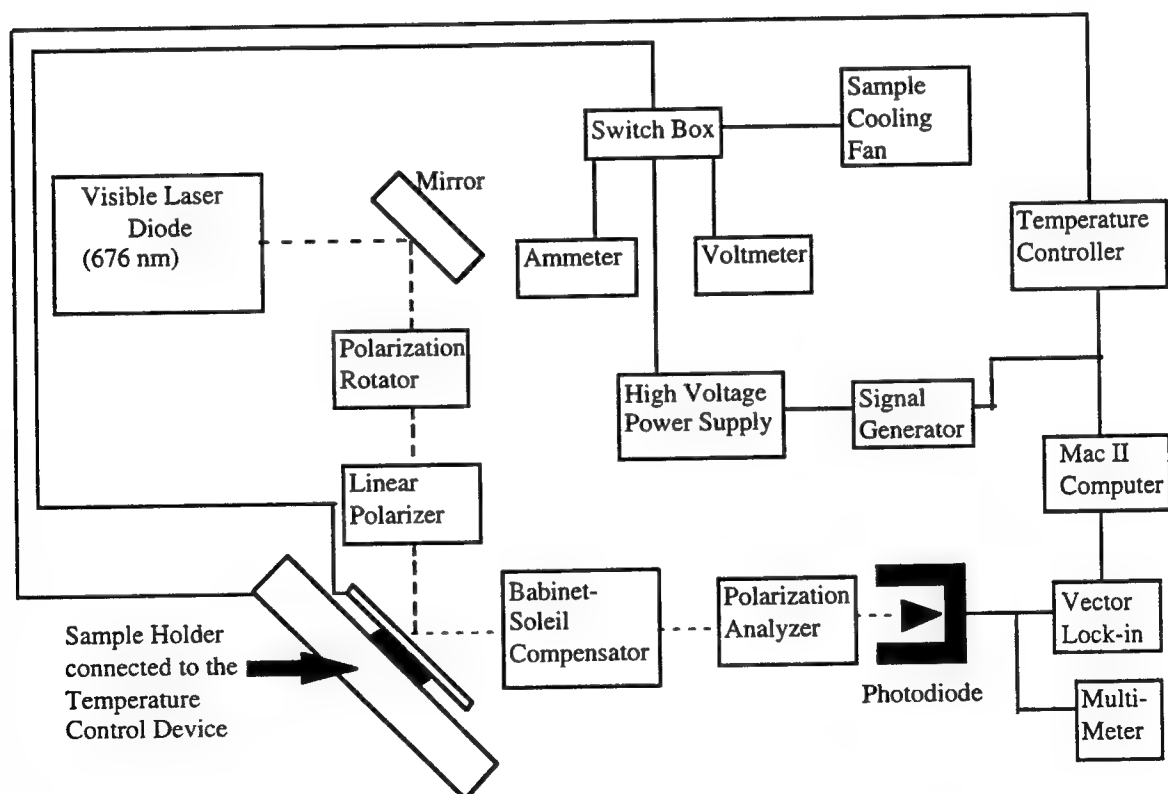


Figure 1. The experimental setup. With this design, we were able to pole polymer samples at different temperatures or measure the decay of the signal versus time.

II. Sample Preparation

The next step was sample preparation and processing. Glass slides which had been coated with indium tin oxide(ITO), an electrically conducting layer that is transparent, were used as substrates for the polymer films. We covered these slides with a self-adhesive clear film, masking about two thirds of the slide. Next, we etched these masked slide in aqua regia consisting of 3 parts hydrochloric acid to one part nitric acid, to remove the ITO from the non-masked part of the slide. After an etch time of one and a half to two minutes in the aqua regia, the ITO slides were rinsed in deionized water and dried with a nitrogen gun to prepare them for spin-coating.

The polymer solutions were prepared by mixing different amounts of the active chromophore in a solution of cyclopentanone containing PMMA. Solutions containing 1%, 5%, 10%, and 15% of DR-1(disperse red one, a common chromophore) were made by adding different amounts of DR-1 (2 mg, 10 mg, 20 mg, or 30 mg) to vials containing 200 mg of PMMA and 2000 mg of cyclopentanone. In a similar way, 1%, 2%, 5%, and 7% solutions of DANS were prepared. These solutions were then mixed for 45 minutes in a mechanical shaker to dissolve all of the chromophore into the PMMA. The solutions were filtered through a two micron filter as the final step before spin coating. The solutions were spin-coated on a Solitec spin-coater for 60 seconds at 750 rpm resulting in a film thickness of one to two microns. After spin coating, the slides were placed in a oven at a temperature of 70° C to dry overnight. Two slides of each DR-1 concentration and one slide for each DANS concentration were prepared. The 1% and 2% DANS solutions were of acceptable quality, but the 5% and 7% DANS particles aggregated in solution during spin-coating and were not of sufficient quality to make any useful measurements on these samples. After curing, portions of the polymer film were removed so that the thickness of the polymer layer could be measured with a Dektak IIA profilometer.

After measuring the thickness, the sample was ready for deposition of metal electrodes. Again the sample was masked, this time with a mask containing three long, rectangular holes which overlapped the small area where there was only polymer and ITO. These openings in the mask allowed gold to be evaporated upon the slides, producing an electrode with which the sample could be poled. Because the gold electrodes have a tendency to become scratched, aluminum contacts were placed on top of the gold electrode and on the ITO end. Figure 2 shows a side-view of a finished electro-optic polymer sample(not to scale).

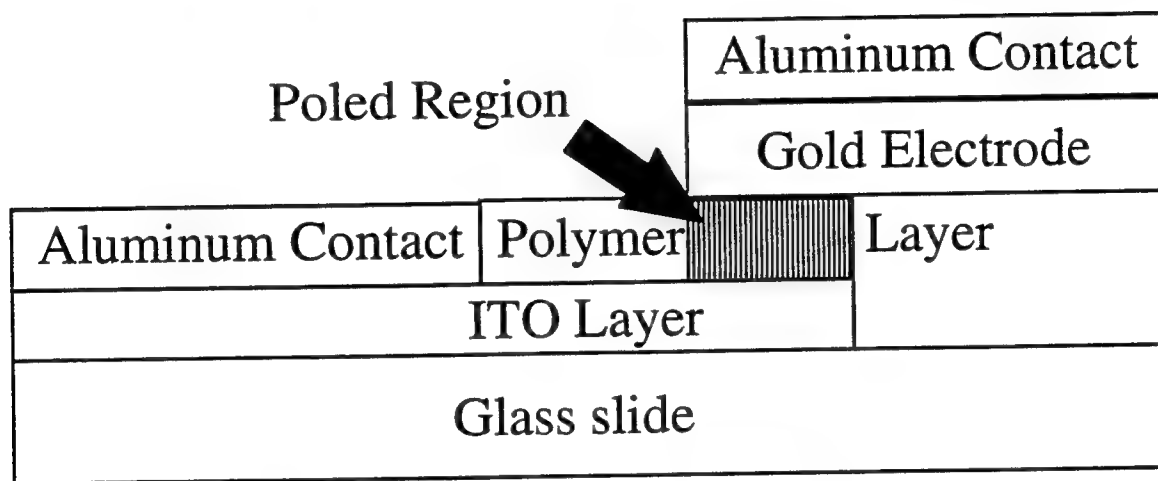


Figure 2. A side view of a completed electro-optic polymer sample ready for characterization. Using connectors attached to the aluminum contacts, a large DC field is applied to the sample at high temperatures to pole the polymers.

III. Polymer Poling and Characterization

In order to establish the necessary baseline data, poling conditions were investigated relating the electro-optic coefficient to the poling temperature (70°C, 80°C, 90°C) and the DC poling field (100 V/ μm , 50V/ μm). The characterization starts by first placing the slide in the sample holder and attached alligator clips to the aluminum contacts.

Next, the optical signal is optimized so that the detection of the reflecting signal was at its maximum (typically this range is 9.60 to 9.80 volts) The minimal signal was then determined by adjusting the Babinet-Soleil compensator. The midpoint of the signal is calculated and the Babinet-Soleil compensator adjusted to this point where the system signal is at its maximum sensitivity (usually 4.9 to 5.1 V). The sample is then heated up to the poling temperature and the DC field applied to the sample. The poling conditions are left to equilibrate for about 10 to 15 minutes, after which the temperature is slowly lowered to room temperature. After the sample temperature reaches about 34° to 36° C, the DC field was removed and the signal from the polymer is monitored for the next 10 to 15 minutes to establish the actual electro-optic coefficient. The following day, the poled polymers were again put back into the experimental setup and the electro-optic coefficient is monitored for 15 minutes to study the decay of the signal versus time.

Results

I. Overall Results

There were four concentrations of DR-1 solution and two concentrations of DANS solution. These polymer solution samples were all poled at 70° C, 80° C, and 90° C with an applied DC poling voltage of 100 V/ μ m. With the poling voltage constant the effect of temperature and chromophore concentration on the electro-optic coefficient could be studied. The DANS sample results were not consistent enough to be of any practical use in establishing a baseline. The electro-optic coefficients from the DANS samples were very low and were probably composed of more background noise than anything else. The DR-1 electro-optic values were of an acceptable quality and will prove useful for future reference and research. A data table containing all of the DR-1 measurement results are presented in Figure 3.

	70 ° C	70° C	80° C	80° C	90° C	90° C
	End of Test	Next Day	End of Test	Next Day	End of Test	Next Day
1% DR1-1	0.61	0.25	0.70	0.39	0.85	0.40
DR1-2	0.50	0.21	0.60	0.32	0.62	0.42
5% DR1-1	2.90	1.03	3.00	1.61	2.65	1.37
DR1-2	2.05	0.74	2.70	1.40	3.50	2.98
10% DR1-1	5.55	3.48	5.90	3.43	6.65	4.01
DR1-2	5.95	2.98	5.05	2.45	5.97	3.51
15% DR1-1	6.85	2.99	9.00	4.40	8.90	4.77
DR1-2	7.01	2.96	7.50	3.59	8.50	4.54

Figure 3. This data table contains the electro-optic coefficient measurements in pm/V taken on each slide both at the end of the test and the next day.

II. End of Test Results

The values measured at the end of the test were taken for 10 to 15 minutes after the voltage had been removed and after the sample temperature was down between 26° C and 28° C.

The different poling temperatures made only a slight difference in the electro-optic measurement of the samples. However, a bigger factor in the end result of the chromophore's electro-optic value was the sample doping concentration. As the doping concentration of the chromophore is increased in the sample, the measured EO coefficient can be seen to rise proportionally. These results are shown in Figure 4.

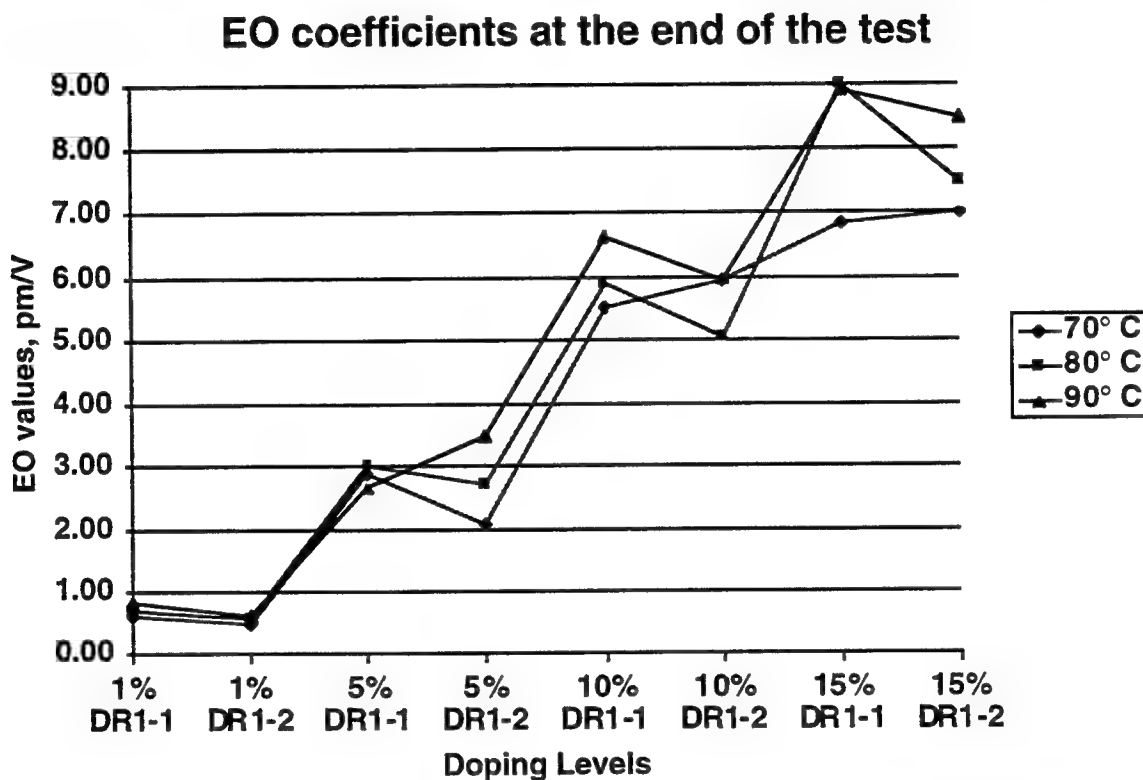


Figure 4. The electro-optic coefficients of DR-1 versus doping levels for three different poling temperatures. The differences in temperature do not show a significant difference, but increasing the dopant concentration clearly results in larger EO values.

The differences seen in the measured values of the slides doped at the same levels, i.e. 1% DR-1 slide one and slide two, can be attributed to many errors. One of these errors could be a difference in actual concentration of the chromophore in the samples. The 1% DR-1 slide two may contain a concentration that is lower than the 1% DR-1 slide one.

A second source of error could be due to the thickness measurements of the polymer films. Sample thickness was measured through a tiny scratch in the middle of the slide. A total of two measurements were taken on each slide and then averaged. The applied poling voltage was then calculated using this thickness measurement to achieve approximately $100 \text{ V}/\mu\text{m}$. If the measurements were taken at a low or high point of the sample, the applied voltage would not be correct. Due to equipment limitations, the applied voltage was not always exactly 100 volts per micron. For example, if the thickness of the sample was 1.53 microns, we would have to round up to 160 volts for that sample. Also there could be differences between the gold and aluminum contacts on each slide. If the gold was scratched/pitted the laser would not reflect the same giving different values for each measurement. Also the temperature and time that the poling voltage was removed before the final measurement started was not consistent for every sample. With all of these errors considered, the differences in the measurements from slide to slide can be understood.

III. Next Day Results

Electro-optic measurements were taken the following day to determine the thermal stability of the chromophore alignment in the host material. The trends and errors affecting the measurements the previous day are still affecting the values the next day. While most of the data tracks values from the previous day, some differences do exist. These differences could be the result of not re-measuring a sample after the same amount of time has passed. For example, sometimes a slide sat for only sixteen hours before it was measured again, other times the slide could have waited for almost twenty-four hours before the final measurement was made. This produces a great amount of difference and error in the next day's measurements.

Figure 5 shows the EO values for the samples measured the following day.

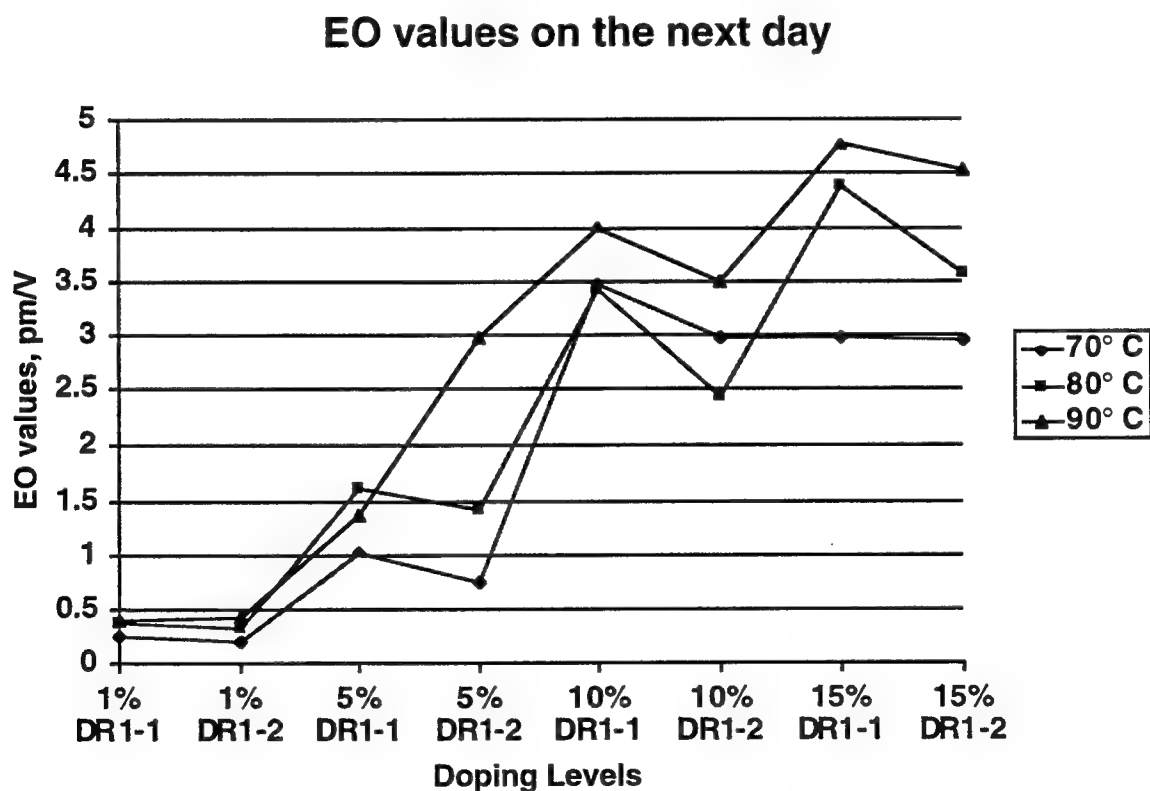


Figure 5. The electro-optic values after a period of time. The same trends can be seen in this graph as in the one of the values at the end of the test. The variations due to temperature do not appear to be significant, but a clear trend shows that higher doping concentrations improve the EO coefficient.

IV. EO Graph

As the data was collected, a computer monitored the measurements for ease in calculations and storage. The program then compiled this data into very neat and precise graphs. One set of these graphs is shown in Figure 6.

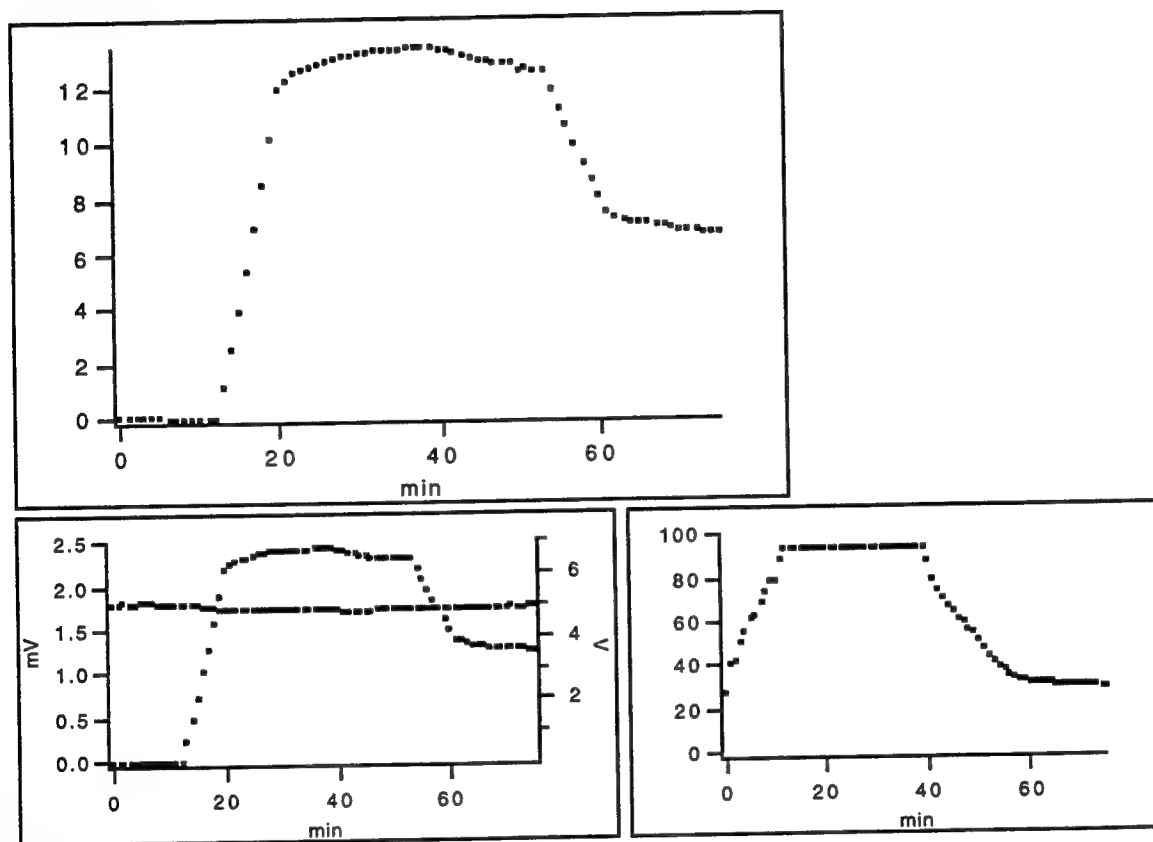


Figure 6. Sample graphs of the data which are collected during the experiments. Along with these graphs, a data table is compiled, showing all comparison of the exact values for each point on every graph, making analysis and comparison easy.

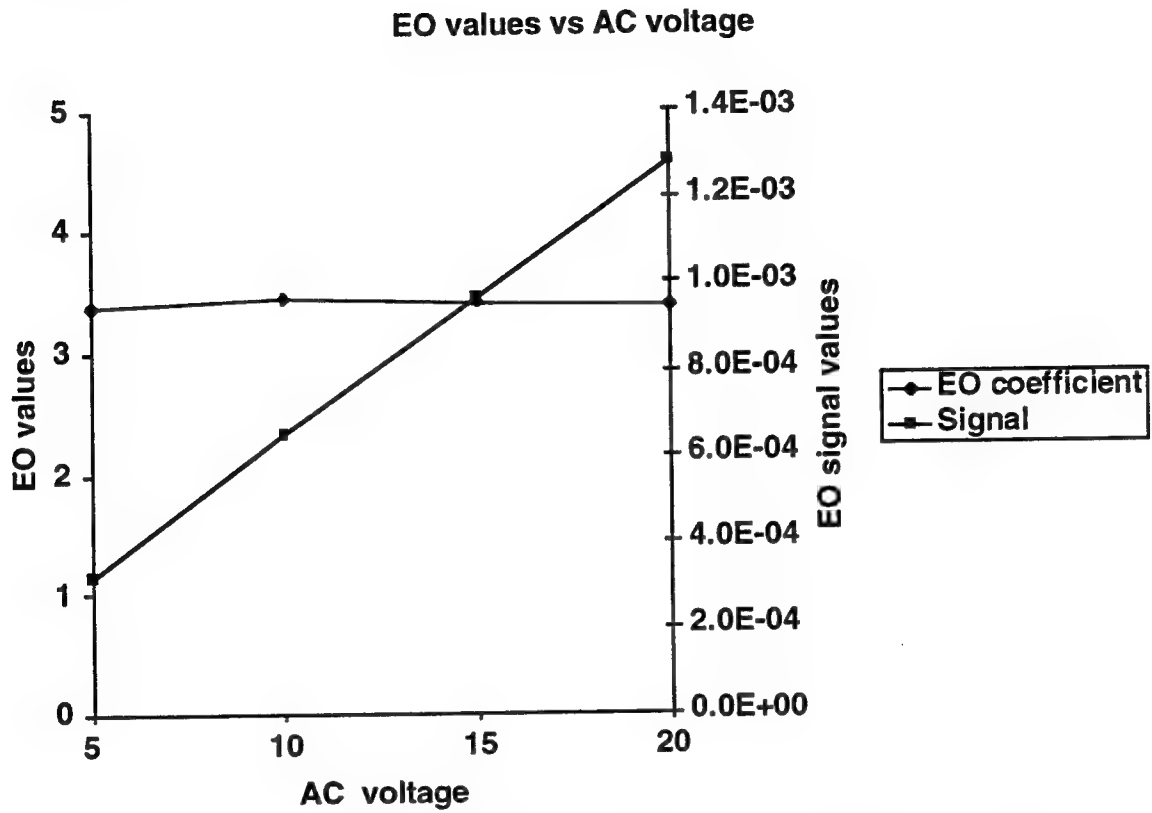
These graphs were made during the poling of the 10% DR-1 slide #1. The poling temperature was 90° C and the voltage that was applied was 160 volts. The largest graph shows the electro-optic coefficient. The smaller one on the right is the temperature and the one on the left contains both the electro-optic signal and the multi-meter signal.

At the beginning of the poling procedure is the measurement of an un-poled sample where the EO value remains flat as the temperature is increased. As soon as the glass transition temperature is reached, the voltage is applied and increased at 20 volts per minute. As the chromophore molecules align under the applied voltage, the EO coefficient begins to increase. The voltage is left on for a period of time to stabilize the sample and then the temperature is slowly lowered. This is indicated by the large, gradual crest in the middle of the graphs. After the sample temperature is low enough, the voltage is brought back down by 20 volts per minute. The sharp decrease at this point in the graphs is from a DC field induced nonlinearity. After the voltage has been completely removed, the program is allowed to run for a short period of time to adequately measure the room temperature EO value of the now poled sample. This is shown by the progressively decreasing points at the end of the graphs. This data format is extremely useful in characterizing the chromophores, but stricter procedures must be made so that the data from every sample can be compared on an equal level.

V. EO versus AC Applied Voltage

When electro-optic values are being measured, the AC voltage which modulates the chromophores is very important. With the application of an AC modulating voltage, an electro-optic signal that is directly proportional to the AC voltage is measured. This occurs because the higher the voltage applied, the more modulation there is in the chromophore, resulting in a larger change in the phase of the laser light. From the electro-optic signal we can calculate an EO coefficient for the sample. This electro-optic coefficient should not vary with the modulation voltage since it is a material property.

Figure 7 shows the relationships of the AC voltage to both the electro-optic signal and coefficient.



	5 AC volts	10 AC volts	15 AC volts	20 AC volts
EO coefficient	3.39	3.45	3.41	3.39
Signal	3.19E-04	6.51E-04	9.64E-04	1.28E-03

Figure 7. The graph and data tables show the direct relationship of the signal to the applied AC modulating voltage and the normalization of the electro-optic coefficient to this voltage.

Conclusion

The design of our experimental setup proved to be quite useful for poling and measuring many polymer samples in a short period of time. There are three main conclusions that can be made about DR-1 from the baseline data: (1) the higher the concentration of disperse red one in the sample, the higher the electro-optic coefficient after poling; (2) the temperature at which DR-1 samples are poled does not make a significant difference as long as the temperature is above the T_g allowing the chromophore molecules to align with the voltage; and (3) the T_g of disperse red one is not high enough for the chromophore to be thermally stable at room temperature after poling, thus resulting in the decay of the electro-optic coefficient with time.

The results of the DANS polings were sufficient enough to conclude that the chromophore is not adequate for electro-optical communications.

Acknowledgments

I would like to thank Drs. Steve Caracci and Steve Hubbard, and Mr. James Drummond for their assistance and support in making these experiments possible. I would also like to recognize Mr. Robert Leese for his help in the fabrication of parts necessary for these experiments.

References

1. C.C. Teng and H.I. Man, "Simple Reflection Technique for Measuring the Electro-Optic Coefficient of Poled Polymers," Appl. Phys. Lett. 56 (18), 1734-1736 (1990).

THE FLIGHT DYNAMICS LAB

Jon M. Graham

**Carroll High School
4524 Linden Avenue
Dayton OH 45432**

**Final Report for:
High School Apprentice Program
Wright Laboratories**

**Sponsored by:
Wright Patterson Air Force Base
Dayton, OH**

and

Wright Laboratories

August 1997

Table of Contents

Title Page.....	16-1
Table of Contents.....	16-2
Abstract.....	16-3
Introduction.....	16-4
Discussion.....	16-4
References.....	16-9
Acknowledgments.....	16-10

THE FLIGHT DYNAMICS LAB

Jon M. Graham
Carroll High School

Abstract

My employment in the Flight Dynamics Lab at Wright Patterson Air Force Base did not consist of a single performed experiment on which data could be retrieved. Rather, it involved various short-term assignments and simple jobs that needed to be done. Even though I did not perform a professional experiment, as it were, the time I spent over the summer was extremely valuable. I learned a great deal about the modern workplace and also about the specific duties and projects of the Flight Dynamics Lab.

THE FLIGHT DYNAMICS LAB

Jon M. Graham

Introduction

During the time I spent at the Flight Dynamics Lab, I was able to complete a number of necessary odd jobs which included all of the following: filing photographs, converting various written reports and pictures to electronic format for use on the labs website, writing a Microsoft Access program for searching the branch library catalog, writing a users guide for a program developed by the lab called VBMS (virtual battlefield management system), printed a presentation for the labs SNAP and NETS projects which involve the networking of simulators around the globe, performed data reduction on information obtained from experiments performed concerning the SNAP and NETS projects, and acted as a "dummy" pilot in a few flight simulation runs.

Discussion

Since I did not perform any particular experiment, it would be difficult to write this paper in the standard research paper format. I have chosen instead to simply provide an explanation for all of the particular jobs which I have listed above in the introduction in this discussion.

Filing the photographs was a simple job which was more like menial labor but it was a very good place to start. It was an easy thing to do and to complete and I was able to learn a lot

about the branch in which I was working, what goes on there, and even its history from the pictures. There were a large amount of pictures, negatives, vu-graphs, and presentations which had to be organized in case they needed to be used. It was something that needed to be done that no one else wanted to do.

Converting reports and pictures to electronic format involved typing the reports onto the computer and scanning the pictures in and saving them onto the local network. This was done to various significant works published by the lab so that they could later be transferred onto the lab's website. This assignment allowed me to learn more about the lab, learn how to scan photographs onto the computer, and improve on my typing skills.

During my tour, the lab's staff was in the process of organizing a branch library in which they could store all of their data, resources, presentations, reports, etc. It was my duty to create a search engine for the library catalog using Microsoft Access. Basically, I generated a list of all the reports in the library and information concerning each report in a large chart. The information on each report included publishing data, title, author, subject matter, and position in the branch library. I then made it possible to search this chart using any of the information on the reports. With this project, I was introduced to Microsoft Access and learned how to use it to write my first "program".

I also wrote a user's guide for one of the most recent programs written by the lab's staff, known as VBMS (virtual battlefield management system). The Flight Dynamics Lab is Wright Patterson's laboratory for flight simulator research. VBMS was developed to assist the staff in

monitoring all simulation runs, it provides the user with a "window" into the database in which the virtual aircraft exists. VBMS has a number of different viewing options and also provides any information that would conceivably be useful in analyzing a simulation run. The program will also save and play back simulation runs so that they may be analyzed later. This project was very useful to the laboratory staff since the VBMS program was to be distributed or possibly sold within the year and no user's manual had yet been made. It was useful to me also in that I had to learn to pay attention to any and all details and had to be sure that everything I wrote was clear and could not be misconstrued.

My mentor, Mr. Ron Ewart had to make a presentation concerning the lab's SNAP and NETS projects. He assigned me to the task of creating a few charts and displays on vu-graph paper which he would be able to use for his presentation. The SNAP and NETS projects are both part of a new intricate system of networking which is being employed by the lab. With this new system, flight simulators and other simulators all over the world can represent virtual vehicles such as planes and interact with each other on the same database. Specifically, these projects involve the measurement of time delays in the networking system using simulation runs conducted simultaneously with a flight simulator in Daimler-Benz Laboratory, Germany. This assignment allowed me to familiarize myself with SNAP and NETS as well as with Microsoft PowerPoint.

Later in my tour, I was asked to assist with the ongoing data reduction for the SNAP and NETS projects. Before my tour began, the laboratory had already conducted a number of test simulation runs concerning SNAP and NETS and had collected a stockpile of data from those

tests. This vast amount of information was useless to the staff as it was just a huge jumble of digits. It was, in part, my job to decipher the data and transfer the important information into a condensed, understandable format. Both the SNAP and NETS data contained the same essential information, just in different formats. The SNAP data was displayed as Microsoft Excel worksheet while the NETS data was in UNIX code. My job, for both sets of data, was to find average time delays between different sections of the network and storing them in a easily read chart. The purpose of these tests was to find out which type of network would work most efficiently or cause the smallest time delays. The different networking methods tested were Ethernet, Scramnet, and ALL-DIS network. One specific example of one of the measured time delays in the tests is the time difference between the movement of a joystick at Wright Patterson to the movement of the represented virtual aircraft on a visual screen in Germany. This delay is known as the stick-to-visual or end-to-end time delay which was the longest delay measured in the tests since it consists of the entire network system yet the actual difference in time between the two is only a few microseconds at worst. Another measurement taken in the tests was the number of PDU packets traveling on the network during the test. Too many packets can clutter the network and increase the time latencies. This specific job introduced me to the UNIX system for the first time and now I understand as well as I do DOS which I have used for a number a years, it also sharpened my skills in the use of Microsoft Excel.

Sometimes during preliminary simulation runs, the laboratory staff simply needed someone to sit in the pilot's seat of the simulator so that they could make sure everything was operating

properly. This was a very exciting privilege for me but it also allowed me to experience the “core” of the laboratory hands-on and I also learned the basic pilot controls for an F-18 and how to read a HUD (heads-up display). For some simulation runs I was allowed to operate the VBMS program to monitor the simulation and act as a navigator for the pilot using the map system provided by the program. This experience was useful in writing the user’s guide I discussed earlier besides the time I spent running saved simulation runs.

References

The only true references I had during my eight week tour were the discussions I had with the staff members of the laboratory in which I worked and what I learned from these people by what they said and what they did. I can classify these discussions as interviews and thus I have interviewed all of the following people:

Mr. Ron Ewart

Cp. Ron Johnston

Lt. Steve Purdy

Lt. Dave Barhardt

Mr. Roger Wuerfel

Mr. Terry Christian

Lt. Rob Subr

Acknowledgments

I would like to extend my deepest thanks to the entire staff of the Flight Dynamics Lab, Bldg. 145 in Area B of Wright Patterson Air Force Base, especially my mentor Mr. Ron Ewart, for looking out for me during my tour, putting up with me, teaching me everything I needed or wanted to know and more, and for being the friendliest group of coworkers I've ever known.

**CAST DUCTILE IRON (CDI)
(A CONTROLLED FRAGMENTATION STUDY)**

Trenton A. Hamilton

**Rocky Bayou Christian School
2101 N. Partin Drive
Niceville, FL 32578**

**Final Report for:
High School Apprenticeship Program
Wright Laboratory, Eglin AFB**

**Sponsored by:
Air Force Office of Scientific Research
Bolling Air Force Base, DC**

and

Wright Laboratory

August 1997

CAST DUCTILE IRON (CDI)
(A CONTROLLED FRAGMENTATION STUDY)

Trenton A. Hamilton
Rocky Bayou Christian School

Abstract

Sub-scale tests were conducted using Cast Ductile Iron (CDI) cases to control case fracture. Data was collected using Celotex collection media, velocity screens, 16 gauge steel witness panels, 10,000 fps high speed camera, and 2 lines of pressure gauges. The primary purpose of the testing was to confirm that the fragments would be of a specified, uniform size (weight). This data was reduced to determine the effectiveness of CDI over soft steel cases. The CDI cases were manufactured to yield a uniform fragment of specified size. Success of this test series will be determined from the percent of total mass recovered for each fragment weight division. Thirty percent fragment mass in the specified division would constitute a successful control of the case break-up. Although the cases did not provide the specified fragment weight distribution, results indicate the case fracture was controlled.

CAST DUCTILE IRON (CDI)
(A CONTROLLED FRAGMENTATION STUDY)

Trenton A. Hamilton

Introduction

Advancements in military technology drive the need to produce smaller munitions with larger capabilities. Because of this need, the CLAW (Compact Lethality Augmented Warhead) program was founded. Its primary purpose is to produce a 1,000 pound class general purpose (GP) bomb that has the lethality, measured in Single Shot Probability of Kill (SSP_k), of a 2,000 pound GP bomb (MK-84). A long term goal of this weapon is to have dual-use capabilities.

There are multiple reasons smaller munitions are required. With the advent of Stealth aircraft, which must carry munitions in internal bays, smaller bombs are needed to accommodate the decrease in storage area. These new aircraft have smaller payload capacities, resulting in the need for lighter warheads. Smaller payloads make the plane faster and more maneuverable. Smaller weapons also accommodate force structure

A lethality study has indicated that under controlled conditions, the SSP_k of a MK-84 is achievable by the CLAW. Through controlling the case fracture (resulting in specific fragment sizes), using enhanced explosives, controlling the height of burst, and controlling the beam spray (placing the frags on the vulnerable area of the target), the CLAW can be comparable to the MK-84.

Many concepts have been introduced to control the fragmentation. One such concept is to score the case wall. Scoring the case walls has been proven to consistently control the case fracture. However, this method is costly. Because of the cost, it was determined that the metal mesh used to score the case wall could potentially use the force of detonation to effectively cut the case wall. In January of this year, this concept was tested. The test was successful, but had one minor drawback. The heat from the explosion welded the mesh to the fragments, resulting in non-uniform fragment weight distribution. To correct the problem, a plastic mesh could be used. Some preliminary testing shows the plastic mesh concept to be promising.

The current idea being worked on is the use of Cast Ductile Iron (CDI) cases. WL/MNME hosted a visit by representatives of Lufkin Industries on 30 Jan 97 who specialize in CDI. They claimed to be able to control the fragmentation of the case by doping it with magnesium, chromium, and small amounts of other metals. The doping and/or heat treatment processes cause the carbon matrix in the iron to be distributed as nodules. The mechanism for

spreading the nodules, although proven to be reproducible, is not clearly understood. These nodules provide a splitting point for the case wall upon detonation. Analogous to this concept would be a car windshield splitting apart. If a rock hits a windshield, it provides a splitting point. If the windshield reaches a certain temperature, it splits from that point. The verification testing on ten sub-scale CDI cases which were acquired from Lufkin will be the subject of this report.

Methodology

Ten CDI cylindrical cases were obtained from Lufkin, Ind. for evaluation. As Table 1 shows, five designs were provided for the tests. Two of the designs were made using dual cases, an outer and inner case. Each model was made to break up into different sized frags of specified weights. For each dual case, the outer can should have produced one size of frag, while the inner core produced another size. Along with the CDI cases, three baseline steel cases were tested to provide a control group to measure the CDI cases against. Composition-B was the explosive used for the testing. Comp-B is desired because of its availability and ease of processing. It also has outstanding capability to fracture the case wall.

Test Name	Case Weight (lbs)			Case Dimensions (in)		Frag Size (grains)	
	Filled	Empty	N.E.W	Height	Outer Dia.		
Baseline 1	93.2	51	42.2	18	7.75	Random	
Baseline 2	93.2	51	42.2	18	7.75	Random	
Baseline 3	95.2	51	44.2	18	7.75	Random	
CDI A-1	90.3	50	40.3	18	7.75	500	
CDI A-2	90.3	50	40.3	18	7.75	500	
CDI B-1	106.1	71	35.1	18	7.75	1000	
CDI B-2	106.3	71	35.3	18	7.75	1000	
CDI C-1 (Dual)	98.3	62	36.3	18	7.75	500	Outer Case Inner Case
					4.50	1000	
CDI C-2 (Dual)	98.7	62	36.7	18	7.75	500	Outer Case Inner Case
					4.50	1000	
CDI D-1 (Dual)	98.0	61	37.0	18	7.75	1000	Outer Case Inner Case
					4.50	500	
CDI D-2 (Dual)	97.6	61	36.6	18	7.75	1000	Outer Case Inner Case
					4.50	500	
CDI E-1	98.0	60	38.0	18	7.75	250	
CDI E-2	97.9	60	37.9	18	7.75	250	

Table 1: Case Properties

Tests were conducted at C-64A. For each shot, the arena setup (Figure1) included two lines of six pressure gauges, ten Celotex bundles, four velocity screens, and three witness panels.

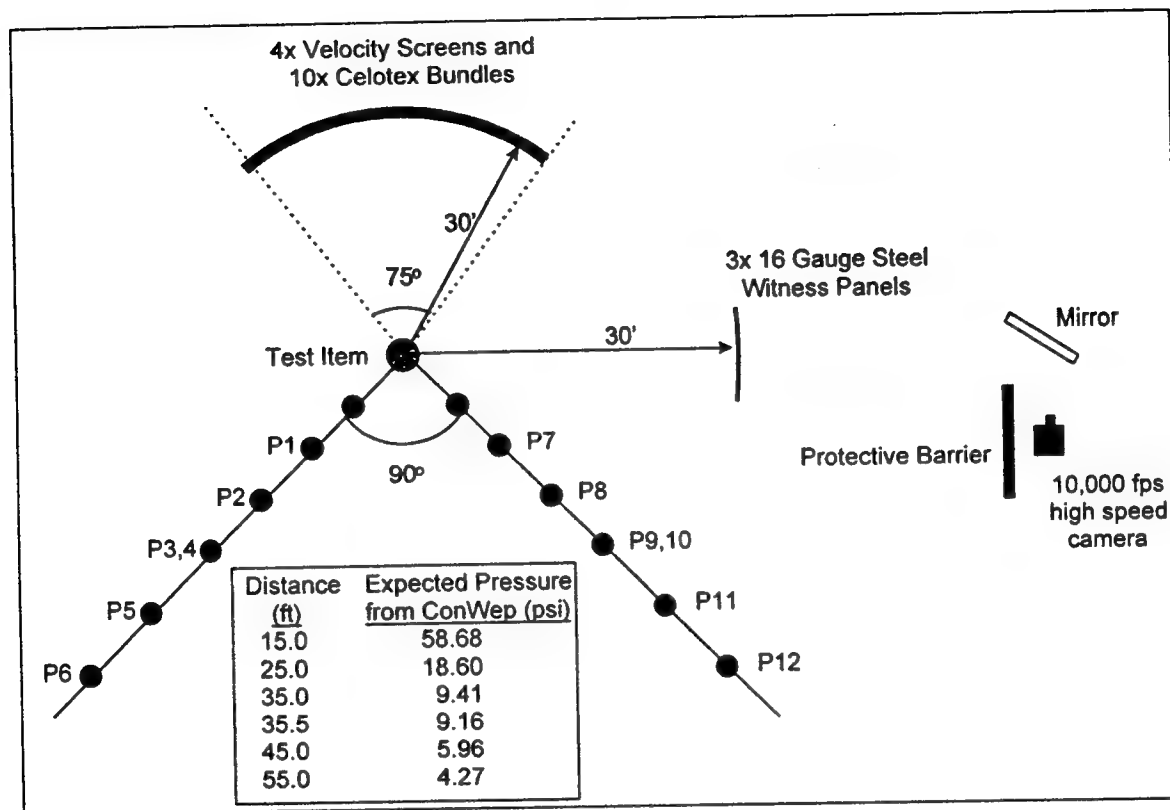


Figure 1: Arena Setup

The pressure gauges were set in two lines of six gauges 90° offset from each other. They were placed at 15, 25, 35, 35.5, 45, and 55 feet from the test item, and calibrated to an expected pressure from the pressure wave. The purpose of Celotex bundles is to catch the fragments. They are 8'x4'x3", with 16 stacked on one stand, with each covering 2.01% of the circumference. The bundles were placed at 30' according to the cubed root of W (W=explosive weight) provided in the Joint Military Effectiveness Manual (JMEM). Attached to the front of the four middle bundles were velocity screens. These screens have a conductive material on the front and back, with a cardboard buffer in the middle. Wires are connected to the front and back, and run back through to a computer. When a fragment goes through, it completes the circuit, causing the computer to register the Time of Arrival (TOA). With this, it calculates the fragment's velocity. Finally, the three witness panels were set up with a high speed camera

filming through a mirror behind them. When the frags break through the panels, they are recorded on the film. Calculations can be done to determine the velocities, again based on TOA.

The pressure data was then reduced, and the CDI pressure data compared against the baseline pressures to determine if there was a difference in case strength. If the steel cases were stronger, they would have resisted expansion for a longer period of time, thus producing a greater pressure wave. Pressure data was collected to certify that there was no difference in the shock wave between the CDI cases and the steel cases. After the Celotex bundles had been scored to retrieve all the frags, the fragments were then sand-blasted to remove the remaining Celotex. Each was then weighed, and data from the weights was reduced. The data collected by the velocity screens was also useful in judging whether or not the CDI cases reacted differently than the steel cases did to the expansion caused by the explosion. As a case resists expansion, it gains more energy. Therefore, the more case inertia, the more energy absorbed by each frag. Faster frags mean greater lethality (higher SSP₀). The high speed camera also aided in determining the fragment speeds.

Results

Fragmentation: After the fragments had been cleaned, weighed, and their weights inputted into a computer, the data was then reduced. The following graphs are the results of the fragmentation reduction.

The frag sizes from the baseline shot (figure 2) were rather random. This is what was expected. The steel cases should have broken up along the easiest lines to relieve the pressure of the explosion. This would result in random sizes of fragments. The baseline shot had fragments ranging from below 25 grains to one over 1200 grains.

CDI Subscale Test Series Fragmentation Results

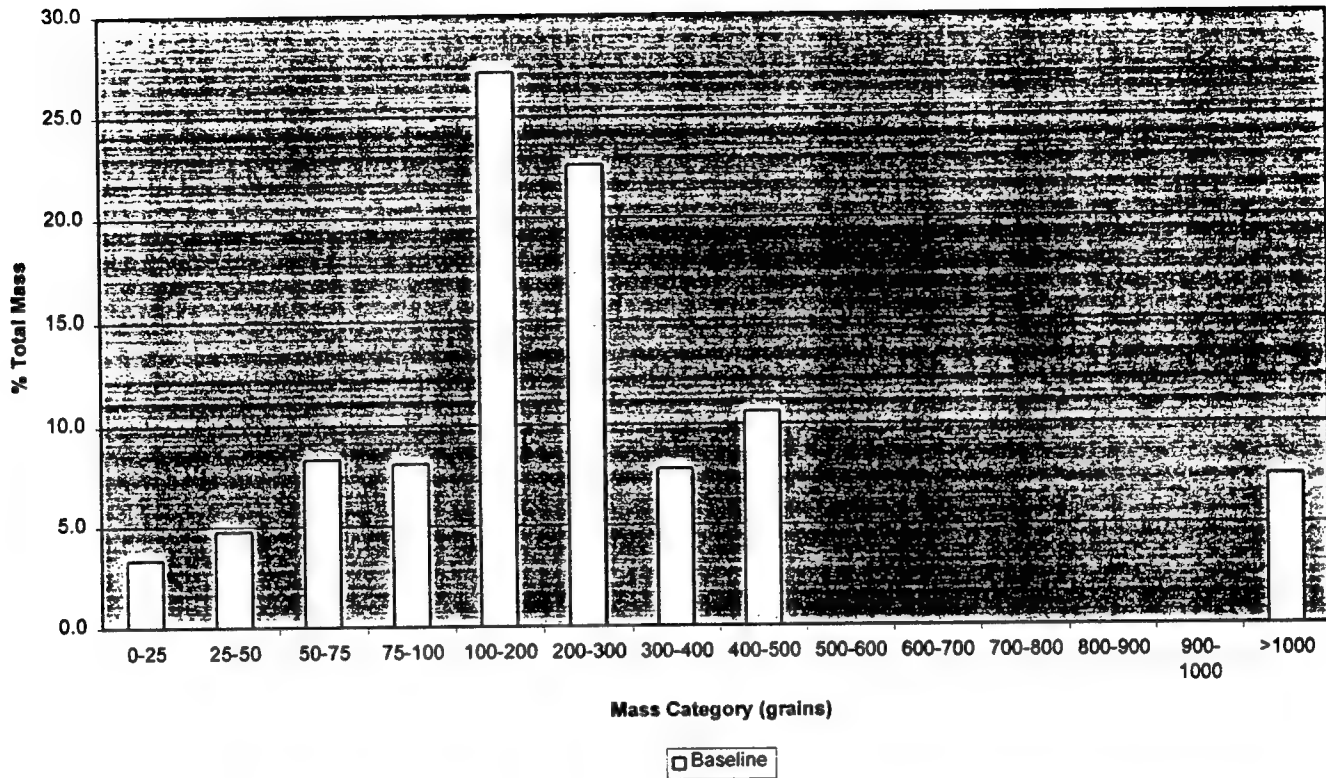


Figure 2: Fragmentation Results (Baseline)

Figure 3 illustrates the desired results from the CDI cases. The 1000 grain case should have had a higher percent of its mass be in the form of 1000 grain fragments, resulting in a peak around the 1000 grain mark. The 500 grain case should have likewise peaked around the 500 grain mark. The 250 grain case should have again corresponded and peaked around the 250 grain mark.

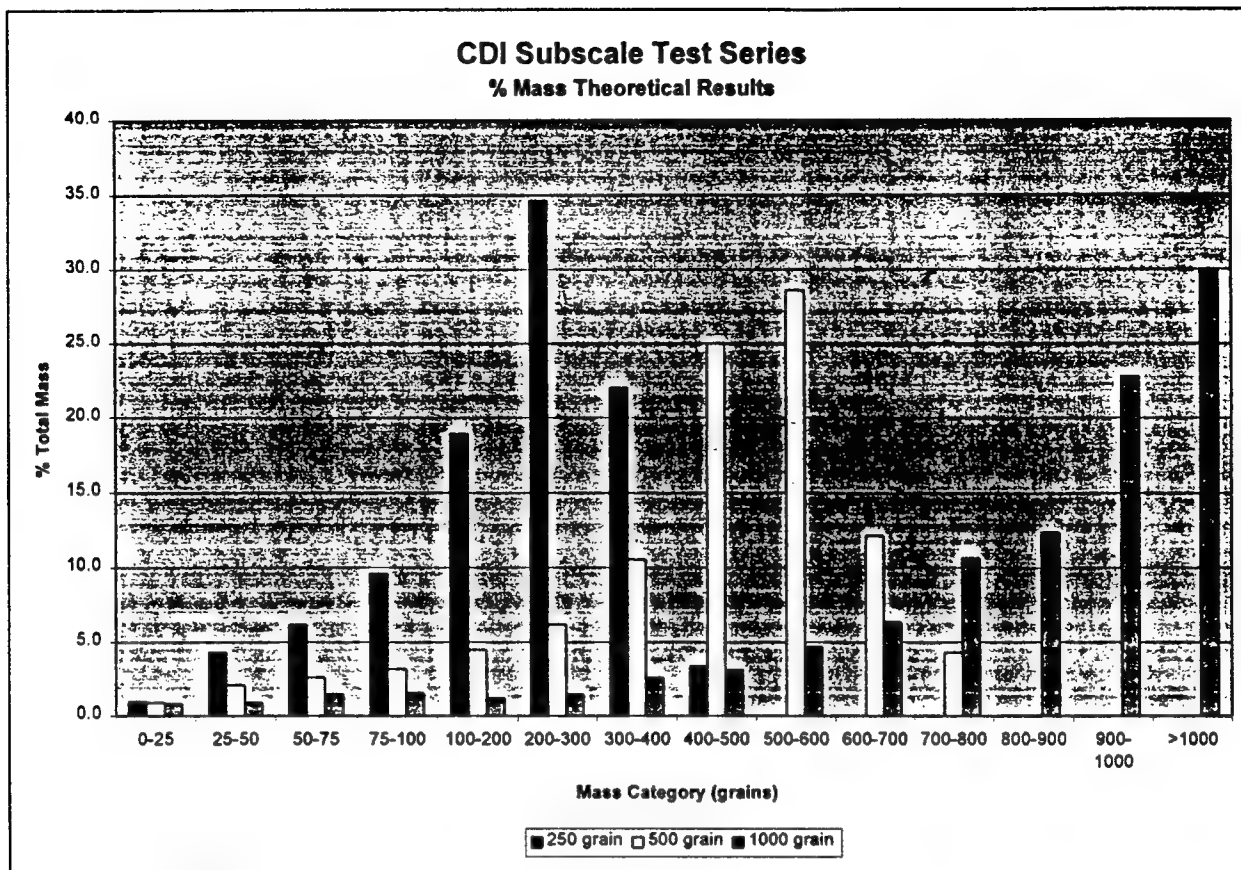


Figure 3: Theoretical Fragmentation Results

From the CDI cases, the fragment sizes were not the predetermined sized. Therefore, at a glance, the fragmentation control did not work. Had the control worked, the cases would have peaked at 1000, 500, and 250 grains, respectively. Those peaks were not there. In fact, the only 1000 grain fragment came from the baseline shot. However, the 1000 grain case does peak at the 100-200 grain mark. It appears from this that the case formulation is off by a factor of 10. Analysis of the 500 grain case proves the same. It peaks at the 50-100 grain region. The proportion of 2:1 (1000:500) also holds true. Along these same lines, the 250 grain case should have peaked at the 25-50 grain mark. There is a slight increase in this area, but not enough to justify a true peak. One probable explanation for this is that frags in the 0-50 grain region are difficult to collect. On average, 50% of the cases were collected. The smaller frags are usually the ones that are overlooked. And many of the smaller frags are turned into dust. The 250 grain case's peak may be missing merely because the fragments were lost. Figure 4 shows the single case fragmentation results.

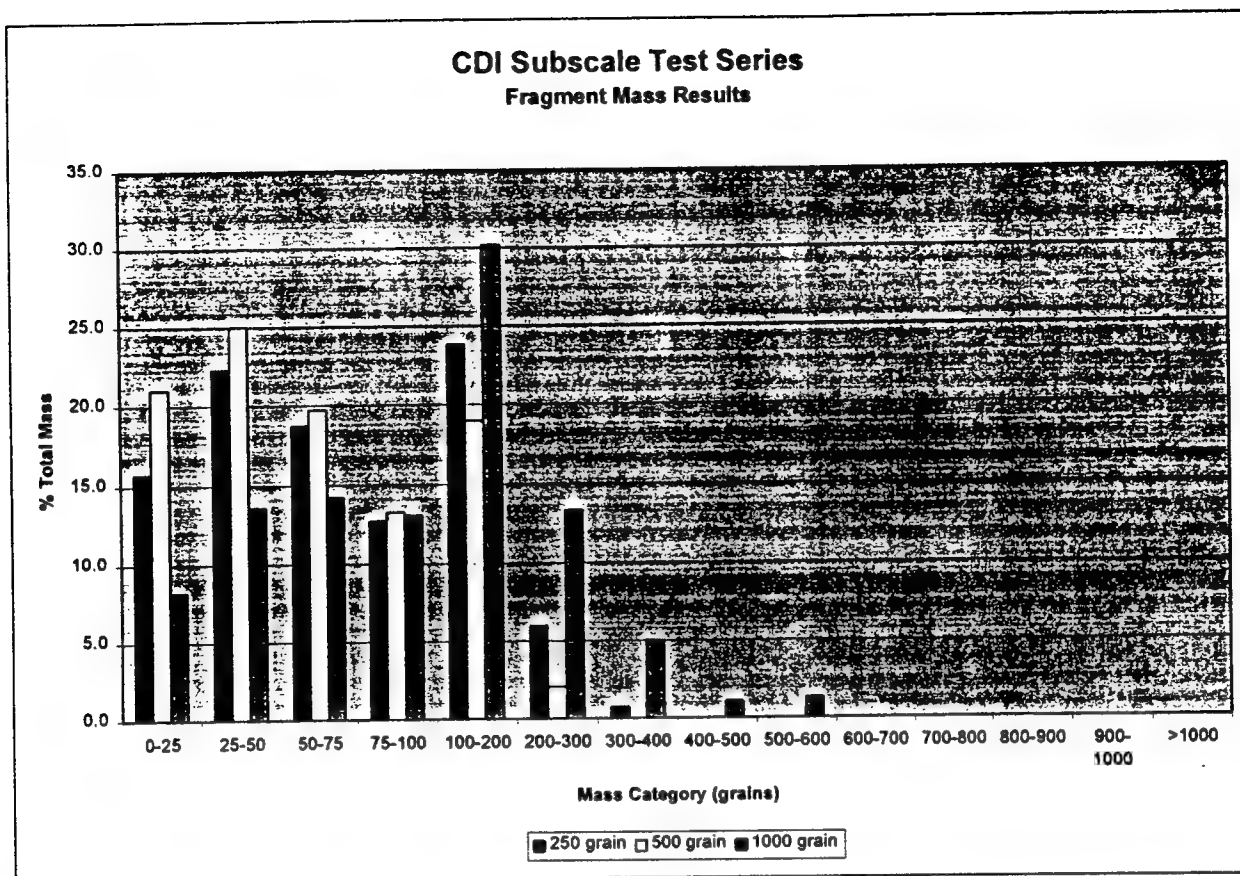


Figure 4: Fragmentation Results (Single Case)

Looking at the graphs from the two dual cases helped confirm that the peaks were in a definite, proportional pattern. The Dual 1 CDI case (figure 5) was made of a 1000 grain outer case with a 500 grain inner case. This should have caused a shift from the 1000 grain case peak over toward the 500 grain case peak. There still should have been frags at the 1000 grain peak, but also some concentrated around the 500 grain peak. When the graphs were looked at, the same pattern is exactly what was seen. There were peaks at the 100-200 grain mark, and also at the 50-100 grain mark.

Likewise, the Dual 2 CDI case (figure 6) consisted of a 500 grain outer case with a 1000 grain inner case. The fragmentation from this case should have been similar to the 500 grain case, with a shift toward the 1000 grain peak. Again, this was seen.

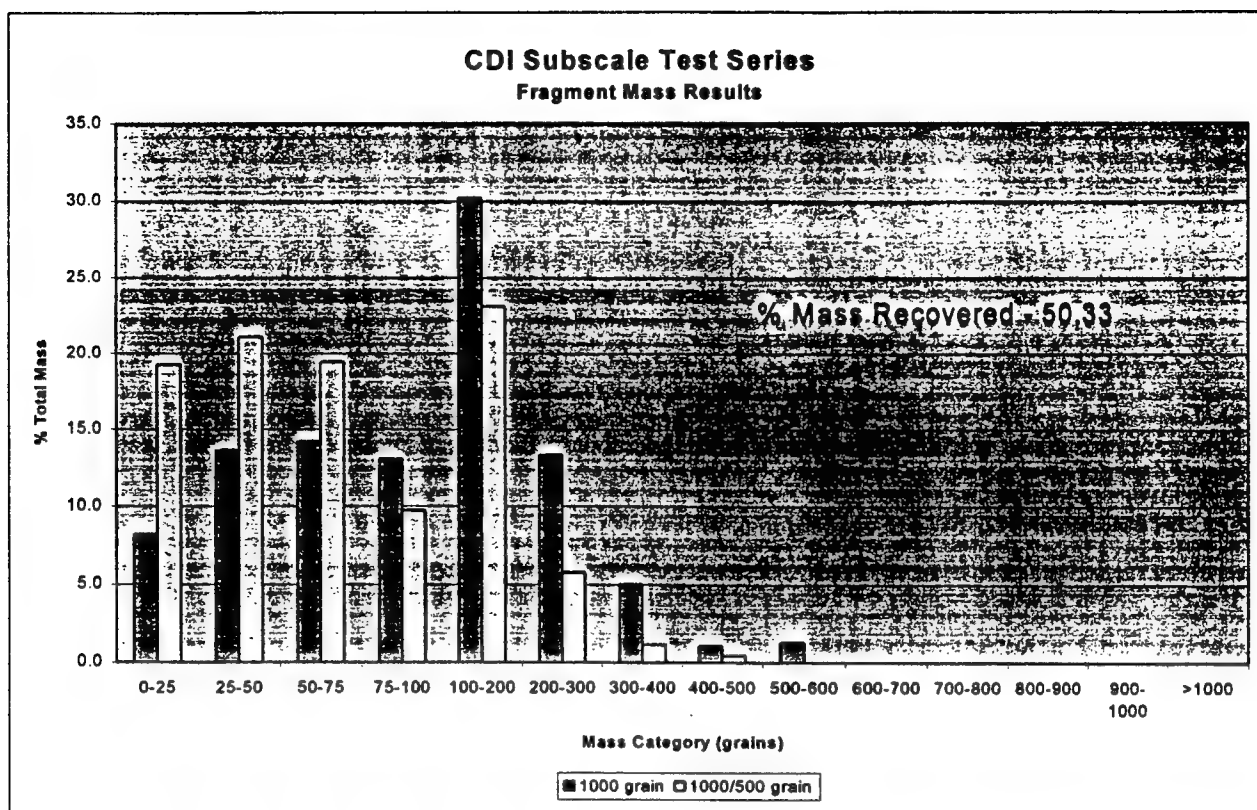


Figure 5: CDI Dual Case 1

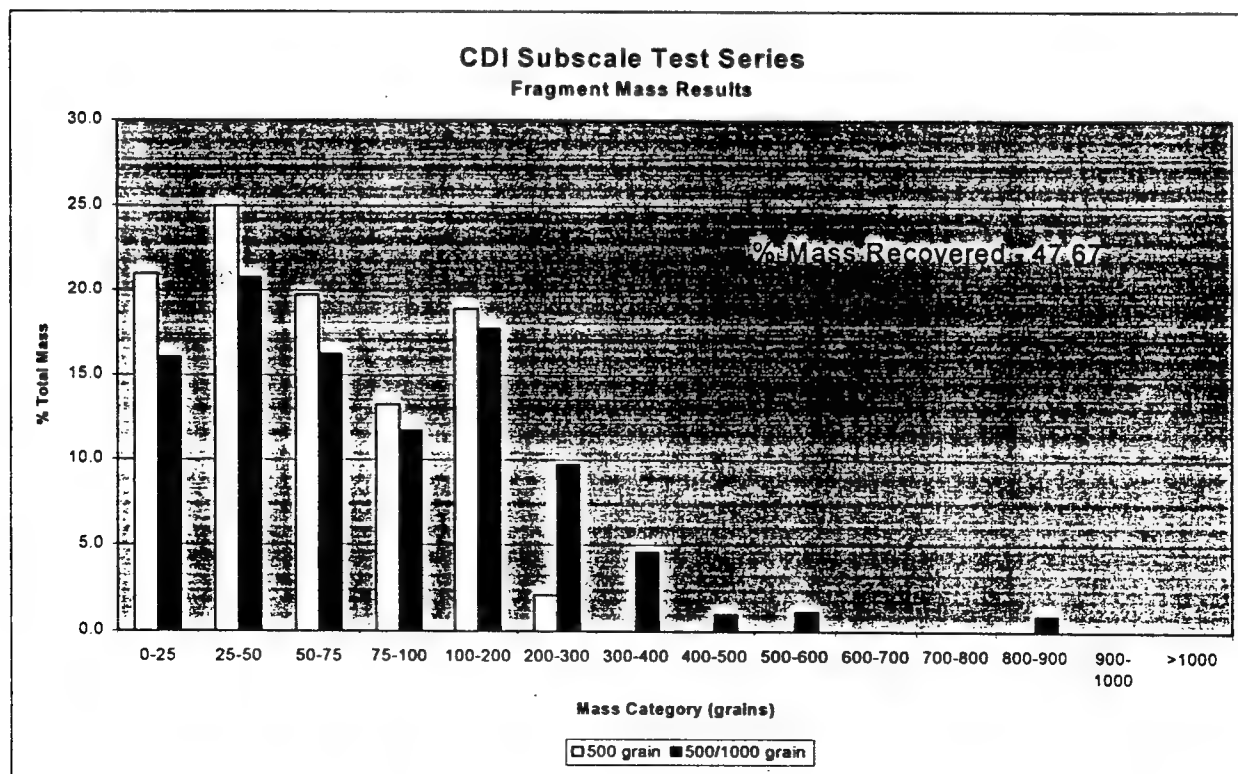


Figure 6: CDI Dual Case 2

The fragmentation results show a definite trend. Although the pattern is not the desired one, it is still proportional to the desired pattern. Either the formulation or the advanced process controls may have been off.

Velocity: Study of the velocity graph (figure 7) indicates the fragment velocities were about the same. The baseline shots had slightly higher velocities than the CDI shots, but the difference was not very great. One goal of the CLAW program is for the fragments to exceed 6000 feet per second (fps). Although the steel cases' velocities are higher than the CDI cases', the CDI cases did meet the goal. Every case excluding the 250 grain case reached the mark with 6000 fps fragments.

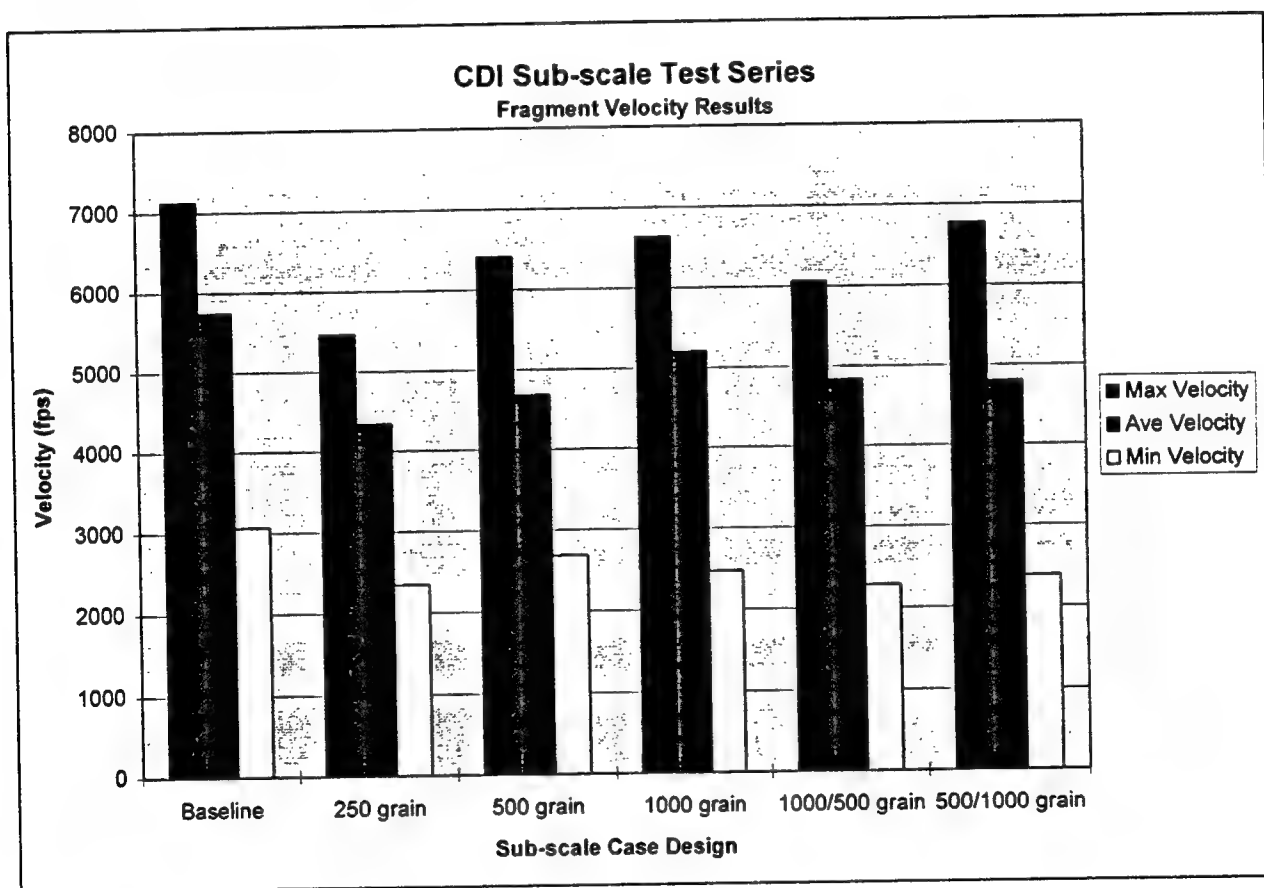


Figure 7: Velocity Results

The velocity results are very important. In a given explosion, as the explosive detonates, the case resists expansion. As the case resists, the fragments gain more and more energy. Therefore, the longer a case can resist the expansion before being blown apart, the faster the fragments will go. Some people thought that the CDI cases

would be blown apart much sooner in the expansion process than the steel cases. This would cause their fragments to be much slower than the baseline frags. Since there was not a significant difference between the velocities of the steel frags and the CDI frags, it can be determined that the CDI cases will have the same lethality as steel cases, assuming the fragment sizes remain constant. This does not mean there is no difference in the expansion process from CDI to steel, but so far no notable difference has been detected.

Pressure / Impulse / TOA: Preliminary graphs of pressure, impulse, and time of arrival indicate only minor differences between the baseline shots and the CDI shots. Since the pressure data has not yet been fully reduced, it cannot be determined if any differences exist.

Summary

Was the fragmentation controlled? A look at the results graphs show that the cases did not break up along the specified parameters. But there were peaks in proportion to each other. These peaks were in a definite pattern. The pattern was not of the specified fragment size, but it does remain constant throughout the test series. This pattern leads us to believe that either the formulation or the advanced process controls were off. This leaves the CDI cases still as a viable option for the fragmentation control section of the CLAW program.

The velocity results indicate that there is no noteworthy difference between the steel and CDI cases. But there still may be a very important difference that has yet to be discovered.

Pressure, impulse and time of arrival results are yet to be reduced. The preliminary look, though, again shows no drastic difference among the cases.

Future tests are in order to provide a more thorough study of the nature of the CDI cases.

**COMPARISON OF EXPERIMENTAL PENETRATION DATA WITH VARIOUS
PENETRATION PREDICTION METHODOLOGIES**

Neil N. Harrison

**Walton High School
555 Walton Road
DeFuniak Springs, FL 32433**

**Final Report for:
High School Apprentice Program
Wright Laboratory**

**Sponsored by:
Air Force Office of Scientific Research
Bolling Air Force Base, DC**

August 1997

**Comparison of Experimental Data with Various
Penetration Prediction Methodologies**

Neil N. Harrison
Walton High School

Abstract

In this study, experimental data from tests done at the AWEF was compared to data from simulations of the same tests using three different penetration prediction codes: PENCVR3D, LaBombA, and EPIC. Six different cases were studied, varying only in the nose shape of the penetrator used in each case. All other conditions of the six tests were the same. Input files were created for each test under each penetration prediction code and the tests were run. Finally, the data received was compared to the data from the experimental tests. The results all ranged from 81.8% to 134.5% of the experimental data. This showed that all three methods used were satisfactory, although LaBombA and PENCVR3D showed slight advantages.

COMPARISON OF EXPERIMENTAL PENETRATION DATA WITH VARIOUS PENETRATION PREDICTION METHODOLOGIES

Neil N. Harrison

Introduction

A study was made to compute and compare the predicted penetration depth of six different penetrator designs for which experimental results were available. The penetrators differed in nose shape and nose length, with the overall length and diameter of the penetrator staying constant. All tests were conducted against similar concrete targets and at near normal impact conditions. Calculations of penetration depth were made with PENCVR3D¹, LaBomba² (with loads model and a Lagrangian Target), and using the EPIC³ code (with the PenCurv model and with a Lagrangian target). Variations within each computational method are described in detail in the appropriate sections. These variations are an attempt to measure the sensitivity of the resulting penetration depth to changes in input parameters.

Methodology

The methodology used in this study is described in the following sections about each penetration prediction code and the experimental data to which the results were compared. In the simulations, either a 6000 or 5000 psi concrete target was used. Some codes would not allow a 6000 psi concrete. The input velocities used were taken from the experimental data for each nose type. All models were run using 4340 RHA Steel as the penetrator material. The percentage listed after the penetration depth in the results tables is a comparison the experimental data for that nose type (prediction/experiment).

Experiments:

The tests⁴ included seventeen shots with seven different variations of nose and body shapes. Six different penetrators, all with cylindrical bodies, were chosen for this computational comparison. The nose shapes included two ogival, two conic, and two biconic nose shapes and nose lengths of four and five inches for each shape (see Figure 1).

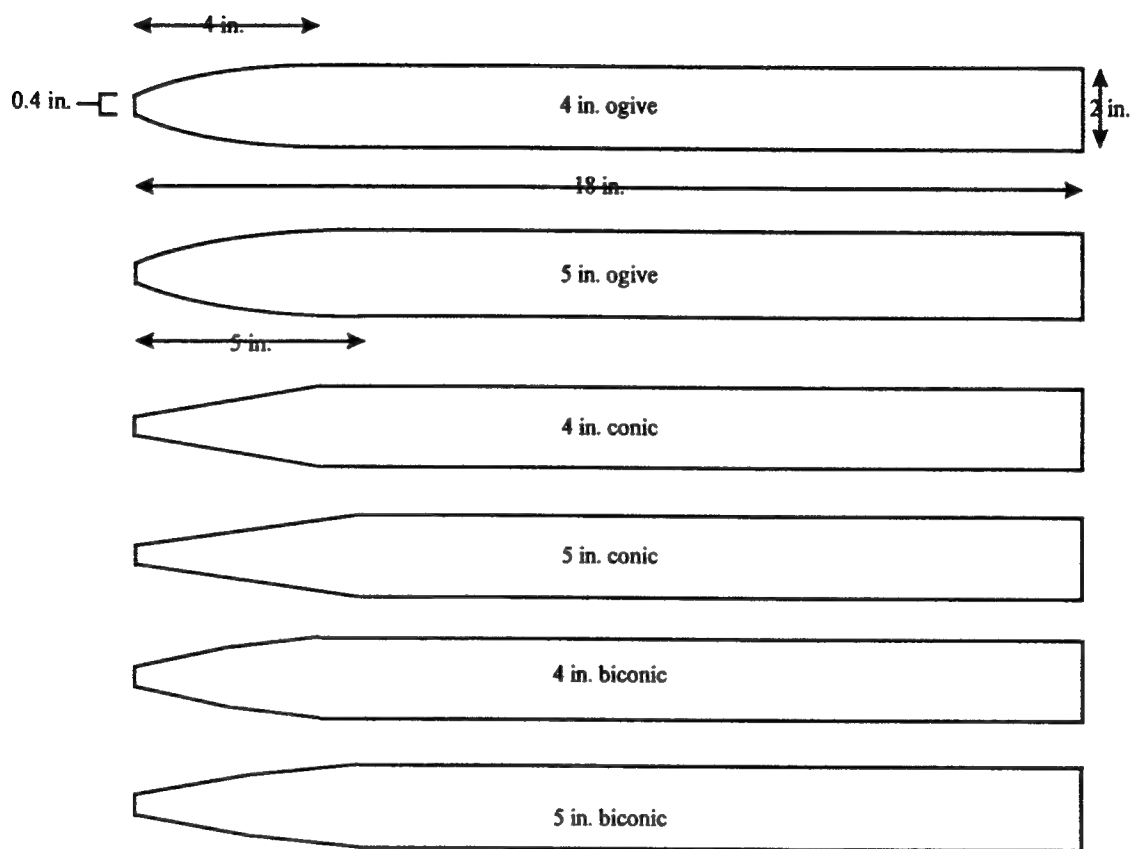


Figure 1: Penetrator Shapes

The tip of each nose had a 0.4 inch diameter blunt tip. For convenience, some simulations used a pointed tip for the penetrator. All targets were concrete with compressive yield strength of around 6000 pounds per square inch (psi). Target dimensions are shown in Figure 2.

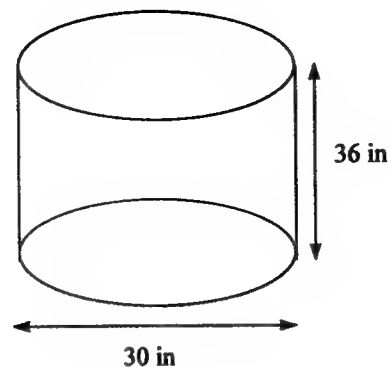


Figure 2: Target Dimensions

Impact conditions (see Table 1) for all tests were near normal and velocities varied from 894 to 956 feet per second (fps).

Nose Type	Impact Velocity	Penetration Depth
4 in. ogive nose	956 fps	23.14 in
5 in. ogive nose	926 fps	23.00 in
4 in. conic nose	899 fps	22.84 in
5 in. conic nose	899 fps	22.40 in
4 in. biconic nose	904 fps	20.44 in
5 in. biconic nose	894 fps	24.13 in

Table 1: Experimental Data

PENCRV3D:

PENCRV3D is a program sponsored by the US Army Corps of Engineers and is used to simulate the penetration of rigid axisymmetric projectiles into a concrete or soil target. The first version of PENCRV was released in a classified report in 1983. It was only usable for two-dimensional (2D) tests. During Operation Desert Storm, interest was renewed in the program and PENCRV V1.0 was released. In

1994, PENCVR V1.5 was released, with improved prediction capabilities. The next year, a 3D version of PENCO2D, the prediction code in PENCVR, was developed and added to PENCVR V1.5.

In the current version, PENCVR3D, three equations can be used to calculate the results: PENCO3D, for normal tests; ISAAC2, for soil half-space tests; and FORRESTAL, for concrete half-space tests. For this study, only PENCO3D was used. The ISAAC2 equation did not apply to this test, and FORRESTAL gave results which were extremely low compared to the actual tests and to other predictions. The user inputs data, including target, projectile, and control information, into P3dShell to create an input file. The file can be edited in P3dShell or any text editor. An input file can also be created in a text editor. PENCVR3D itself must be run under DOS. Typical runtimes on a 486 DX2 machine were less than 10 seconds.

Target information includes target dimensions and information about the material constants (S-Number or density and yield strength is needed). The target can have multiple layers if needed. Projectile information includes shape and size. These are given by choosing a nose type and entering information about the radius, nose length, ogive radius or conic angle, and total projectile length. Weight, location of the center of gravity, and moments of inertia are also needed. They were calculated by Moments96, programmed by Josh Weaver (HSAP 95-96). Control data consists of stop conditions (Maximum time, minimum velocity, maximum Euler angles, etc.), initial position, velocity, information controlling output of steps, and the analysis type that is to be used, PENCO3D, FORRESTAL, or ISAAC2. An example of a PENCVR3D input file is shown in Appendix 1.

Two output files are generated for each run. One output file is a text file containing data for each step in the test and the final results of the test, with maximum penetration depth, ending time of the test, and angular values. The second output file is used in the PLTCRV3D program to plot the projectile penetration. Plots can be obtained for the projectile shape, the trajectory path, and 20 other variables that can be plotted against time or position (velocity, acceleration, and angular values). This file was also useful because it could be easily manipulated to move to Microsoft Excel for further analysis.

The speed of using PENCVR3D and the simplicity of changing the input files made running many variations of the tests more realistic. All penetrators were run against 5000 and 6000 psi concrete targets. Also, to use for comparison with Lagrangian models such as LaBombA and Epic, tests were run with penetrators similar to the ones used in the experiments, but with the nose extended to a point. This was done because experience has shown that the use of pointed noses against Lagrangian targets is much more computationally efficient and gives more accurate results. Runs were also made with density variations in the target material at 6000 psi. Density ranged from 0.0001917 to 0.0002343 lbf-s²/in⁴ ($\pm 10\%$ of the baseline density). Also, penetrators with blunt noses were run against 7000 and 8000 psi concrete at normal density. The variations in density and yield strength were made to study the sensitivity of the penetration depth to these factors. PENCVR3D results are shown in Table 2.

	blunt 5000psi	blunt 6000psi	blunt 7000psi	blunt 8000psi	pointed 5000psi	pointed 6000psi	blunt/6000p si low density	blunt/6000p si high density
4 in. ogive	26.0 (112.4%)	23.2 (100.3%)	21.1 (91.2%)	19.7 (85.1%)	27.0 (116.7%)	24.2 (104.6%)	23.9 (103.3%)	22.5 (97.2%)
5 in. ogive	26.5 (115.2%)	23.4 (101.7%)	21.5 (93.5%)	20.1 (87.4%)	27.8 (120.9%)	24.8 (107.8%)	24.3 (105.7%)	22.8 (99.1%)
4 in. conic	24.2 (106.0%)	21.8 (95.4%)	20.0 (87.6%)	18.7 (81.9%)	26.1 (114.3%)	23.5 (102.9%)	22.3 (97.6%)	21.1 (92.4%)
5 in. conic	26.2 (117.0%)	23.3 (104.0%)	21.6 (96.4%)	20.1 (89.7%)	28.2 (125.9%)	25.2 (112.5%)	24.1 (107.6%)	22.9 (102.2%)
4 in. biconic	27.5 (134.5%)	24.8 (121.3%)	24.3 (118.9%)	22.5 (110.1%)	26.9 (131.6%)	24.2 (118.4%)	26.9 (131.6%)	25.7 (125.7%)
5 in. biconic	29.4 (121.8%)	26.2 (108.6%)	22.8 (94.5%)	21.2 (87.9%)	28.4 (117.7%)	25.7 (106.5%)	25.3 (104.8%)	24.2 (100.3%)

Table 2: PENCVR3D Results

LaBombA:

LaBombA (Lagrangian Bomb Aalysis) is a penetration hydrocode being developed by Dr. William Cook to simulate penetration of axisymmetrical penetrators using either a loads model or a

Lagrangian Target. A graphical model is displayed on the screen while the simulation is running, which can display the strain, pressure, heat, stress, or damage on each element using a color-coded scale.

LaBombA is an interactive program in which data is input via a series of menu screens. Due to its early stage of development (only the Alpha version is available), input options are limited and only 2-dimensional simulations are available. Enough options are available, however, to create and run the models that were needed. One of the biggest advantages of LaBombA is that it is a full hydrocode that runs on a PC platform. In addition to its full hydrocode capabilities, it also has several engineering empirical options. Another advantage of LaBombA is its interactivity. With options such as easy bombs and easy targets, a full simulation can be set up in two or three minutes for many types of penetrators.

Input parameters for LaBombA include a geometry file for the projectile, the shape and size of the target, and other information such as velocity, minimum time step, ending time, and other information common to all penetration codes. The geometry file is created by entering in all of the points, connecting them by entering in lines, then forming polygons with the lines. Number and size of elements created when the file is meshed is determined by the number of nodes the user chooses to put on the individual lines when creating the geometry file. An example geometry file is shown in Appendix 2.

After all of the geometry has been entered, the file is meshed. This divides the projectile (and target if the Lagrangian model is used) into elements. After the file has been meshed, finite element analysis is performed. Current velocity, depth, cycle number, and time are at the bottom of the screen while the program is running. No output file is generated, but when the job is completed, the final penetration depth and other information is on the screen.

For this study, tests were run with a pointed nose against a 5000 psi concrete target using the loads model and a Lagrangian target. Yield strength of the target cannot currently be modified within LaBombA. The easy bomb option was used to set up the conic and biconic tests, but the ogive geometry files had to be created without this option. Using the loads model, the runs in this study took about 15-20 minutes on a 200 MHz Pentium Pro. The runs done using the Lagrangian target took around an hour. Results for LaBombA are shown in Table 3.

	pointed/5000 psi Lagrangian	pointed/5000 psi Loads Model
4 in. ogive	22.1 (95.5%)	27 (116.7%)
5 in. ogive	24.8 (107.8%)	28.3 (123.0%)
4 in. conic	21.4 (93.7%)	26.3 (115.1%)
5 in. conic	23.7 (105.8%)	28.4 (126.8%)
4 in. biconic	20.5 (100.3%)	27.4 (134.1%)
5 in. biconic	23.4 (97.0%)	28.1 (116.5%)

Table 3: LaBombA Results

EPIC:

EPIC (Elastic Plastic Impact Computations) is a penetration hydrocode first developed for the Ballistic Research Laboratory (BRL) in 1977, but has been primarily supported by Wright Laboratories since this time. For 13 years, EPIC-2, for 2D simulations, and EPIC-3 for 3D simulations, were separate programs. They both underwent many changes, adding improved pre- and postprocessing capabilities, improved material modeling, eroding interfaces, and many other options. The 1990 version of EPIC combined the 2D and 3D versions. Between then and 1997, 6 new versions were released, each with more options and improvements over previous versions. The current EPIC 97 version was used in this study.

EPIC uses many different algorithms to compute the penetration cases. It has many options, including 1D, 2D, and 3D geometry, different element types, and sliding, contact, and erosion algorithms. Smooth Particle Hydrodynamics (SPH) algorithms are also available. If SPH is used, the penetrator and target are not broken up into elements, like in most cases. Instead, the code deals with particles. This allows for more severe distortions of shape, which are often present during high-velocity impacts. Various material models are available, including seven basic material types: Solid (metal) materials, explosive

materials, crushable/concrete materials, liquid materials, brittle (ceramic) materials, reactive explosive materials, and RDG solid (metal) materials.

Input files for the 2D EPIC calculation were created using EPEG, a graphic user interface written by Dann Holmes (HSAP 96). Velocity, minimum time steps, ending time, target information, and projectile information were required. Points were entered to describe the projectile, and the material was chosen from a menu. The target information included radius, depth, and material. After input files were created, they were run on a workstation. Results are shown in Table 4.

Nose Type	Pointed/5000 psi Lagrangian
4 in. ogive	18.93 (81.8%)
5 in. ogive	21.79 (94.7%)
4 in. conic	19.58 (85.7%)
5 in. conic	23.73 (105.9%)
4 in. biconic	18.97 (92.8%)
5 in. biconic	21.54 (89.3%)

Table 4: EPIC Results

Conclusions:

Results from the most closely matching PENCVR3D runs (blunt/6000 psi) ranged from 95.4% to 121.3% of the experimental data. Results from the LaBombA lagrangian runs ranged from 93.7% to 107.8% of the experimental data. LaBombA loads model results ranged from 115.1% to 134.1% of the experimental data. Epic results ranged from 81.8% to 105.9% of the experimental data.

Bibliography

1. M. D. Adley, R. P. Berger, J. D. Cargile, H. G. White, and D. C. Creighton, *Three-Dimensional Projectile Penetration Into Curvilinear Geologic/Structural Targets: User's Guide for PENCVR3D*, U.S. Army Corps of Engineers, Vicksburg, MS, 1997.
2. W. H. Cook, personal interview
3. G. R. Johnson, R. A. Stryk, T. J. Holmquist, and S. R. Beissel, *User Instructions for the 1997 Version of the EPIC Code*, Alliant Techsystems Inc., Hopkins, MN, 1997
4. Optimum Penetrator Shape Study

Appendix 1: PENCVR3D input file

4 in blunt ogive nose/5000 psi

*** CONTROL INFORMATION ***

NSTP, NPRINT, IFFSEL, ISI
75,2,1,1
VEL, FREKOT, PHIMIN
11472,.5,0
GAMMA, PSI
180,0
XTIP, YTIP, ZTIP
0,0,0
ALFXZ, ALFYX, ALFYZ
0,0,999
VX, VY, VZ
0,0,0
W1, W2, W3
0,0,0
DTMIN, DTMAX
.00000001,.1
TIMEI, TIMEF, FREQI
0,.01,.5
XSTOP, YSTOP, ZSTOP, VELF
30,30,-36,100
GAMSTP, ALSTP, PSISTP, PHISTP
270,360,360,360

*** PROJECTILE INFORMATION ***

NEM, IOPSHP, ARATIO
12,5,1.25
RB, EJ, RJ
.2,0,10.4
RC, RO, RN
.000000001,1,.2
XFA, XFF, THETAF
0,0,0
XLP, XCG, SN, THETAN
18,9.7775,4,0
WEIGHT, XICG, YICG, ZICG
14.58,27.028232,27.028232,5.648929

*** TARGET INFORMATION ***

NLAY
2
SNUM(J), DENSITY(J), YIELD(J), FRICAT(J), FRICCT(J), J=2toNLAY
0,.000213,5000,0,0
NSURF(J), J=2toNLAY
2
YSURF(IJ), ZSURF(IJ), I=1toNSURF(J), J=2toNLAY
-15,0,15,0

Appendix 2: LaBomba geometry file

Summary of Geometry

Point Summary:

Point	x	y
1	0.000e+000	0.000e+000
2	4.500e-001	0.000e+000
3	4.500e-001	2.000e-001
4	9.500e-001	0.000e+000
5	9.500e-001	1.965e-001
6	9.500e-001	3.930e-001
7	1.450e+000	0.000e+000
8	1.450e+000	3.739e-001
9	1.450e+000	5.580e-001
10	1.950e+000	0.000e+000
11	1.950e+000	4.656e-001
12	1.950e+000	6.950e-001
13	2.450e+000	0.000e+000
14	2.450e+000	5.400e-001
15	2.450e+000	8.060e-001
16	2.950e+000	0.000e+000
17	2.950e+000	5.970e-001
18	2.950e+000	8.910e-001
19	3.450e+000	0.000e+000
20	3.450e+000	6.378e-001
21	3.450e+000	9.520e-001
22	3.950e+000	0.000e+000
23	3.950e+000	6.620e-001
24	3.950e+000	9.880e-001
25	4.450e+000	0.000e+000
26	4.450e+000	6.700e-001
27	4.450e+000	1.000e+000
28	1.845e+001	0.000e+000
29	1.845e+001	6.700e-001
30	1.845e+001	1.000e+000
31	-3.600e+001	0.000e+000
32	-3.600e+001	1.500e+001
33	0.000e+000	1.500e+001
34	0.000e+000	0.000e+000

Line Summary:

Line	Nodes	Point A	Point B	Constraint
1	2	1	3	16384
2	2	3	2	0
3	2	2	1	4096
4	2	2	3	0
5	2	3	6	16384
6	3	6	4	0
7	2	4	2	4096
8	2	4	5	0
9	2	5	8	0
10	3	8	7	0
11	2	7	4	4096
12	2	5	6	0
13	2	6	9	16384
14	2	9	8	0
15	2	8	5	0
16	3	7	8	0
17	2	8	11	0
18	3	11	10	0

19	2	10	7	4096
20	2	8	9	0
21	2	9	12	16384
22	2	12	11	0
23	2	11	8	0
24	3	10	11	0
25	2	11	14	0
26	3	14	13	0
27	2	13	10	4096
28	2	11	12	0
29	2	12	15	16384
30	2	15	14	0
31	2	14	11	0
32	3	13	14	0
33	2	14	17	0
34	3	17	16	0
35	2	16	13	4096
36	2	14	15	0
37	2	15	18	16384
38	2	18	17	0
39	2	17	14	0
40	3	16	17	0
41	2	17	20	0
42	3	20	19	0
43	2	19	16	4096
44	2	17	18	0
45	2	18	21	16384
46	2	21	20	0
47	2	20	17	0
48	3	19	20	0
49	2	20	23	0
50	3	23	22	0
51	2	22	19	4096
52	2	20	21	0
53	2	21	24	16384
54	2	24	23	0
55	2	23	20	0
56	3	22	23	0
57	2	23	26	0
58	3	26	25	0
59	2	25	22	4096
60	2	23	24	0
61	2	24	27	16384
62	2	27	26	0
63	2	26	23	0
64	3	25	26	0
65	40	26	29	0
66	3	29	28	0
67	40	28	25	4096
68	2	26	27	0
69	40	27	30	0
70	2	30	29	0
71	40	29	26	0
72	41	31	32	0
73	49	32	33	0
74	41	33	34	0
75	49	34	31	4096

Polygon Summary:

Polygon	Line1	Line2	Line3	Line4
1	1	2	3	9983404
2	4	5	6	9983404
3	8	9	10	9983404
4	12	13	14	9983404
5	16	17	18	9983404
6	20	21	22	9983404
7	24	25	26	9983404
8	28	29	30	9983404
9	32	33	34	9983404
10	36	37	38	9983404
11	40	41	42	9983404
12	44	45	46	9983404
13	48	49	50	9983404
14	52	53	54	9983404
15	56	57	58	9983404
16	60	61	62	9983404
17	64	65	66	9983404
18	68	69	70	9983404
19	72	73	74	9983404

Angela Helm's report was not available at the time of publication.

WINDOW DESIGN FOR LASER VELOCIMETER DATA ACQUISITION

Anna S. Hill

**Carroll High School
4524 Linden Avenue
Dayton, OH 45432**

**Final Report for:
High School Apprentice Program
Wright Laboratory**

**Sponsored by:
Air Force Office of Scientific Research
Bolling Air Force Base, Washington, DC**

And

Wright Laboratory

August 1997

WINDOW DESIGN FOR LASER VELOCIMETER DATA AQUISITION

Anna S. Hill
Carroll High School

Abstract

In the project TESCO, the airflow velocity profile at stage two needed to be measured to find out why the test had failed in the past. A silica window, along with a metal holder, was designed using mechanical engineering techniques. The obstacles to these designs were a flat window had to be placed in a circular compressor case, with the width equal to one blade pitch of stator one and the length had to be as long as possible given the confinements of the compressor case. Two laser beams will be directed through this window and used to measure the velocity of the airflow between the second rotor and the stator, which is where the problems were in the past. However, the experiment is not complete at this time, due to a September testing date. At that time the suitability of the window designed will be determined.

WINDOW DESIGN FOR LASER VELOCIMETER DATA ACQUISITION

Anna S. Hill

Introduction

In order to determine the reason why rotor two did not start in the initial run of TESCOM, a second attempt is scheduled to run in September of 1997. The overall objective of the TESCOM project is to achieve an 8:1 pressure ratio in three stages; to build, design, and test stage-by-stage; and to employ counter-swirl (high reaction) for increased work. In the early eighties a single stage test was completed with two different rotor designs and good performance was demonstrated. In the early nineties a initial stage two test was completed. There was a performance setback with pressure ratio and efficiency; the second stage rotor did not start. This resulted in an investigation into the possible causes of why the second stage rotor did not start.

A laser window is required to allow access into the compressor for the TESCOM measurements. Laser anemometry measurements are used to determine the velocity of small particles (approximately one micron), which are carried by the airflow, and assumed to represent the actual fluid velocity. The window allows two laser beams to measure the velocity of the airflow between the second rotor and stators, as well as between the rotor blades. This measurement is taken by intersecting the two beams at a specific point, where the separate beams form an interference pattern (fringe pattern). As a particle moves through the fringe pattern, the intensity of the light reflected from the particle will vary at a frequency directly related to the particle's velocity.

Discussion of Problem

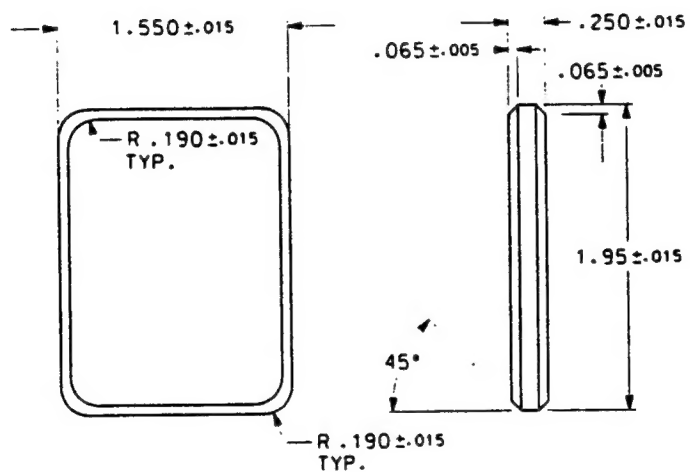
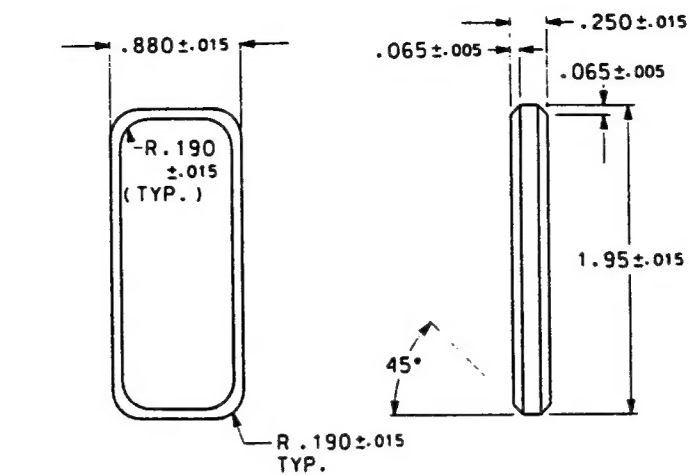
The challenge was to design a window, which consists of a metal holder and the corning 7940 fused silica window. The window had to be flat because the laser beams are rotated around a common axis. If the window was not flat, then the beams would not cross at the planned specific point and the exact position of the measurements would not be accurate. The construction of the window was difficult because it needed to have the largest surface area possible, without affecting the tip flow due to a change in the curvature of the compressor case.

Methodology

First, the compressor case had to be taken apart in order to ensure that accurate measurements of the future window site could be taken. The designated site of the window had to be decided. This was determined by the largest area along the casing that was not obstructed by experimental equipment. Once the site was decided, measurements were taken of the length, width, and the thickness of the case. Using these measurements, an engineering draft of the window was created. This drawing of the window was then sent to Bond Optics to be fabricated.

Next, the window holder was designed to fit securely around the silica window, to ensure that the window would not move during testing. The window will be held in place by the use of teflon tape and rubber "O" rings. This will reduce the amount of friction between the window and the metal holder. To this date, the window drawings have been completed; however, the holder drawings have yet to be finished. Eventually, the drawings will be sent to the machine shop and manufactured for testing in September.

Results



MATERIAL: CORNING 7940 FUSED SILICA

UNLESS OTHERWISE SPECIFIED DIMENSIONS ARE TO THIERES TOLERANCES ARE:		CONTRACT NO.		WRIGHT LABORATORY AERO PROPULSION & POWER DIRECTORATE	
PRECISION	RESEARCH	APPROVALS	DATE	TITLE	
DO NOT SCALE (PRINTING)		R.T. McEVY 25 JUN 97		TESCOM WINDOW	
DESIGNED BY		H. LAW 10 JUL 97		DRAWN BY	
CHECKED BY		C. WILLIAMS 25 JUN 97		SCALE	
APPROVED BY		G. HOWELL 25 JUN 97		1/1	
SHEET NO.		1 OF 2		1 OF 2	

Conclusion

Due to the scheduling of the test, no conclusions can be drawn at this time. At the completion of testing it will be decided if the window was suitable for the TESCOM procedure. Also, the cause of the initial setback will hopefully be discovered at that time.

References

Battle, G.C. Connolly, Tom. Keese, Anne M. Laser Window and Mirror Materials. Vol.9. IFI/ Plenum Data Co. New York. 1977

Drain, L.E. The Laser Doppler Technique. John Wiley & Sons. New York. 1980

Durst, F. Melling, A. Whitelaw, J. H. Principles and Practice of Laser-Doppler Anemometry. Academic Press. New York. 1980

Introduction to Lasers. Laser/Electro-Optics Tech. Series. Vol. 1. Second edition. Center for Occupational Research and Development. Waco, TX. 1990

Klein, Claude A. Mirrors and Windows for High Power/High Energy Laser Systems. The Society of Photo-Optical Instrumentation Engineers. Bellingham, WA. 1989

Laser Anemometry Advances and Applications: Proceedings of the Fifth International Conference. The International Society for Optical Engineering. Bellingham, WA. 1993